

Self-organizing structure and metrics of complex networks

Dissertation

zur Erlangung des Doktorgrades
der Naturwissenschaften

vorgelegt beim Fachbereich Physik
der Goethe Universität
Frankfurt am Main

von

Jan Carsten Scholz

aus Gießen

Frankfurt, 2010

(D30)

vom Fachbereich Physik der

Goethe Universität als Dissertation angenommen.

Dekan: Prof. Dr. Michael Huth

Gutachter: Prof. Dr. Martin Greiner, Prof. Dr. Joachim Maruhn

Datum der Disputation:

Contents

German summary	v
1. Introduction	1
2. Brief Résumé of Graph Theory	5
2.1. Graph Theory notation	5
2.2. Empirical networks and network models	10
2.2.1. Small world graphs	11
2.2.2. Scale-free graphs	12
2.3. Geometric- p model	14
3. Game Theory on networks	19
3.1. The Prisoner's Dilemma	20
3.2. Games and Graphs	23
3.3. Prisoners' Dilemma Network Game	27
3.4. Related network structure modeling	29
4. Iterated prisoners dilemma network game	33
4.1. Iterated Prisoner's Dilemma (IPD)	34
4.2. Neighborhood Exploration Schemes	37
4.3. Existence of NNEs	38
4.4. Perturbation dynamics of NNEs	42
4.5. Properties of stationary NNEs	47
5. Incentives for cooperation	53
5.1. Underlying interaction model	53
5.2. Incentive model and distribution strategies	55
5.3. Comparison of incentive distribution strategies	56
6. Communication throughput of networks	59
6.1. Data Traffic Model and Load	59
6.2. Derivation of Throughput Capacity T_{e2e}	61
6.3. Influence of network structure on data throughput	62
7. Advanced routing	65
7.1. Weights and metrics	66
7.2. Routing weight assignments	68

Contents

7.3. Effects of metrics on distances and loads	71
7.4. Hybrid metric	75
7.5. Comparing T_{e2e} -scaling of the metrics	80
7.6. Self-organizing (SO) metric	88
7.7. The $\log(k_i k_j)$ -metric	91
8. Conclusion	95
A. AS-level data table	99
B. Coauthored publications	103
Proactive robustness control of heterogeneously loaded networks	105
Optimized network structure and routing metric in wireless multihop ad hoc communication	109
Bibliography	127
Acknowledgments	135
CV	137

Zusammenfassung in deutscher Sprache

Die vorliegende Arbeit befasst sich mit der Charakterisierung und Optimierung von Prozessen auf komplexen Netzwerken. In Natur, Gesellschaft und Technik existiert eine Vielzahl ungeordneter Systeme, für die die Emergenz makroskopischer Eigenschaften aus mikroskopischen Wechselwirkungen charakteristisch sind. Diese makroskopischen Eigenschaften sind in den einzelnen mikroskopischen Bestandteilen nicht erkennbar, sondern entstehen erst durch das Zusammenspiel einer großen Anzahl derselben. Beispiele für emergente Eigenschaften sind Phasenübergänge wie sie im Magnetismus und in der Perkolation, aber auch in biologischen und sozialen Systemen auftreten. Weitere bedeutende Beispiele sind komplexe technologische Systeme, insbesondere solche, bei deren Entwicklung eine hohe Ausfallsicherheit ohne zentrale Kontrollinstanz eine wichtige Rolle spielt. Die wahrscheinlich prominentesten Beispiele hierfür sind das Internet, bestehend aus weltweit vernetzten Routern, sowie das World-Wide-Web, die (virtuelle) Struktur, gebildet von Homepages und ihren Verbindungen durch Hyperlinks. Eine verblüffende Gemeinsamkeit vieler solcher in der Natur auftretender vernetzter Systeme ist die Struktur der Netzwerke, die sich weder durch reguläre Gitter, noch durch rein zufällige Verbindungen beschreiben lassen.

Der mathematische Rahmen zur Beschreibung von Netzwerken ist die Graphentheorie. Deren Ursprünge finden sich bereits bei [Euler \[1736\]](#), aber auch heute stellt sie ein aktives Forschungsfeld der Mathematik dar [z.B. [Erdős und Rényi, 1960](#), [Bollobás, 1985, 1998](#)]. Im Formalismus der Graphentheorie werden vernetzte Strukturen als Menge von Knoten dargestellt, welche durch Kanten miteinander verbunden sind. Durch computergestützte Datenaquise und -verarbeitung wurden in den zwei vergangenen Jahrzehnten empirische Datensätze zu Netzwerkstrukturen zugänglich, deren Größe die zuvor manuell ermittelten Datensätze um Größenordnungen übertrifft. Exemplarisch für diese Entwicklung ist die Zahl der Knoten in Soziologischen Studien zu sehen. Untersucht [Zachary \[1977\]](#) das soziale Netz zwischen 34 Mitgliedern eines Karateclubs und [Klov Dahl \[1985\]](#) das Netzwerk sexueller Kontakte zwischen 40 HIV infizierten Personen, so extrahieren [Ebel et al. \[2002\]](#) das soziale Netz zwischen 6000 Kieler Studenten durch die Analyse ihrer eMail-Kommunikation, und [Palla et al. \[2007\]](#) untersuchen ein Netzwerk von über 4 Millionen Nutzern eines Mobilfunkanbieters.

Viele wissenschaftliche Forschungsgebiete, die zuvor vornehmlich im Bereich der mikroskopischen Wechselwirkungen quantitativ gearbeitet haben, erfahren durch die Anwendung der Graphentheorie eine Analyse ihres makroskopischen

Verhaltens. Den so genannten *Small World Effekt*, von [Milgram \[1967\]](#) in sozialen Netzwerken beschrieben als den Umstand, dass jeder Bewohner der USA mit jedem Anderen im Mittel über eine Kette von ca. 6 Bekanntschaften verbunden ist, finden [Watts und Strogatz \[1998\]](#) in Netzwerken unterschiedlichsten Ursprungs: Im Netzwerk der Neuronen des Wurms *Caenorhabditis elegans*, in der Verbindungsstruktur des Stromnetzes der westlichen USA, und in einem Graphen, der die Zusammenarbeit zwischen Filmschauspielern beschreibt. [Watts und Strogatz](#) definieren den Small World Effekt als das gemeinsame Auftreten enger lokaler Vermaschung (*Clustering*), und eines kurzen mittleren Abstands zwischen den Knoten des Netzes auf globaler Ebene. Wenig später folgt die Entdeckung der skalenfreien, d.h. einem Potenzgesetz folgenden Verteilung der Anzahl der Nachbarn von Knoten in Netzwerken, im Fall des Internets durch [Faloutsos et al. \[1999\]](#), sowie für das World Wide Web durch [Albert et al. \[1999\]](#). Zahlreiche Studien folgen, die sowohl den Small World Effekt, als auch die Skalenfreiheit als Gemeinsamkeit einer Vielzahl unterschiedlichster realer Netze bestätigen. Stellvertretend seien hier soziale Netzwerke (Zitierungen wissenschaftlicher Artikel [Newman \[2001a\]](#) und die bereits erwähnten Email-Netzwerke [[Ebel et al., 2002](#)]), biologische Netzwerke (Interaktionen im Zellstoffwechsel [[Jeong et al., 2000](#), [Wagner und Fell, 2001](#)] und Protein-Protein Wechselwirkungen [[Yook et al., 2004](#)]) und die bereits vorgestellten technologischen Netzwerke erwähnt, weitere Beispiele finden sich in unterschiedlichsten Bereichen von Ökologie bis Ökonomie. Aber auch umgekehrt katalysiert die Entdeckung des Small World Effekts und der Skalenfreiheit in empirischen Netzwerkdaten, die von dem Standardmodell für zufällige Grafen [[Erdős und Rényi, 1960](#)] nicht reproduziert werden, das Interesse und die Weiterentwicklung der Graphentheorie. Die interdisziplinäre Vereinigung von Forschungsgebieten durch die Gemeinsamkeiten der als Netzwerk abstrahierten Strukturen, sowie die Suche nach Erklärungen für deren Emergenz bilden das junge Forschungsgebiet der komplexen Netzwerke. Hier helfen Methoden der Physik, wie Generalisierung und Reduktion auf grundlegende Eigenschaften, die Aufmerksamkeit von implementationspezifischen Details der mikroskopischen Dynamik auf makroskopische Folgen zu lenken. Speziell die Konzepte und Methoden der Statistischen Physik erweisen sich im Umgang mit komplexen Netzwerken als nützlich.

In klassischen Anwendungen der statistischen Physik sind die Wechselwirkungen zwischen den mikroskopischen Bestandteilen durch physikalische Gesetze gegeben. In Systemen deren mikroskopische Wechselwirkungen beeinflusst werden können, sei es weil sie technologischen Ursprungs sind, oder weil sie eine (gewisse) Intelligenz besitzen, ergibt sich eine aufregende Perspektive: Werden die Wechselwirkungen verändert, so kann dies durch die Mechanismen der Emergenz und Selbstorganisation das makroskopische Erscheinungsbild des Systems quantitativ und qualitativ drastisch verändern. Ein physikalisches Beispiel hierfür findet sich in der Perkolation. In der Nähe einer kritischen Dichte können kleine Änderungen der Dichte einen Phasenübergang, z.B. vom Isolator zum Leiter bewirken.

Ein mathematischer Formalismus zur Beschreibung von lokalen, eigenständig

handelnden Entitäten ist die Spieltheorie. Diese beschreibt das Verhalten und die Entscheidungsfindung von Agenten bzw. Spielern, die eigenständig und eigennützig ihr Verhalten, charakterisiert durch ihre Strategie, optimieren. Zunächst zur Beschreibung ökonomischer Vorgänge angewandt [von Neuman und Morgenstern, 1944] entwickelt sich die Spieltheorie zu einem eigenständigen Gebiet der Mathematik [z.B. Nash, 1950, Vega-Redondo, 1996], spieltheoretische Prinzipien werden jedoch auch in der Natur gefunden, wie sie etwa Kerr et al. [2002] in Populationen des Bakteriums *Escherichia coli* beschreiben. In der vorliegenden Arbeit werden Interaktionen zwischen Knoten von Netzwerken durch Spiele im Sinne der Spieltheorie modelliert.

Ein archetypisches Beispiel eines komplexen, selbstorganisierten Systems, gesteuert durch eigennützig handelnde Einheiten, sind Kommunikationsnetzwerke, insbesondere das Internet. Die vorliegende Arbeit zieht jedoch nicht das Internet in seiner Gesamtheit mit allen Details als Beispiel heran, sondern beschränkt sich auf eine höhere organisatorische Ebene des Internets, das so genannte *AS-level*. Das AS-level beschreibt die weltweite Verbindungsstruktur der Internetprovider untereinander.

Für die vorliegende Arbeit wurde aus mehreren Gründen das Internet als Beispielsystem verwendet: Die grundlegende Funktionsweise der Bestandteile (Router und Datenleitungen) ist bekannt, im Gegensatz zu klassischen Systemen der statistischen Physik ist das makroskopische Verhalten jedoch noch nicht grundlegend verstanden. Als weiteren Grund ermöglicht die Tatsache, dass es sich um ein technisches System handelt (wenigstens prinzipiell) ein Eingreifen in die Regeln der mikroskopischen Wechselwirkungen und damit eine Anwendbarkeit gewonnener Erkenntnisse. Des weiteren liegt durch die immense Bedeutung von Kommunikationsnetzen im Allgemeinen und die des Internets im Besonderen für die heutige moderne Gesellschaft die Suche nach Optimierungsmöglichkeiten auf der Hand. Auch wenn das Internet als Beispiel gewählt wird, schränkt dies die Allgemeinheit der Betrachtungen nicht ein, da durch die Abstraktion der Annahmen zum Datenverkehr die Übertragbarkeit auf andere Transportprozesse gewährleistet ist.

In der vorliegenden Arbeit folgt auf eine Einleitung mit Kapitel 2 eine Einführung in die wesentlichen Konzepte der Graphentheorie und die verwendete Notation, zusammen mit der Vorstellung einiger Algorithmen zur Generierung zufälliger Graphen, die verschiedene Charakteristika empirischer Netzwerke reproduzieren. Weiterhin werden drei Projekte vorgestellt, die sich der Sammlung und Archivierung der Verbindungsstruktur des Internets verschrieben haben und deren Daten innerhalb der vorliegenden Arbeit als Referenz verwendet werden. Das Kapitel zur Graphentheorie wird durch die Vorstellung eines eigenen Modells, genannt *geometric-p Modell*, zur Generierung skalenfreier Graphen mit wählbarem Clustering in Kapitel 2.3 abgeschlossen.

Kapitel 3 gibt anhand des *Prisoner's Dilemma* (PD) eine Einführung in die Spieltheorie und erläutert die Verknüpfung von Spieltheorie und Graphentheorie als Modell komplex wechselwirkender vernetzter Systeme. Mit numerischen Untersuchungen zur Reorganisation vernetzter Systeme durch mit dem Netz gekoppelte

Spieldynamik in den Kapiteln 3.3 und 3.4 schließt der einführende Teil zur Graphentheorie. Das Konzept der Reorganisation von Netzwerken durch Kopplung an Spieldynamiken wird durch Kapitel 4 mit einer Variante des Prisoners's Dilemma, dem *Iterated Prisoner's Dilemma* (IPD), wiederaufgenommen. Im Gegensatz zum PD erlaubt das IPD eine Beeinflussung der Reorganisationsdynamik durch kontinuierliche Änderung der Spielparameter und ermöglicht damit eine Optimierung der Spieldynamik in Bezug auf Eigenschaften der emergenten Netzstruktur. Die vorgestellte Art der selbstorganisierenden Netzwerkoptimierung wird exemplarisch für eine von Holme und Ghoshal [2006] vorgeschlagene Quantifizierung der Netzwerkperformanz demonstriert. In Abhängigkeit des gewählten Spielparameters wird im Vergleich zu Zufallsgraphen eine Erhöhung der Performanz um den Faktor 1.2 bis 1.9 erreicht. Eine andere Herangehensweise zu Spielen auf Netzwerken und deren Optimierung wird in Kapitel 5 verfolgt, indem die Kooperativität von PD Spielen auf dem Netz, gemäß Ohtsuki et al. [2006], anhand der *fixation probability* quantifiziert wird. Kapitel 5.2 schlägt Strategien zur individuellen Verteilung von Anreizen vor, die die Kooperativität des Systems in effektiverer Art und Weise zu erhöhen, als dies durch globale Anreize möglich ist und bestätigen die Wirkung durch numerische Simulationen. Die vorgeschlagenen Strategien zur individuellen Anreizverteilung resultieren relativ zur globalen homogenen Verteilung derselben Summe der Anreize zu einer um den Faktor 5 erhöhten Kooperativität.

An die spieltheoretischen Betrachtungen anschließend liegt das Hauptaugenmerk der folgenden Kapitel auf Kommunikationsnetzwerken. Nach der Vorstellung relevanter vorangegangener Arbeiten stellt Kapitel 6 die verwendete Modellierung des Datenverkehrs vor und leitet einen graphentheoretischen Ausdruck für die Performanz (*Throughput Capacity*) entsprechender Kommunikationsnetze her. Kapitel 6.3 untersucht den Einfluss der Netzwerkstruktur, durch Verwendung des in Kapitel 2.3 eingeführten Netzwerkmodells insbesondere des Clusterings, auf die Performanz. Die Optimierung von Netzwerken wird in Kapitel 7 erneut aufgenommen, hier im Rahmen von Kommunikationsnetzwerken mit gegebener Struktur, die eine Optimierung durch intelligente Wahl der benutzten Pfade (*Routing*) ermöglicht. Die Wahl der benutzten Pfade wird durch Assoziation von Gewichten zu Kanten des Graphen erreicht und als Metrik des Netzes bezeichnet. Zusätzlich zu durch andere Arbeiten vorgeschlagenen Metriken, führen die Kapitel 7.4, 7.6 und 7.7 drei weitere Metriken ein, von denen sich zwei, die *Hybrid Metrik* und die *log_{k_ik_j}* Metrik, als äußerst erfolgreich im Sinne einer Optimierung der Throughput Capacity erweisen, was durch ausführliche numerische Simulationen belegt wird. Die Vorteile der hier eingeführten Metriken liegen im Fall der Hybrid Metrik in der unter den verglichenen Metriken besten resultierenden Performanz für Netze mit mehr als 3000 Knoten, mit einer mittleren Steigerung um den Faktor 7 im Vergleich zur Performanz ohne Metrik. Für Netze mit bis zu 3000 Knoten erreicht die von Danila et al. [2006b] vorgestellte Metrik zwar eine leicht höhere Performanz, sie ist jedoch wegen ihrer extremen numerischen Anforderungen für größere Netze nicht anwendbar. Im Falle der *log_{k_ik_j}* Metrik ist die numerische Komplexität vernachlässigbar, dieser Vorteil an vermindertem numerischen Aufwand wird jedoch durch

eine leichte Reduktion des Performanzgewinns erkaufte, nichtsdestotrotz bewirkt auch diese Metrik eine mittlere Performanzsteigerung um den Faktor 5 und erreicht damit die Größenordnung der Hybrid Metrik.

Die drei in der vorliegenden Arbeit verfolgten Ansätze zur Charakterisierung und Optimierung vernetzter Systeme betrachten hochgradige Idealisierungen realer Systeme. Dies resultiert jedoch nicht in einer Beschränkung der Allgemeinheit, im Gegenteil, die Abstraktion ermöglicht den Transfer der Methoden und Ergebnisse auf weiterführende Anwendungen.

So legt schon die Sprache der Spieltheorie auf Netzwerken, die Knoten mit Spielern assoziiert die Verbindung zu sozialen Netzen nahe. Aber obwohl soziale Netze tatsächlich die Inspiration für die vorliegenden Untersuchungen gaben, sind Anwendungen auf viele andere Systeme denkbar. Betrachtet man beispielsweise zelluläre Stoffwechsel oder Protein-Netzwerke, deren mikroskopische Wechselwirkungen von den Gesetzen der Biochemie bestimmt werden, so ist eine globale Änderung der Spielparameter, wie in Kapitel 4 untersucht, vergleichbar mit unspezifisch wirkenden chemischen Stoffen. Noch prägnanter ist die Ähnlichkeit zu der individuellen Verteilung von Anreizen in Kapitel 5, die im Kontext biochemischer Netzwerke der gezielten Wirkung von Medikamenten auf spezifische Proteine entspricht. In beiden Fällen ist der Einfluss von Änderungen der mikroskopischen Wechselwirkung auf die emergenten Eigenschaften, hier das Verhalten der Zelle, von Interesse. Für solche und ähnliche Untersuchungen bieten die vorgestellten abstrakten Methoden einen Rahmen für ähnliche Optimierungsansätze.

Ähnliches gilt für die Betrachtungen zur Optimierung von Kommunikationsnetzen. So gelten die vorgestellten Ansätze für jeglichen Transport von unterscheidbaren Gütern mit definiertem Ausgangsort und Ziel und können daher generell auf vielfache logistische Probleme angewandt werden. Ein Beispiel hierfür mag der Straßenverkehr sein, wo Gewichte auf Verbindungen durch Ampeln und Geschwindigkeitsbegrenzungen realisiert werden können, oder innerhalb der Software von Navigationsgeräten eingesetzt werden können.

Selbstverständlich ist die Untersuchung detaillierterer und realistischerer Systeme von ebenso großem Interesse, da durch die zum Teil hohe Sensitivität der emergenten Phänomene auf Änderungen der mikroskopischen Wechselwirkungen ein Einfluss implementationsspezifischer Details zu erwarten ist. Aber auch für diese Fälle bietet die hier vorgestellte Methodik einen Rahmen und eine Einschätzung der prinzipiellen Möglichkeiten verteilter, selbstorganisierender Ansätze. Dies bringt uns zu vielen denkbaren Möglichkeiten der Fortsetzung und Vertiefung der vorliegenden Arbeit. Naheliegend ist eine Anwendung der spieltheoretischen Ansätze auf ökonomische Systeme, in denen der Gewinn oder Verlust eines Spielers sich direkt monetär darstellt, das verwendete Spiel aber sicherlich ein Spiel mit unvollständiger Information wäre. Eine weitere hochinteressante theoretische Studie im Bereich der Netzwerkmetriken stellt die Anwendung von Metriken nicht nur zur Erhöhung der Performanz, sondern für eine Steigerung der Ausfallsicherheit, beispielsweise gegenüber Kaskadeartigen Ausfällen in vereinfachten Stromnetzmodellen dar. Für eine solche Anwendung stellt insbesondere die $\log k_i k_j$ Metrik

German summary

einen interessanten Kandidaten dar, da sie durch ihre geringe numerische Komplexität Reaktionen auf Ausfälle von Netzwerkkomponenten innerhalb kürzester Zeiträume ermöglichen kann.

1. Introduction

In nature, society and technology many disordered systems exist, that show emergent behavior, where the interaction of numerous microscopic agents result in macroscopic, systemic properties, that may not be present on the microscopic scale. Examples include phase transitions in magnetism and percolation, for example in porous unordered media, biological, and social systems. Also technological systems that are explicitly designed to function without central control instances, like their prime example the Internet, or virtual networks, like World Wide Web, which is defined by the hyperlinks from one web page to another, exhibit emergent properties.

A common theme of many of these systems is the ubiquity of networked structures, that are neither strictly regular lattices, nor completely random, but show organization principles beyond the rules that apply on the individual's level. The mathematical framework for the description of networks is graph theory, in hindsight founded by Euler [1736] and an active area of research in pure mathematics [Erdős and Rényi, 1960, Bollobás, 1985, 1998] since then.

Applied graph theory flourished through the advent of large scale data set, made accessible by the use of computers. The availability and tractability of these data sets ignited the application of graph theory to new scientific disciplines. The increasing size of the investigated data sets is especially pronounced in mathematical sociology, where the size of the empirical data sets increased from a network of 40 HIV infected persons studied by Klovdahl [1985], over the email contacts between approximately 6000 students analyzed by Ebel et al. [2002], to the data acquired by Palla et al. [2007], which covers a network of over 4 million mobile phone users.

Many fields, that employed quantitative analysis only on the microscopic level, experienced quantitative, graph theoretic analysis on a coarse grained, system level. The small world effect described by Milgram [1967] for social networks, has been found to be the rule, rather than the exception by Watts and Strogatz [1998], who discovered small-world structure in the neural network of the worm *Caenorhabditis elegans*, the power grid of the western United States, and a collaboration graph of film actors. The discovery of the small world effect was followed by the discovery of a scale-free degree distribution in the Internet by Faloutsos et al. [1999] and the World Wide Web by Albert et al. [1999]. Many successive studies confirmed numerous networks in nature that exhibit the small world effect and scale-free degree distributions. These networks include social networks (e.g. citation networks Newman [2001a] and email networks [Ebel et al., 2002]), biological networks (e.g. metabolic networks [Jeong et al., 2000, Wagner and Fell, 2001] and protein interaction networks [Yook et al., 2004]), the previously mentioned technologi-

1. Introduction

cal networks, and various other networks found across scientific disciplines from ecology to economy. The study of the common network characteristics found in previously seemingly unrelated fields of science and the urge to explain their emergence, form a scientific field in its own right, the science of complex networks. In this field, methodologies from physics, leading to simplification and generalization by abstraction, help to shift the focus from the implementation's details on the microscopic level to the macroscopic, coarse grained system level. By describing the macroscopic properties that emerge from microscopic interactions, statistical physics, in particular stochastic and computational methods, has proved to be valuable tools in the investigation of such systems.

While for classical subjects of statistical physics, the interactions of the basic constituents at the microscopical level are defined by physical constraints, the investigation of systems based on man-made basic constituents offers a thrilling new possibility: If the constituents of a system are man-made, then their rules of interaction can be changed by the implementer. Through the mechanisms of self-organization, the (perhaps tiny) changes on the microscopical level may propagate to the macroscopic scale and result in qualitatively different behavior there. A prominent example for a physical system that presents similar sensitivity in its macroscopic behavior to changes on the microscopical level is percolation, where small modifications of the density around a critical density results in a phase transition of the material, for example from insulator to conductor.

As paradigm for microscopic interactions among entities that locally optimize their behavior to increase their own benefit is game theory, the mathematical framework of decision finding. With first applications in economics [e.g. [von Neuman and Morgenstern, 1944](#)], game theory is an approved field of mathematics [e.g. [Nash, 1950](#), [Vega-Redondo, 1996](#)], however there are systems found in nature, that exhibit typical game theoretic behavior, for example populations of the bacterium *Escherichia coli*, discovered by [Kerr et al. \[2002\]](#). In the present work, game theory is used to model the interaction of selfish agents that form networks.

The archetypal example of a complex, self organized system, governed by selfish, local rules, that is used frequently in the present work, are communication networks, in particular their most prominent instance, called the Internet. In this work, the Internet will not be treated on its most detailed level, but instead on the so called AS-level, which represents a coarse grained organizational level of the network structure. The Internet is chosen as the example system for several reasons. First it displays a classical parallel to systems subject to classical statistical physics. Its microscopic constituents are (in principle) well known and understood (obviously, as its constituents are man-made). In contrast to classical statistical physics, the properties on the macroscopic scale are not yet well understood. As a second reason, the fact that it's constituents are man-made plays another important role, as for example newly discovered rules can (at least in principle) be applied to the system, yielding a rather direct applicability of gained insights. As a third reason, the humongous importance of communication networks in general, and the Internet in particular, for our modern way of life, makes the importance of possible means of

optimization apparent for both the lay man and the expert. Although the Internet is used as an example, the assumptions made for the transported entities, in the case of the Internet data packets, and the transport mechanisms are rather general, to assure that other transport processes could be treated as well.

The present work is laid out as follows: Chapter 2 reviews the basic notation and facts of graph theory, presents several algorithms that allow to create random graphs, that reproduce stylized facts of empirical graphs, and presents three projects, that are dedicated to measure the connectivity structure of the Internet, along with their data sets. The presentation of existing models of networks is accompanied by the proposition of a new network model, which will be used in the later chapters of the present work, in Section 2.3. The review of graph theory is followed by the analog endeavor for game theory in Chapter 3. Using the famous prisoners dilemma as an example, basic game theoretical concepts like the Nash equilibrium and how these are merged with graph theory to what we call games on graphs are described. This review is then rounded off by a numerical study of games that reshape the network structure in a self-organizing way in Sections 3.3 and 3.4. To allow for more sophisticated dynamics of reshaping, Chapter 4 proposes to couple a variant of the prisoner's dilemma, the iterated prisoner's dilemma, to the network structure and thoroughly investigates its influence on the emergent topologies. Chapter 5 approaches the subject of games on graphs from another perspective. Here a static network structure is assumed, and strategies of incentive distribution and their ability to enhance cooperative behavior of the agents is investigated. The game theory centered studies are followed by investigations that focus on communication networks, starting in Chapter 6 with a review of previous work on communication networks and the derivation of a graph theoretical estimate for the performance of a communication network, the throughput capacity. This Chapter is topped off by the investigation of the network structure's influence on the throughput capacity, using the graph model proposed in Section 2.3. The usage of weights to influence the paths chosen for packets in communication networks, known as metrics of networks, is the focus of Chapter 7. Here the concept of metrics in concert with communication networks, along with some well known metrics is reviewed. Following this, Sections 7.4, 7.6 and 7.7 introduce three new metrics, two of which turn out to be very successful with respect to the enhancement of networks transport capacity, as verified by thorough numerical investigations. A summary, concluding remarks, and an outlook to interesting possibilities for continuation and extensions of the present work's concepts is given in Chapter 8.

2. Brief Résumé of Graph Theory

The mathematical framework to formally describe and study the structure of networks is graph theory. Other than the term *network*, which refers to the connectivity structure and further properties of the vertices and edges, that then are called nodes and links, a *graph* solely describes the connectivity structure. Nevertheless, the terms *graph* and *network*, and even more frequently *vertex* and *node*, and *edge* and *link* are used synonymously in the network literature, since the risk of ambiguities is small.

2.1. Graph Theory notation

This section gives a short résumé of graph theory, introducing the notation used in the present work, which mainly sticks to the conventions of [Bollobás \[1998\]](#) and [Diestel \[2005\]](#), two excellent textbooks on graph theory.

A *graph* \mathcal{G} is an ordered pair $\mathcal{G} = (\mathcal{V}, \mathcal{E})$ of the sets of *vertices* \mathcal{V} and *edges* \mathcal{E} . The vertex set of a graph \mathcal{G} is referred to as $\mathcal{V}(\mathcal{G})$, its edge set as $\mathcal{E}(\mathcal{G})$. The *order* of a graph is the number of vertices $N = |\mathcal{V}(\mathcal{G})|$, the number of edges $M = |\mathcal{E}(\mathcal{G})|$ is called the *size* of \mathcal{G} . Indices or arguments of expressions, that indicate the corresponding graph may be omitted, if the correspondence is clear from the context, for example the vertex set may be referred to as \mathcal{V} instead of $\mathcal{V}(\mathcal{G})$.

The elements of $\mathcal{E} \subseteq \mathcal{V}^2$ are the graph's edges and two vertices $a, b \in \mathcal{V}$ are *joined* by an edge e_{ab} if $e_{ab} := (a, b) \in \mathcal{E}$. Vertices that are joined by an edge are said to be *adjacent*. Generally the graphs considered in the present work are undirected graphs, the edge e_{ab} has no direction, i.e. the order of vertices in an edge is of no relevance, $e_{ab} = e_{ba}$. The *neighborhood* of a vertex $a \in \mathcal{V}$ is the set of vertices

$$\mathcal{N}(a) := \{b \in \mathcal{V} : e_{ab} \in \mathcal{E}\} \quad (2.1)$$

that are connected to a by an edge. The number of neighbors of a vertex a defines its *degree*

$$k_a := |\mathcal{N}(a)|. \quad (2.2)$$

If all vertices of a graph \mathcal{G} have the same degree $\forall a \in \mathcal{V}(\mathcal{G}) : k_a = k$, the graph is a *regular graph*. We define the *edge neighborhood* of an edge e_{ab} as the set

$$\mathcal{L}(e_{ab}) := \{e_{ij} \in \mathcal{E} : |\{a, b\} \cap \{i, j\}| = 1\} \quad (2.3)$$

2. Brief Résumé of Graph Theory

of edges, that have one common vertex with e_{ab} . Analogous to the vertex degree, we define the *edge degree*

$$\ell_{e_{ab}} := |\mathcal{L}(e_{ab})| = k_a + k_b - 2. \quad (2.4)$$

The *line graph* $\widehat{\mathcal{G}}(\mathcal{G})$ of a graph \mathcal{G} is a graph, whose vertices $\widehat{\mathcal{V}}(\widehat{\mathcal{G}})$ are given by the set of edges of \mathcal{G} : $\widehat{\mathcal{V}}(\widehat{\mathcal{G}}) = \mathcal{E}(\mathcal{G})$. Two vertices $i, j \in \widehat{\mathcal{V}}$ in the line graph are connected by an edge $e_{ij} \in \widehat{\mathcal{E}}$, if and only if the corresponding edges i and $j \in \mathcal{E}$ have exactly one common vertex in \mathcal{V} . Using the identity of $\widehat{\mathcal{V}} = \mathcal{E}$ edge related properties of \mathcal{G} can be related to vertex properties of $\widehat{\mathcal{G}}$, e.g. $\mathcal{N}^{\widehat{\mathcal{G}}}(i) = \mathcal{L}^{\mathcal{G}}(i)$.

It is often convenient, to write graph theoretic expressions in a algebraic way using matrices, instead of using the set theoretic notation. The most important matrix in this respect is the *adjacency matrix* $A(\mathcal{G})$ of a graph. It is an $N \times N$ matrix with the elements

$$a_{ij} = \begin{cases} 1 & \text{if } e_{ij} \in \mathcal{E}(\mathcal{G}). \\ 0 & \text{else.} \end{cases} \quad (2.5)$$

For example, the degree of a vertex can be calculated from the adjacency matrix by column-wise summation $k_i = \sum_{j=1}^N a_{ij}$.

A graph $\mathcal{G}'(\mathcal{V}', \mathcal{E}')$ is a *subgraph* of $\mathcal{G}(\mathcal{V}, \mathcal{E})$ if $\mathcal{V}' \subseteq \mathcal{V}$ and $\mathcal{E}' \subseteq \mathcal{E}$, alternatively denoted by the shorthand notation $\mathcal{G}' \subseteq \mathcal{G}$. A *path* $\mathcal{P}(\mathcal{V}_{\mathcal{P}}, \mathcal{E}_{\mathcal{P}}) \subseteq \mathcal{G}$ is a subgraph with $\mathcal{V}_{\mathcal{P}} = \{v_0, v_1, \dots, v_l\}$ and $\mathcal{E}_{\mathcal{P}} = \{(v_0, v_1), (v_1, v_2), \dots, (v_{l-1}, v_l)\}$ such, that the vertices v_i are all distinct. Note, that from demanding distinct vertices, it follows immediately, that the edges of a path are distinct as well. The vertices v_0 and v_l are the path's *endvertices*. Although in principle a path has no direction, sometimes it is necessary to specify, that a path \mathcal{P} is traversed from v_0 to v_l . In that case v_0 will be referred to as the *initial* and v_l as the *terminal* vertex of \mathcal{P} . The set of all paths in a graph \mathcal{G} is denoted as $\text{paths}(\mathcal{G})$. With

$$\text{paths}(s, t) := \{\mathcal{P} \in \text{paths}(\mathcal{G}) : s = v_0 \wedge t = v_l\} \quad (2.6)$$

we denote the set of all paths from vertex s to vertex t . The *length* of a path $\mathcal{P} \in \text{paths}(\mathcal{G})$ is the number of edges contained in the path

$$\text{length}(\mathcal{P}) := |\mathcal{E}(\mathcal{P})|. \quad (2.7)$$

An important subset of the set of all paths from s to vertex t is the set of *shortest paths*

$$\text{spaths}(s, t) := \underset{\mathcal{P} \in \text{paths}(s, t)}{\text{arg min}} (\text{length}(\mathcal{P})). \quad (2.8)$$

The length of the shortest paths defines the *distance*

$$d(s, t) := \min_{\mathcal{P} \in \text{paths}(s, t)} (\text{length}(\mathcal{P})) \quad (2.9)$$

of two vertices. If there is no path connecting s and t , $\text{paths}(s, t) = \emptyset$, the distance $d(s, t) := \infty$ is set to infinity.

A graph \mathcal{G} is *connected*, if for every pair of its vertices a and b , a path \mathcal{P} exists, that connects the vertices, $\text{paths}(a, b) \neq \emptyset$. If for a connected subgraph $\mathcal{G}' \subseteq \mathcal{G}$ the neighborhoods of each vertex in \mathcal{G}' and \mathcal{G} are identical $\forall a \in \mathcal{V}(\mathcal{G}') : \mathcal{N}'(a) = \mathcal{N}(a)$, then the subgraph is a *maximal connected subgraph*, called a *component*. The component of a graph with the maximal number of vertices is the *giant component*.

A *cycle* of length l is a subgraph $\mathcal{C} \subseteq \mathcal{G}$ with $\mathcal{V}(\mathcal{C}) = \{v_1, \dots, v_l\}$ such that there exists a path $\mathcal{P} \subseteq \mathcal{C}$ with $\mathcal{V}(\mathcal{P}) = \{v_1, \dots, v_l\}$, $e_{v_1 v_l} \in \mathcal{E}(\mathcal{C})$, and $e_{v_1 v_l} \notin \mathcal{E}(\mathcal{P})$. Cycles of length $l = 3$ are *triangles*. A graph without cycles is a *forest* and a connected forest is a *tree*, in other words: if every component of a graph is a tree, then it's a forest.

The properties of graphs introduced up to here are mainly in the form of predicates, for example “Graph \mathcal{G} is a cycle”, and the like. There are, however, many important properties of graphs that quantify the nature of a graph. Instead of being the subject of pure graph theory, these properties, tend to be used mainly by branches of science that apply graph theory as a tool of investigation, e.g. social sciences, biology, and neuro science. Maybe it is the binding region between the applications of graph theory and pure graph theory, that is best described as the statistical physics of complex networks. Exhaustive reviews of this field include [Albert and Barabási \[2002\]](#), [Newman \[2003\]](#), and [Dorogovtsev and Mendes \[2003\]](#).

Here we introduce but a few of the most prominent quantitative properties of vertices and edges that are used in the following chapters. A property of a vertex, quantified by a map $\mathcal{V} \mapsto \mathbb{R}$ from vertex space to the real numbers is called a *vertex centrality*, or short *centrality*. Similarly, an *edge centrality* is determined by a map $\mathcal{E} \mapsto \mathbb{R}$. Often there is a straight forward generalization of a vertex centrality to a corresponding edge centrality, or vice versa. For a thorough collection of centralities see [Koschützki et al. \[2005\]](#).

The perhaps most trivial centrality is the *degree centrality* k_i of a vertex i , usually simply called the *degree*, which has already been introduced in Equation (2.2). Its counterpart, the *edge degree centrality* ℓ_e , short *edge degree*, has been defined in Equation (2.4). A more involved centrality is the *clustering coefficient* \mathbb{C}_i of a vertex i . In the language of social networks, where people and social interactions among them, e.g. friendships, are represented by vertices and edges, it quantifies how likely it is, that two of your friends are friends as well. It is defined as the ratio

$$\mathbb{C}_i = \frac{|\{\forall e_{ab} \in \mathcal{E}(\mathcal{G}) : a, b \in \mathcal{N}(i)\}|}{\frac{1}{2}k_i(k_i - 1)} \quad (2.10)$$

of connections between the k_i neighbors of a vertex i and the maximal number of connections among k_i vertices. This definition is the same as taking the ratio of the number of triangles that contain i and the number of paths of length 3 with i as the central vertex.

An example of a centrality that does not only depend on the immediate neighborhood of a vertex, like the degree and the clustering coefficient, but on the whole

2. Brief Résumé of Graph Theory

component the vertex is located in, is the so called *closeness*. For a connected graph \mathcal{G} the closeness of a vertex i is defined as

$$c_i = \sum_{j \in \mathcal{V}(\mathcal{G})} \frac{1}{d(i, j)}. \quad (2.11)$$

[Holme and Ghoshal \[2006\]](#) define a variant of closeness, that normalizes the closeness of a vertex by its degree:

$$s_i = \frac{c_i}{k_i}. \quad (2.12)$$

Another commonly used, non-local centrality is the *betweenness centrality* introduced by [Freeman \[1977\]](#) in the context of social networks. It quantifies the centrality of a vertex $v \in \mathcal{V}$ by the amount of shortest paths that contain the vertex.

$$b_v := \sum_{i, j \in \mathcal{V}} \frac{|\{\mathcal{P} \in \text{spaths}(i, j) : v \in \mathcal{V}(\mathcal{P})\}|}{|\text{spaths}(i, j)|}. \quad (2.13)$$

The betweenness centrality of an edge $e \in \mathcal{E}$ is defined analogously:

$$b_e := \sum_{i, j \in \mathcal{V}} \frac{|\{\mathcal{P} \in \text{spaths}(i, j) : e \in \mathcal{E}(\mathcal{P})\}|}{|\text{spaths}(i, j)|}. \quad (2.14)$$

The sums in these definitions account for the number of shortest paths that contain the vertex or edge, respectively. If there are multiple shortest paths between a pair of vertices $i, j \in \mathcal{V}$ and a vertex or edge is only part of a subset of the shortest paths, the contribution in the corresponding term is normalized by the number of shortest paths $|\text{spaths}(i, j)|$. This normalization is due to the idea, that if a vertex or edge is central because it is situated on a shortest path, then it is considered less central if there are alternative shortest paths that do not contain it.

Instead of discussing the values of a centrality C itself, often the probability distribution of the centrality $p(C)$ is investigated, which denotes the probability of a randomly chosen vertex i to have centrality $C(i)$. The most prominent example is clearly the *degree distribution*

$$p(k) := \frac{|\{i \in \mathcal{V} : k_i = k\}|}{|\mathcal{V}|}, \quad (2.15)$$

that is often written as p_k .

Using global averages of centralities

$$\langle C_{\mathcal{V}} \rangle := \frac{1}{|\mathcal{V}|} \sum_{i \in \mathcal{V}} C(i) \quad (2.16)$$

allows to condense centralities into a single number. Global average graph properties that will be used in the present work include the *average degree*

$$\langle k \rangle := \frac{1}{|\mathcal{V}|} \sum_{i \in \mathcal{V}} k_i \quad (2.17)$$

$$= 2 \frac{|\mathcal{E}|}{|\mathcal{V}|}, \quad (2.18)$$

the average clustering coefficient $\langle \mathbb{C} \rangle$, average closeness $\langle c \rangle$, [Holme and Ghoshal's](#) variant of average closeness $\langle s \rangle$, and the average distance

$$\langle d \rangle = \frac{1}{N(N-1)} \sum_{i,j \in \mathcal{V}} d(i,j). \quad (2.19)$$

Although here the discussion of distributions and global averages has been shown for vertex-based centralities, the same is of course possible for edge-based centralities, by replacing \mathcal{V} with \mathcal{E} in the definitions.

As the degree is the most basic quantitative property of a vertex, it is commonly used to condition other observables to get an observable of a functional form, for example the degree dependent clustering coefficient

$$\mathbb{C}(k) := \langle \mathbb{C}_i | k_i = k \rangle, \quad (2.20)$$

which is read as the average clustering coefficient of vertices, given the degree is k .

[Erdős and Rényi \[1960\]](#) proposed a simple model of a random graph, the *ER-graph*. Generation of an ER-graph is done in the following way: Take a constant number of vertices N and connect each pair of vertices with probability p . The number maximal number of edges in a graph is $N(N-1)/2$. If each of these edges is present with probability p , the expectation value for the total number of edges is

$$\langle M \rangle = p \frac{N(N-1)}{2}. \quad (2.21)$$

As the presence or absence of edges is independent, the degree distribution, see Equation (2.2), is binomial

$$p(k) = \binom{N-1}{k} p^k (1-p)^{N-1-k}. \quad (2.22)$$

In the limit $N \rightarrow \infty$ and $p(N-1) = \langle k \rangle$, the distribution $p(k)$ takes the form of a Poisson distribution

$$p(k) \simeq \frac{\langle k \rangle^k}{k!} e^{-\langle k \rangle}, \quad (2.23)$$

2. Brief Résumé of Graph Theory

hence ER-graphs are usually called *Poissonian graphs*. The standard deviation of k is $\sigma = \sqrt{\langle k \rangle}$, so most of the nodes have a degree close to the average.

The average path length $\langle d \rangle$ of Poissonian graphs can be estimated [see e.g. [Newman, 2003](#)] as $\langle d \rangle = \frac{\log N}{\log \langle k \rangle}$. Let for example a random graph consist of 10000 vertices with an average number of $\langle k \rangle = 10$ neighbors, then the average distance between two randomly chosen vertices is only $\langle d \rangle = 4$, a surprisingly small number. Also the cluster coefficient \mathbb{C}_i as defined in Equation (2.10) is easily derived for Poissonian graphs. Vertex i has k_i neighbors which can be connected by a maximum of $k_i(k_i - 1)$ edges. On average $pk_i(k_i - 1)$ of these edges are present, hence

$$\mathbb{C}_i = \frac{pk_i(k_i - 1)}{k_i(k_i - 1)} = p = \frac{\langle k \rangle}{N}, \quad (2.24)$$

which, for constant $\langle k \rangle$, lets $\mathbb{C}_i \rightarrow 0$ for $N \rightarrow \infty$.

2.2. Empirical networks and network models

To compare results of graph theoretical considerations with networks found in nature, data on these networks has to be gathered. Historically, this had been a tedious task and data acquisition had been confined to small data sets, for example the network of sexual contacts of 40 HIV infected persons, collected by [Klovdahl \[1985\]](#). About a decade ago, aided by the computerization of data collection, information on large scale networks became available. Connectivity of the Internet was investigated by [Faloutsos et al. \[1999\]](#), connectivity of the World Wide Web through hyperlinks from homepage to homepage by [Albert et al. \[1999\]](#). Data on social networks of increasing size became available among others through the work of [Newman \[2001a,b\]](#) (scientific cooperation networks) and [Ebel et al. \[2002\]](#) (email network among users of the university of Kiel). Investigated biological networks include metabolic networks [[Jeong et al., 2001](#)] and protein interaction networks [[Yook et al., 2004](#)]. The necessity of automated data acquisition is especially evident for the network of 4 million mobile phone users by [Palla et al. \[2007\]](#).

Several projects (e.g. ROUTE VIEWS [[University of Oregon, 2001](#)], NETDIMES [[Shavitt and Shir, 2005](#)], and CAIDA [[CAIDA Macroscopic Topology Project Team, 2000–2006](#)]) have been monitoring the Internet's structure during the current decade. This is achieved using different techniques, ranging from distributed traceroute scans¹ to extraction of routing tables from a set of routers [see e.g. [Krioukov et al., 2007](#)]. Chapters 6 and 7 of the present work use the publicly available connectivity information of the Internet provided by the above projects to demonstrate the effectiveness the traffic optimization proposed in those chapters. Specifically the following snapshots of connectivity data are used:

¹Traceroute is a standard computer program available in practically every UNIX-like operating system. It determines the route of a data packet in an Internet Protocol (IP) network in a stepwise fashion.

ROUTEVIEWS	weekly snapshots, Mar–May 2001
NETDIMES	monthly snapshots, Oct 2004–Dec 2005
CAIDA	monthly snapshots, 2000–2006

For the size of the giant component and the average degree of these snapshots, see Table A.1 in the Appendix. These Internet scans represent the Internet’s structure on the level of autonomous systems, the AS-level. An AS is a set of Internet routers under the control of a single technical administration, using an interior protocol to route traffic within the AS, and an exterior gateway protocol to route traffic to other ASs [Rekhter and Li, 1995].

2.2.1. Small world graphs

In their seminal article Watts and Strogatz [1998] show that the neural network of the worm *Caenorhabditis elegans*, the power grid of the western United States, and the collaboration graph of film actors exhibit a property, that cannot be reproduced by Erdős and Rényi’s model of random graphs. These graphs have, like the Poissonian graphs, a small average distance, but in contrast to the former, a large clustering coefficient, similar to regular grids. For the simultaneous occurrence of high clustering and short distances, the authors coined the name *small world*, inspired by Milgram [1967]. As a model that is able to reproduce this behavior Watts and Strogatz [1998] propose a model that is able to interpolate between regular grids and Poissonian graphs.

Construction of the model is done by starting from a regular graph, for example a ring or a two dimensional grid. Every edge of the initial graph is then rewired with a probability p , i.e. removed from the graph and reinserted between two random vertices. For probability $p = 0$ the outcome is obviously simply the initial regular graph with high clustering and long average path lengths, while for $p = 1$ the result is a Poissonian graph without clustering but with short paths. However, between these extremes is a regime that shows the small world characteristic. Figure 2.1 illustrates a few first steps of the rewiring process. For small p the

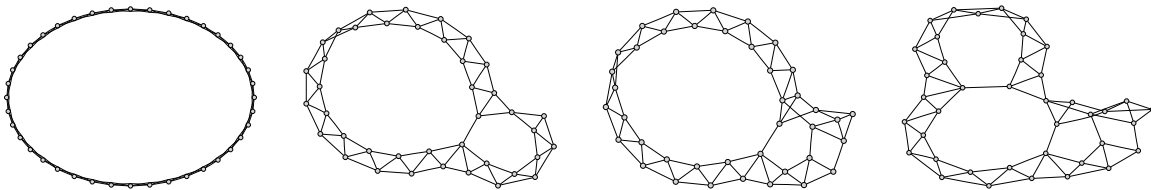


Figure 2.1.: Random rewiring of a regular network. From left to right random links of a ring network of average degree $\langle k \rangle = 4$ are rewired. This leads to small world characteristics of the generated network.

network essentially stays close to the regular network, for $p = 1$ all links are rewired, thus the emerging network is a Poissonian network. Choosing the value

2. Brief Résumé of Graph Theory

of p allows an interpolation between the regular lattice and the completely random Poissonian network. The effect of rewiring links with an increasing probability

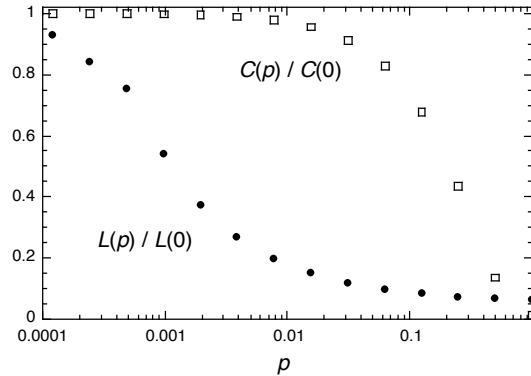


Figure 2.2.: Change of average cluster coefficient and average path length in dependence on the rewiring probability p . With an increasing rewiring probability p the cluster coefficient $C(p) := \langle \mathcal{C} \rangle(p)$ and the average path length $L(p) := \langle d \rangle$ both decrease. However, the average path length decreases rapidly already at small values of $p \lesssim 0.001$, while the clustering coefficient sustains the large value typical for regular grids up to $p \approx 0.1$. The plot shows values averaged over an ensemble of 20 realizations of graphs with $N = 1000$ vertices and an average degree $\langle k \rangle = 10$. Figure from [Watts and Strogatz \[1998\]](#).

p on the cluster coefficient and the average path length is shown in Figure 2.2. With increasing p the average path length drops rapidly to sizes comparable with Poissonian networks. However, for $p \approx 0.1$ the cluster coefficient $\langle \mathcal{C} \rangle$ is still almost as large as for the regular network.

2.2.2. Scale-free graphs

Following the discovery of the apparent ubiquity of the small world property in natural networks, [Faloutsos et al. \[1999\]](#), [Albert et al. \[1999\]](#), and [Barabási and Albert \[1999\]](#) found another property of natural networks, that is neither reproduced by Poissonian graphs, nor by small world graphs as proposed by [Watts and Strogatz \[1998\]](#). Unlike Poissonian graphs, the investigated networks show a degree distribution p_k , see Equation (2.15), that is not peaked around its mean value $\langle k \rangle$, but, at least for large k , follows a power law of the form

$$p_k := p(k) \sim k^{-\gamma}. \quad (2.25)$$

Graphs whose degree distribution follows a power law are called *scale-free graphs*.

Subsequent studies, partly already mentioned above, found scale-freeness of degree distributions to be similarly ubiquitous as the small world property [see

e.g. [Albert and Barabási, 2002](#), [Dorogovtsev and Mendes, 2003](#), [Newman, 2003](#)]. Although it is possible to construct a graph that is scale-free, for example using the *configuration model*,² this fails to offer an explanation of the underlying mechanisms that generate the scale-free degree distributions. [Barabási and Albert \[1999\]](#) propose two basic principles to be responsible for the emergence of scale free graphs in nature: growth and preferential attachment. Growth of the network is realized by starting from an initial seed of m_0 connected vertices and subsequent addition of new vertices, that are connected to $m \leq m_0$ already existing vertices. When connecting to the existing vertices, preferential attachment enters the game. The vertices to connect to are selected randomly with a probability $p \sim k$ proportional to their current degree. Figure 2.3 shows a few first steps of a growing a BA-network. In the limit $k \gg m$ it approaches a scale-free distribution $p_k \sim k^{-\gamma}$, with $\gamma = 3$ and an average degree $\langle k \rangle = 2m$.

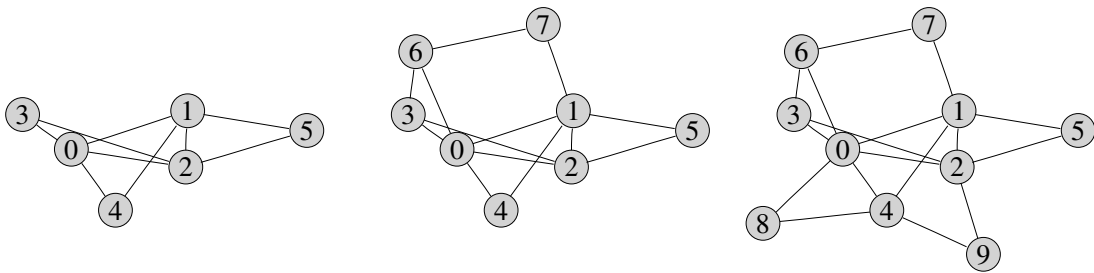


Figure 2.3.: Growth Process of a BA-network. The figure shows the growth of a BA-network with $m = 2$ at three different time steps $t = 3$, $t = 5$, and $t = 7$ of the growth process. The vertex labels denote the sequence of vertex addition. Vertices 0, 1, and 2 are the initial seed of m_0 connected vertices.

The model put forward by [Barabási and Albert \[1999\]](#) emphasizes the importance of growth and preferential attachment for the emergence of a scale-free degree distribution. However, even those real world networks that have the same scale-free exponent $\gamma = 3$ differ from the graphs generated by the BA-model significantly in other graph theoretic observables, which is exemplified in Figure 2.4 by comparing the average clustering coefficient $\langle \mathbb{C} \rangle$ of the CAIDA Internet graphs with clustering coefficients of BA networks with average degree $\langle k \rangle$ and graphs generated by the configuration model with the same scale-free exponent $\gamma = 2.22$. To generate for example graphs that have similar properties as the measured graphs of the Internet on AS-level, depending on the desired accuracy of matching certain observables, there is more than a handful of graph generator to choose from, see e.g. [Jin et al. \[2000\]](#), [Medina et al. \[2000\]](#), [Chang et al. \[2003, 2004\]](#), [Li et al. \[2004\]](#), [Zhou and](#)

²The configuration model is a method to construct graphs with arbitrary degree distributions p_k . It is described in detail in Section 2.3, where a generalization is proposed, that allows to tune the clustering coefficient.

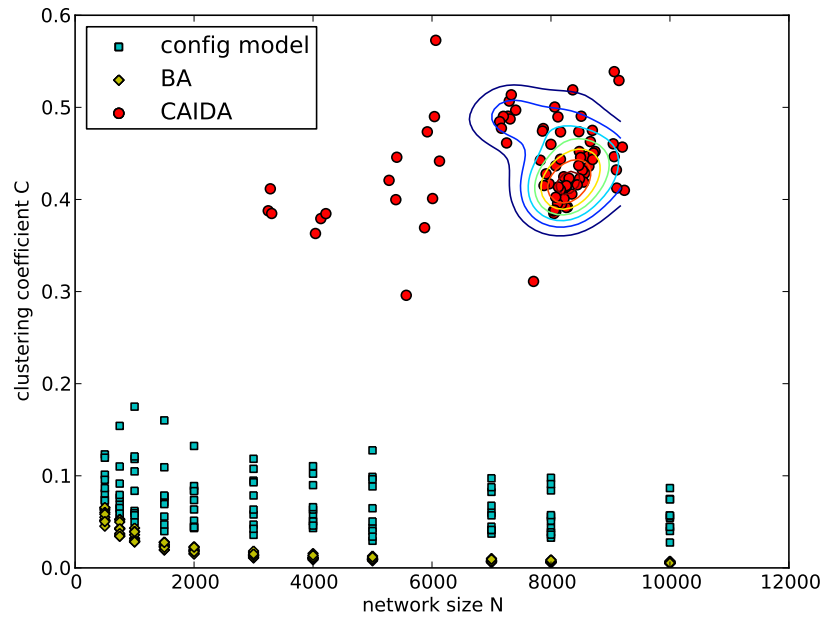


Figure 2.4.: Average clustering coefficient $\langle \mathcal{C} \rangle$ vs. number of vertices N of CAIDA Internet snapshots compared with BA networks and networks generated using the configuration model. The colored lines highlight the region where most of the CAIDA networks are situated.

Mondragon [2004], Krioukov et al. [2007]. A dedicated generator for synthetic AS-level Internet topologies that will be used in Chapter 7 of the present work, is proposed by Zhou and Mondragon [2004]. Based on a nonlinear preferential attachment process, the positive-feedback preference (PFP) model is able to reproduce the degree distribution, the average clustering coefficient $\langle \mathcal{C} \rangle$ and other structural features of the Internet scans like rich-club connectivity, short cycles, disassortative mixing, and betweenness centrality [e.g. Newman, 2003].

2.3. Geometric- p model

From Figure 2.4 we learn, that properties of real Internet scans, like the average clustering coefficient, cannot be reproduced by simple network generators such as the BA-model or the configuration model. Instead more sophisticated, fine tuned generators have to be employed, for example the PFP model, presented by Zhou and Mondragon [2004]. Its parameters are chosen, to reproduce many statistical properties of the empirical data, once the number of nodes has grown to approximately 11000, which is roughly the size of the specific snapshot that has been used to fit the parameters of the model. However, to investigate the influence

of a high clustering, it is desirable to have a model, that is not only able to generate graphs with $\langle \mathbb{C} \rangle$ comparable to the empirical data, but also allows to smoothly adjust the clustering.

For this purpose, here a generalization of the configuration model is proposed that allows to tune the resulting average clustering coefficient in the range $0 \lesssim \langle \mathbb{C} \rangle \lesssim 0.6$. To modify the configuration model to create graphs with high clustering, we use the fact, that geometric networks, with a connectivity constrained by an underlying geometry, have a large clustering coefficient naturally. Take as an example disc graphs. Here vertices are positioned randomly across a plane, and edges are created between those pairs of vertices that have an euclidean distance less than some radius r . The radius obviously determines the average degree, but, for sufficiently large radii, $\langle \mathbb{C} \rangle \approx 0.6$, independent of r [Dall and Christensen, 2002].

To construct networks with fixed degree distribution, but tunable clustering coefficient, we interpolate between the configuration model without any geometric constraints ($\lim_{N \rightarrow \infty} \langle \mathbb{C} \rangle = 0$) and a geometric network. We denote this model as *geometric- p networks*, where $0 \leq p \leq 1$ represents the interpolation parameter. The construction process consists of four steps:

1. Each of the $1 \leq i \leq N$ vertices is initialized with a random position $\vec{r}_i = (x_i, y_i)$ on a square area drawn from a uniform distribution and a target degree t_i drawn from the desired degree distribution $p(t)$.
2. For every vertex i generate a list Δ_i , which contains all other vertices sorted by ascending Euclidean distance $|\vec{r}_j - \vec{r}_i|$. Periodic boundary conditions are assumed, which turn the square into a torus.
3. Create for each vertex i , a number of edge stubs corresponding to the node's target degree.
4. The vertices are connected according to the following iteration:
 - a) From all stubs pick one randomly. Let i denote the vertex it is attached to.
 - b) With probability p a short-range connection is built by creating an edge to the first vertex $j \in \Delta_i$ of the sorted list with $k_j < t_j$ that is not yet in the neighborhood $\mathcal{N}(i)$.
 - c) With probability $(1 - p)$ a long-range connection is built to a vertex j that belongs to a randomly drawn stub and is not yet linked to i .
 - d) After the creation of either a short- or long-range connection, the two used stubs are removed from the respective lists.

Through this iteration scheme, for $p = 0$ only random links are constructed. This limit corresponds to random networks with a given degree distribution and the construction rule is exactly recovering the configuration model as it is defined in [Newman, 2003]. For $p = 1$ a selected stub is always connected to the closest

2. Brief Résumé of Graph Theory

possible vertex and the network closely follows the geometric constraints, respecting the desired degree distribution. We denote this case the geometric network limit. Employing parameter values in the range $0 < p < 1$, we can generate networks, that smoothly interpolate between the random and geometric limit.

Figure 2.5 shows the complementary cumulative degree distribution $P(k) = \int_k^\infty p(k')dk'$ resulting from a scale-free target degree distribution $p(t) \sim t^{-\gamma}$ with exponent $\gamma = 2.3$. The target degrees have been limited to $1 \leq t \leq k_{\max}$ with cutoff $k_{\max} = N^{1/(\gamma-1)}$. At this cutoff³ the expected number of vertices with a degree of k or higher, given by $N \int_k^\infty p(k)dk$, drops below 1. The complementary cumulative

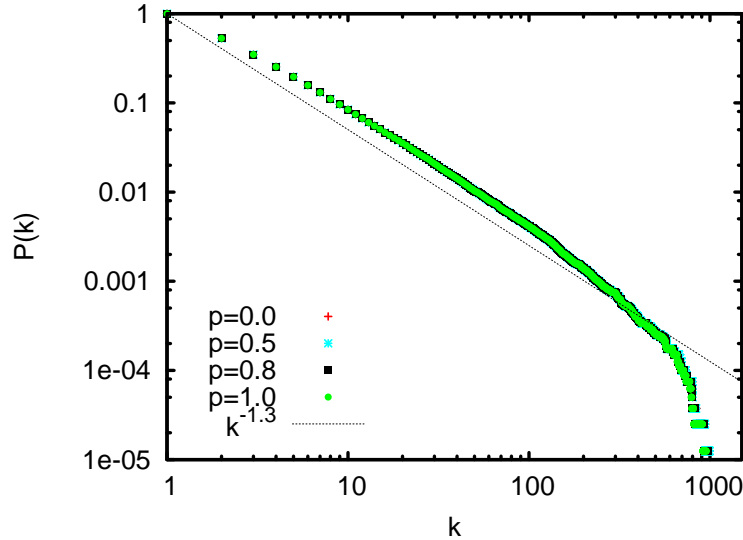


Figure 2.5.: Complementary cumulative degree distribution $P(k)$ of various geometric p networks resulting from a scale-free target degree distribution $p(k) \approx p(t) \sim t^{-\gamma}$ with $\gamma = 2.3$ and $N = 8000$. For comparison, a power law with exponent $\gamma - 1 = 1.3$, which corresponds to the exponent of the complementary cumulative target degree distribution is shown.

distributions of the put in target distribution and the generated degree distribution shows comfortable agreement. In the small and medium degree range the scale-free exponent is reproduced. Towards the end of the construction (4a-4d) it may happen that especially for high-degree vertices some of their prospective links are dropped because the last remaining stubs would produce either already existing links or self-links. This explains the bending down of the resulting distribution for very large k and the slight probability enhancement at small and medium degrees. No dependence on the interpolation parameter p is observed.

³For $\gamma = 2.3$ we get $k_{\max} \approx 200, 700, 1000$ for $N = 1000, 5000, 8000$. A $\gamma = 2.2$ yields $k_{\max} \approx 1700$ for $N = 8000$. This is in good agreement with $k_{\max} \approx 1000-2000$ for $N \approx 8000$ AS scans.

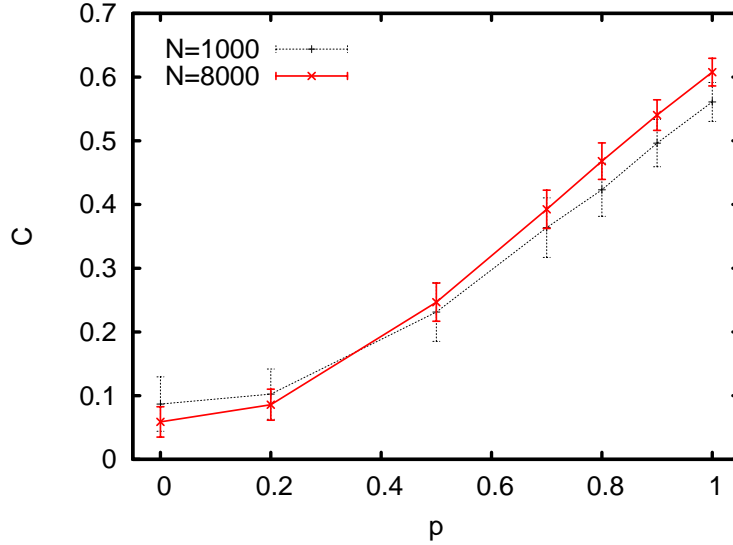


Figure 2.6.: Clustering coefficient as a function of the interpolation parameter p for scale-free geometric p networks with $\gamma = 2.3$ and $N = 1000$ (dashed), $N = 8000$ (solid). The plotted values are averages from an ensemble of 10 realizations, the error bars show the standard deviation of the mean.

The clustering coefficient of scale-free geometric p networks is illustrated in Figure 2.6. As expected, it increases from a very small value $\langle \mathcal{C} \rangle \approx 0.05$ at $p = 0$ to a large value $\langle \mathcal{C} \rangle \approx 0.60$ at $p = 1$. Between $p = 0.3$ and 1.0 it increases almost linearly, which makes the model convenient to use for investigations of the influence of clustering on other network properties.

Figure 2.7 shows the degree-dependent clustering coefficient $\mathcal{C}(k)$. For $p = 0$ there is no dependence of $\mathcal{C}(k)$ on k for small and medium k , which is the expected result for random networks generated by the configuration model, see Vázquez et al. [2002]. The k -dependence observed for large degrees is an effect of the finite system size. With increasing p the degree-dependent clustering coefficient increases significantly for small and medium degrees. For $p = 1$ it exhibits a power-law form $\mathcal{C}(k) \sim k^{-\beta}$ with $\beta \approx 0.8$, which is in good agreement with $\beta \approx 0.75$ reported by [Vázquez et al., 2002] for Internet scans of the years 1997 to 1999.

To sum up, real networks, like for example the Internet, often exhibit a high degree of clustering. Neither the BA scale-free graph model, nor the configuration model generate graphs that reproduce this property. By enforcing geometrical constraints during the construction, the present section proposes a generalization of the configuration model, the *geometric- p model*. This generalization allows to tune the amount of clustering in the generated graph. The interpolation between the pure configuration model ($p = 0$) and the pure geometric case ($p = 1$) allows for clustering coefficients in the range of $\langle \mathcal{C} \rangle \approx 0$ to $\langle \mathcal{C} \rangle \approx 0.6$.

2. Brief Résumé of Graph Theory

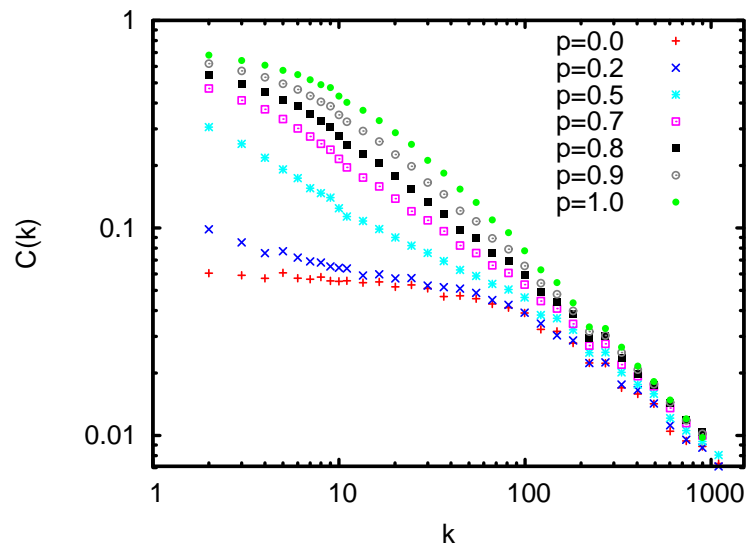


Figure 2.7.: Degree-dependent clustering coefficient $\mathcal{C}(k)$ for various scale-free geometric- p networks with $\gamma = 2.3$ and $N = 8000$. For large degrees it shows a power law behavior $\mathcal{C}(k) \sim k^\alpha$. This is especially pronounced for $p = 1$, where $\alpha \approx 0.8$.

3. Game Theory on networks

In this and the two following chapters, we address the optimization of networked systems with respect to global properties of the topology. Performing global optimizations in rugged fitness landscapes typically suffers from a vast search space, causing the required algorithmic effort to grow to unfeasible extents. Fortunately, for practical applications, it is often not necessary to find the best solution exactly, as long as a solution with a performance close to the global optimum can be found with less effort. Renouncing to find the global optimum, opens up the possibility of optimizing in a distributed, self organized manner. Instead of a central instance, that has to know all the details of the whole system and knows which changes to apply to reach the global optimum, distributed optimization employs a large number of agents following simple rules while accessing only information about their immediate environment. Because of the restriction to local information, none of the agents can actually determine the values of the global properties to be optimized, still, as will be demonstrated in Chapter 4, significant optimization of global properties may emerge from application of local rules.

As a consequence of the confinement to local information, it is obvious, that the key to a successful distributed optimization scheme lies in the rules which determine the agents' actions. Given a certain global observable to be optimized, the challenge is to find corresponding local rules. To achieve this, two approaches are possible: The first, perhaps more obvious, approach is to translate the global objectives to local objectives. This however may be difficult or impossible to do, as for example global information that cannot be approximated locally might be necessary. The second approach is to neglect the global objective and to come up with rather arbitrary rules that are tunable by a single or maybe a few parameters. The values for these parameters are then to be determined by classical optimization techniques. However, the space of parameters to be searched is reduced from the high dimensional space of the global optimization, to the space of the handful of parameters that tune the local update rules, which ideally is also smoother than the original space.

Having in mind real networks like the Internet as described in Section 2.2, the agents driving the optimization are thought of as the economic entities that own parts of the network and, by establishing business relations among each other, determine the structure of the network. Assumed to be driven by financial interests, these intelligent agents will inevitably pursue their own goals and therefore exhibit selfish behavior. The behavior of agents, their decision making and choice of strategies, is the subject of *Game Theory*, developed to a large extent by [von Neuman and Morgenstern \[1944\]](#), with important contributions by [Nash \[1950, 1951\]](#).

3. Game Theory on networks

Apart from the pragmatic use as a framework to describe and implement distributed optimization, more motivation for studying Game Theory on networks is given by the parallels to social networks, which (for the most part) also consist of intelligent agents following more or less simple rules. Looking at the structure of society with network Game Theory in mind, the question if and how changes to the rules of social interaction, be it by new forms of interaction made possible by modern technology or by a change of ethics, influence the structure of society.

After a short, non-extensive, introduction of concepts of game theory and game theory on networks in the present Chapter, the following Chapters will apply it to networked systems. Chapter 4 investigates the influence of games played on the network to the network structure and attempts to utilize the game to optimize the structure. Chapter 5, on the other hand, investigates the influence of the structure on the behavior of the agents and attempts to use structural information to encourage cooperation among the players.

3.1. The Prisoner's Dilemma

The so called *Prisoner's Dilemma* is a simple game that demonstrates why two players might not cooperate, even if it was in the interest of both. We will use this game as a guide through some basic game theory principles. To get familiar with the subject of game theory, let's start with the following, close-to-real-life example of a Prisoner's Dilemma:

Bank robbery! Two suspects under arrest! — Amy W.
and Bill G. were arrested after a bank had been robbed, but the police has insufficient evidence for a conviction, although minor charges, like illegal gun possession, are obvious.

The two suspects were separated and interrogated but neither made a confession until the police decided to offer both of them the same deal: Testify, get mitigating circumstances as the principal witness and be set free, or remain silent and get a full ten-year sentence in case the other suspect testifies against you. If both remain silent, the minor charges cannot be dropped, resulting in minor sentences of six months for both. However, if both testify, then only the bank robbery can be dropped, resulting in sentences for is reduced to five years.

Read the full story and background on pages 20–22.

3.1. The Prisoner's Dilemma

Formally a simple two-player game $\mathcal{D}(\mathcal{S}_A, \mathcal{S}_B, \mathcal{P}_A, \mathcal{P}_B)$ between the players A and B is defined by the strategy spaces \mathcal{S}_A and \mathcal{S}_B , which contain the strategies (actions) that players can choose from, and the payoff matrices $\mathcal{P}_A : \mathcal{S}_A \times \mathcal{S}_B \rightarrow \mathbb{R}$ and $\mathcal{P}_B : \mathcal{S}_B \times \mathcal{S}_A \rightarrow \mathbb{R}$ that map the players choice of strategies to a real valued payoff. Except for the excursion in Section 5, the games we consider below will be symmetric games, i.e. both players have the same set of strategies $\mathcal{S}_A = \mathcal{S}_B =: \mathcal{S}$ to choose from and the payoffs are determined by identical payoff matrices $\mathcal{P}_A = \mathcal{P}_B =: \mathcal{P}$. In that case, we abbreviate $\mathcal{D}(\mathcal{S}, \mathcal{P}) := \mathcal{D}(\mathcal{S}, \mathcal{S}, \mathcal{P}, \mathcal{P})$. Note that this does not imply identical payoffs for both players, as the payoff matrix itself is generally not symmetric.

In the case of Amy and Bill mentioned above, both have the same two strategies to choose from. The received sentence depends only on the chosen strategies, not on some other property of the suspect and both are offered the same deal, resulting in a symmetric game. The strategies they can choose from are to *cooperate* (C) with the other by remaining silent or to *defect* (D) from the other. The strategy space $\mathcal{S}_{PD} = \{C, D\}$ of the Prisoner's Dilemma contains the two strategies cooperate and defect.

When two players encounter, each player i picks a strategy $s_i \in \mathcal{S}_i$ from their respective strategy portfolio. The outcome of the game is then given by the corresponding entry in the payoff matrix: Player A collects a payoff $p_A = \mathcal{P}_{s_A, s_B}$, given by the entry of the payoff matrix in the row corresponding to his own strategy s_A and the column corresponding to the opponents strategy s_B .

Coming back to our real-life example the length of the time in jail has to be translated in payoffs. \mathcal{P}_{PD} is a 2×2 matrix, in win-loose terminology it reads

$$\mathcal{P}_{PD} = \begin{pmatrix} \text{win} & \text{lose much} \\ \text{win much} & \text{lose} \end{pmatrix}.$$

According to custom, the entries of the prisoner's dilemmas payoff matrix are named T , R , P , and S

$$\mathcal{P}_{PD} = \begin{pmatrix} R & S \\ T & P \end{pmatrix}. \quad (3.1)$$

These abbreviations stem from the following names: The payoff both get when mutually staying silent is called the *reward for cooperation* R , while the payoff for mutual defection is simply called *punishment* P . Naturally the highest payoff from the perspective of one of our prisoners corresponds to being released right after the interrogation, this payoff is named the *temptation to defect* T , the lowest payoff, which obviously corresponds to the full ten-years sentence, is called the *suckers payoff* S . Comparing the magnitudes of the payoffs of Amy and Bill, we find

$$T > R > P > S. \quad (3.2)$$

This characterizes a prisoner's dilemma. The condition

$$2R > T + S \quad (3.3)$$

3. Game Theory on networks

assures that even in a repeated game, the average payoff for mutual cooperation is greater than the payoff of alternating cooperation and defection.

A frequently used [e.g. [Hauert and Doebeli, 2004](#), [Ohtsuki et al., 2006](#), [Szabó and Fáth, 2007](#)] and beautiful parametrization of the payoff matrix, emphasizes the costs c of cooperating and the benefits b of encountering a cooperator in the prisoner's dilemma:

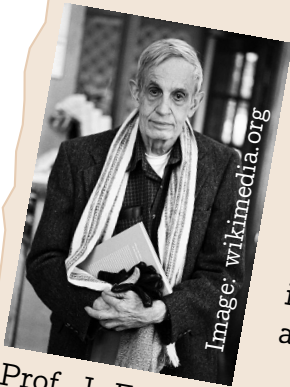
$$\mathcal{P}_{\text{PD}} = \begin{pmatrix} b - c & -c \\ b & 0 \end{pmatrix}. \quad (3.4)$$

This line of thought assumes, that the player has to invest a certain amount c when deciding to cooperate, while a defector refuses to invest. When collecting the payoff however, it's not the player's, but the opponent's strategy, that determines the benefit of the interaction. With a cooperating opponent, a benefit b is collected, but from the interaction with a defector there is no benefit. Assuming b and $c > 0$ Inequation (3.2) is fulfilled if the benefit $b > c$ outweighs the cost, while Inequation (3.3) is automatically fulfilled by the cost/benefit parametrization

Being offered the deal, which strategies will Amy and Bill choose? To answer this we have to make assumptions about the players: We assume they behave rationally on an individual level, an assumption introduced by [Nash \[1950, 1951\]](#). This assumption might not be too realistic in the example of our two suspects, especially if they knew each other beforehand or happened to be friends, but thinking for example of business interactions between companies, rationality is assumed to be valid.

Given the payoff matrix \mathcal{P}_{PD} as given in Equation (3.1), together with Inequality (3.2), Amy may assume that Bill will cooperate, then her payoff would be R if she cooperated as well, but T if she defected. If, however, Bill defects, then Amy's payoff as a cooperator would be S , while by defecting she'd get P . As a result, since $T > R$ and $P > S$ Amy will always choose to defect. From Bill's perspective the same arguments hold, so he will choose to defect, too. To summarize, a rational player will realize, that no matter what strategy the opponent picks, the own payoff will increase if he chose to defect.

States like this, where no player is able to increase his payoff by an unilateral change of strategy, are called *Nash Equilibria*. From above it is obvious, that a Nash Equilibrium does not have to be anywhere close to the global optimum. In Amys and Bills case the global optimum in the sense of a minimal overall time to do, is mutual cooperation, resulting in a 6 month sentence for both. However, even if they know the global optimum, their selfish behavior makes it impossible for them to realize that strategy configuration without interaction outside of the game, for example by promising to each other to remain silent. It is the rationality and selfishness, that turns the prisoner's problem into a dilemma.



Prof. J. F. Nash

Amy and Bill sentenced for bank robbery! — At first, the suspects denied any responsibility for the robbery. Even the officers who arrested them, considered it “hard to imagine, that these guys robbed the bank.” However, during the interrogations Amy and Bill changed their minds and got surprisingly eager to give a full plea of guilty. It is rumored that they were offered a deal by the authorities.

Game theory godfather Prof. J. F. Nash: “This is exactly what my theory predicts. They should have read my paper: [Nash \[1950\]](#).”

3.2. Games and Graphs

Merging of games and graphs is achieved by explicit identification of n players $P = \{p_1, \dots, p_n\}$ with the N vertices of a graph \mathcal{G} , $p_i \Leftrightarrow v_i \in \mathcal{V}(\mathcal{G})$ and accordingly $n = N = |\mathcal{V}(\mathcal{G})|$. These players interact pairwise with each other by playing a game \mathcal{D} as sketched in the previous section. However, interactions are only possible between players that are located on adjacent vertices, i.e. vertices that are connected by an edge $e \in \mathcal{E}(\mathcal{G})$ of the graph $\mathcal{G}(\mathcal{V}, \mathcal{E})$. As a consequence of the identification of players and vertices, the terms player, vertex, and node are used synonymously, although player is used to emphasize game theory aspects, vertex refers to graph theoretical viewpoints, and node tends to be used to point out the connection of both. In principle the game played among two players can vary from pair to pair, meaning that each player may have his own set of strategies and is rewarded according to an individual payoff matrix. Generally the players $p_i, p_j \in P$, located at the vertices $v_i, v_j \in \mathcal{V}(\mathcal{G})$, engage in the game $\mathcal{D}(\mathcal{S}_i, \mathcal{S}_j, \mathcal{P}_i, \mathcal{P}_j)$. Many studies restrict themselves to symmetric games, i.e. all players choose from the same strategy portfolio and receive payoffs determined by the same payoff function. In this case the common strategy space $\mathcal{S} = \mathcal{S}_1 = \dots = \mathcal{S}_n$ and payoff function $\mathcal{P} = \mathcal{P}_1 = \dots = \mathcal{P}_n$ define the game $\mathcal{D}(\mathcal{S}, \mathcal{P})$.

The connection of game theory and graph theory in this manner has been pioneered by [Nowak and May \[1992, 1993\]](#) who located the players on a two dimensional grid, allowing interactions only between neighbors on that grid. The payoff

3. Game Theory on networks

of a player is defined as the sum of payoffs

$$p_i := p_i^* = \sum_{j \in \mathcal{N}(i)} \mathcal{P}_{s_i, s_j}, \quad (3.5)$$

resulting from the interactions with the neighbors. Especially when considering graphs with a very heterogeneous degree distribution, a common choice is to define the payoff of a node as the average payoff per interaction

$$p_i := \bar{p}_i = \frac{1}{k_i} \sum_{j \in \mathcal{N}(i)} \mathcal{P}_{s_i, s_j}, \quad (3.6)$$

which results from normalization with respect to the node degree k_i .

[Nowak and May](#) let the players update their strategies by imitating the best scoring neighbor

$$s_i \leftarrow s_j : j = \arg \max_{l \in \mathcal{N}(i)} p_l. \quad (3.7)$$

To emphasize the motivation from evolution, subsequent work refers to the imitation as a *death-birth process* [e.g. [Ohtsuki et al., 2006](#)] where a node that got vacant (*death*) is taken over by the offspring (*birth*) of the most successful player from the adjacent nodes. Another common update rule, the *best response* update

$$s_i \leftarrow \arg \max_{s \in \mathcal{S}(\mathcal{D})} p_i(s), \quad (3.8)$$

assumes players to know all available strategies and pick the one that yields the highest payoff, given the neighbors current strategies are fixed. In their seminal work [Nowak and May](#) showed the emergence of complex patterns of cooperators and defectors caused by the confinement to the underlying geometry. In principle games on regular lattices are *cellular automata* like for example *John Conway's Game of Life* [[Gardner, 1970](#)], but the interpretation as a game allows for a much more concise formulation of the update rule, which would “look horrendous if expressed in canonical cellular automata terms” [[Nowak and May, 1992](#)]. This quotation tries to set apart spatial games from cellular automata by pointing out, that although it is possible to express the game's update rule in terms of the canonical description of cellular automata, as used by [Wolfram \[1983, 1984\]](#), the corresponding code is lengthy and hard to grasp,¹ while the formulation in terms of a game and an update rule is straight forward and comprehensible. Furthermore, this formulation allows straight forward generalization to irregular lattices as described by graphs.

¹For the case of the square neighborhood the strategy update of a player depends on the state of 25 cells, i.e. the cell itself, its 8 immediate neighbors, and the neighbors' neighbors. The canonical code of the update rule is a 2²⁵-digits binary number, or 2²¹-digits hexadecimal, whichever the reader feels more comfortable to visualize.

Motivated by the abundance of complex network structures found in biological and social networks [Watts and Strogatz, 1998], the Internet [Faloutsos et al., 1999], the World-Wide-Web [Albert et al., 1999], and so forth (see Section 2.2), the dynamics of various games on structures defined by graphs have been explored. Hauert and Doebeli [2004] confirm that cooperation among the players is enhanced if the prisoners' dilemma is played on a regular network, as opposed to the classical scenario taking place in a *well stirred* population, represented by a complete graph. However, they raise the awareness, that this is not the case for all kind of games, by showing that for the *snowdrift game* with imitation update given in Equation (3.7) the evolution of cooperation can even be inhibited by regular spatial structure. On the contrary, implementing the same game dynamics on scale-free graphs Santos and Pacheco [2005] find that the heterogeneous structure of graphs grown according to preferential attachment yields cooperation as the dominant strategy for either the prisoners' dilemma or the snowdrift game.

Approaching from the perspective of statistical physics, Ebel and Bornholdt [2002a] investigate the reaction of the system of prisoners' dilemma players on a random network of the Erdős and Rényi [1960] type when perturbed from the Nash equilibrium state. The perturbation from an equilibrium state is done by forcing a suboptimal strategy at a random node, as a consequence other nodes may now adjust their strategies to take advantage of the suboptimal strategy in the neighborhood. The consecutive changes of strategies propagate through the network, forming avalanches, whose size distribution depends on the parameter T in the prisoners' dilemma payoff matrix. Three phases are identified: A subcritical phase, with local avalanches that die out fast, a supercritical phase, with avalanches that span the whole network and die out only after a number of time steps which are by magnitudes larger than the system size, and a critical phase, between the two other phases, which exhibits avalanche sizes that follow a scale-free distribution.

While the work mentioned above considers game dynamics that take place on *static* graphs, there are two main lines of research, that investigate the interplay of games with the growth and reshaping of graph topologies. The first line of research does not identify players and vertices, but considers the graph structure as the outcome of a game played by n players. Games with more than two players are a classical field of game theory [von Neuman and Morgenstern, 1944, Nash, 1950], where n players are facing the problem of competitively optimizing their utilities. The payoff p_A of a certain player A depends on his own strategy s_A and the strategy choices of all $n - 1$ other players.

$$p_A := p_A(s_1, \dots, s_A, \dots, s_n)$$

Applied to the creation of network structures, n players engage in a game that encodes properties of the network, e.g. connectedness [Bala and Goyal, 2000, Haller and Sarangi, 2005, Schneider and Kirkpatrick, 2005] or the ability to reach certain vertices on preferably short paths [Anshelevich et al., 2003, Fabrikant et al., 2003], in the player's payoff functions. The players may achieve the goals encoded in

3. Game Theory on networks

the payoff function by means of changes to the network structure, for example by adding edges to the graph. Costs incurred by the topology changes reduce the investing player's payoff and result in a classical n -player game.

The second line sticks to the identification of players and nodes as put forward by [Nowak and May \[1992\]](#) and adds a degree of freedom to the nodes behavioral repertoire: The neighborhood of a node is considered part of the players strategy, accordingly the player is able to change the members of its neighborhood, i.e. to change its *social environment*. Like [Ebel and Bornholdt \[2002b\]](#) put it: "If the fish you bought on the fish market is spoiled you will probably switch the dealer next time."

Early studies investigated the propagation of strategy and neighborhood switch avalanches for the imitation (3.7) and best response (3.8) update rule [see [Zimmermann et al., 2001](#), [Ebel and Bornholdt, 2002b](#), resp.]. The influence of these local updates on the overall network structure is characterized by changes in global graph observables, like the cluster coefficient (2.10) [[Zimmermann et al., 2004](#)] and the cluster coefficient and average path length (2.19) [[Ebel and Bornholdt, 2002b](#)]. In addition to the dependence on parameters in the payoff matrix [Pacheco et al. \[2006a,b\]](#) point out the sensitivity of the dynamics on the relative frequency of strategy to topology updates. In terms of the degree distribution (2.15) the emergent structures of such self organizing topology dynamics have been elaborated upon by [Scholz and Greiner \[2007\]](#), which will be detailed in Section 4.

Including the closeness (2.11) of the node in its payoff function, [Holme and Ghoshal \[2006\]](#) create an update rule that depends on the whole network structure, instead of restricting the needed information to the 1- or 2-hop neighborhood. Naturally this results in a higher computational complexity, as the computation of global observables scales at least like $\mathcal{O}(N)$, while observables that only depend on the neighborhood typically do not scale with the system size. By sacrificing the restriction to local information, [Holme and Ghoshal](#) buy the possibility to use the framework of network game theory to directly optimize for global network properties.

The global property of guaranteeing network connectivity is of special interest in wireless communication networks. In wireless communication networks the existence of edges is determined indirectly by the power level of a node's radio transmitter, which defines a sphere of direct reachability. Interpreting its chosen power level as the strategy of a node, and incorporating the draining of battery power and the network connectivity in the payoff, [Eidenbenz et al. \[2003\]](#) create a game dynamics, that ensures a connected wireless communication network. Compared to non-game theoretic approaches [see e.g. [Glauche et al., 2003](#)], this approach has the disadvantage of converging into any of many Nash equilibria, which vary vastly in the cost, measured by summing up the overall power consumption.

To sum up this sections mini-review of relevant network game theory, the exhaustive review of game theory, with an emphasis of games taking place on graphs, given by [Szabó and Fáth \[2007\]](#) has to be mentioned.

3.3. Prisoners' Dilemma Network Game

As a concrete example of a game dynamic coupled to a network, this section investigates the prisoners' dilemma network game. The system consists of a graph $\mathcal{G}(\mathcal{V}, \mathcal{E})$ with $N = |\mathcal{V}|$ vertices, connected by the edges \mathcal{E} , and N players $\{p_1, \dots, p_N\} = \mathcal{P}$. Each player p_i is associated $p_i \Leftrightarrow v_i \in \mathcal{V}$ with a distinct vertex. The game is symmetric in the sense, that all players can pick their strategy $s_i \in \mathcal{S}$ from the same set of strategies $\mathcal{S} := \mathcal{S}_{\text{PD}} = \{C, D\}$ and the payoffs resulting from an interaction between two players p_i and p_j is determined by the same payoff matrix \mathcal{P} for all interactions. The payoff matrix $\mathcal{P} := \mathcal{P}_{\text{PD}}$ is the prisoner's dilemma payoff matrix (3.1), well known from the example given by Amy and Bill in Section 3.1, with its entries T , R , P , and S adhering to the inequalities (3.2) and (3.3). With these definitions the game played is $\mathcal{D} := \mathcal{D}(\mathcal{S}, \mathcal{P})$. The payoff a player p_i collects after playing a round of games against his neighbors $\mathcal{N}(v_i)$ is the sum of payoffs $p_i := p_i^*$ as defined in Equation (3.5).

The players may now update their strategies according to the best response update rule (3.8). These updates are done in a round robin fashion, i.e. at every time step a random player p is allowed to update his strategy. This player then updates its strategy to the strategy that results in the highest possible payoff, given the neighbors' strategies are fixed. Analogous to the decision finding process in the 2-players prisoner's dilemma faced by Amy and Bill in Section 3.1, rational players that encounter multiple opponents recognize, that no matter what the opponents' strategies are, the own payoff is greater when defecting, instead of cooperating. Iteration of the update process results in a network where all players have switched to defect, the system's unique Nash equilibrium. The iteration of the update process until the Nash equilibrium is reached is depicted in Figure 3.1.

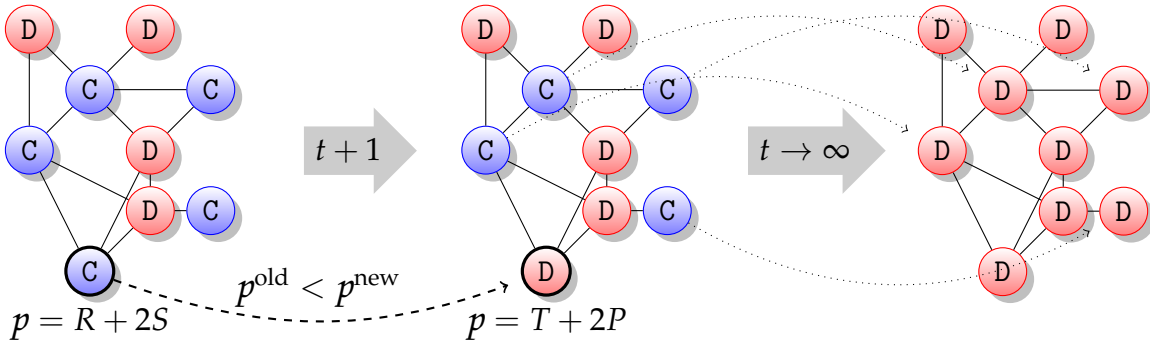


Figure 3.1.: Prisoners' dilemma on a network. The three pictures show a network at time steps t_0 , t_1 , and t_{NE} . From t_0 to t_1 the highlighted player updates his strategy from cooperate (C) to defect (D), thereby changing his payoff from $p = R + 2S$ to $p = T + 2P$, which according to Equation (3.2) is an increase. During the time between t_1 and t_{NE} further strategy changes symbolized by the dotted arrows have occurred, until at at time t_{NE} , the Nash equilibrium, consisting solely of defectors, has been reached.

3. Game Theory on networks

As this is not particularly exciting, we grant the players an additional degree of freedom: They are allowed to pursue the maximization of their payoff not only by adjusting their strategy, but they might as well adjust their neighborhood. However, to avoid explosion or extinction of the number of edges in the network, the players must not change the number of neighbors they are connected to. To ensure the fixed number of edges in the network, players who build a new connection have to remove an old one simultaneously. For the sake of simplicity the number of neighbor exchanges is limited to one per player and time step. The neighborhood update is depicted in Figure 3.2.

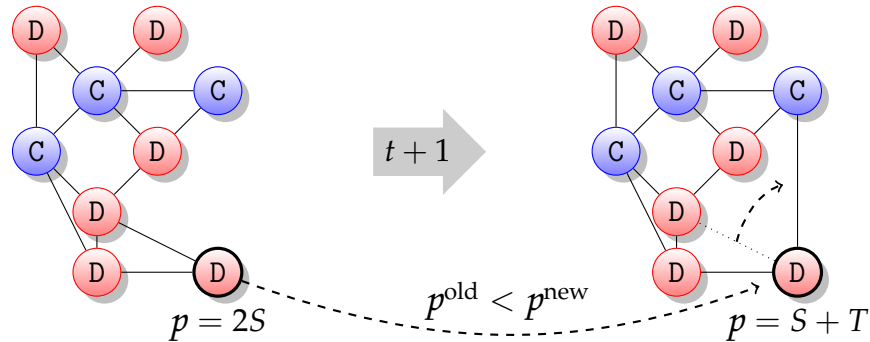


Figure 3.2.: Prisoners dilemma neighborhood update. The highlighted player has already optimized his strategy to defect (D), but is still able to increase the payoff from $p = 2S$ to $p = S + T$ by connecting to a cooperating player instead of a defector.

After a sufficient number of update steps, eventually no player will be able to increase his payoff, neither by a change of strategy nor neighborhood. A network Nash equilibrium (NNE), as defined by Ebel and Bornholdt [2002b], has been reached. Despite the greater freedom of choice, for the prisoners' dilemma the choice of strategies in the network Nash equilibrium are the same as on the static network. After a player has exchanged one of his defecting neighbors for one of the still cooperating players in the network, he will still choose to defect for the same reasons as before. The possibility of increasing the payoff by creating an edge to an arbitrary player and removing another edge, lets the updating player act quite predictably: The player creates an edge to some cooperating player and removes an edge which connects him to a defector. Therefore, as soon as every player that has been cooperating initially had the chance to update his strategy and neighborhood, all players are defecting and no further changes, neither in strategy nor in connectivity, will increase any player's payoff.

Although during the neighborhood updates no player has changed his own degree, the degree of the affected neighbors is not conserved, which leads to a change of the overall topology. To find out the system's reaction to small perturbations from the equilibrium, once a network Nash equilibrium is reached, we force a random player to use a suboptimal strategy, and observe the chain of changes that follows. As, depending on T , the number of changes until a NNE is reached may be small

compared to the number of edges in the system, the process of perturbation and consecutive settling into an equilibrium has to be applied repeatedly until the network configuration reaches a stationary state. This simple rule leads to a network with a scale-free degree distribution $p_k \sim k^{-\gamma}$ with $\gamma \approx 2$, shown in Figure 3.3.

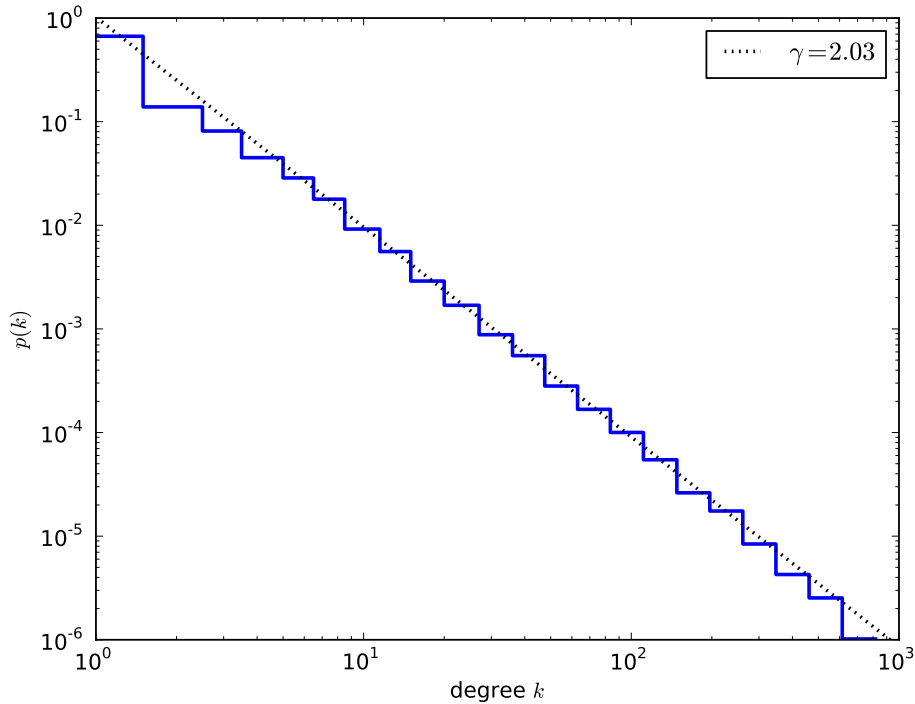


Figure 3.3.: Degree distribution emerging from playing the prisoners' dilemma with network topology updates. Here networks with $N = 1000$ nodes and an average degree $\langle k \rangle = 6$ have evolved through 3000 consecutive NNEs. The degree distribution shown is the average over 40 realizations. Shown as a dotted line is a powerlaw $k^{-\gamma}$ with $\gamma = 2.03$.

3.4. Related network structure modeling

Because of the strict dominance of defection over cooperation in the Prisoners' dilemma as described in the previous section, it is straightforward to describe the same dynamics without employing game theory. Consider the following update rule, that starts from a state corresponding to the all-D Nash equilibrium, but instead of forcing a random player to use the suboptimal C strategy, we *tag* the corresponding vertex $v' \in \mathcal{V}(\mathcal{G})$ to make it stand apart from the other vertices of the graph \mathcal{G} . The corresponding topology update process is modeled as follows:

- Generate an initial network

3. Game Theory on networks

- iterate the following update rule
 - tag a random vertex $v' \in \mathcal{V}(\mathcal{G})$
 - select a random vertex $w \in \mathcal{V}(\mathcal{G})$
 - create an edge (v', w) , but only if there hasn't been an edge before
 - if an edge has been added, remove a random edge from w to one of its neighbors $\mathcal{N}(w)$
 - repeat while $v' \neq w$

The condition in the update process that terminates the current update round, when the random vertex w is identical to the tagged vertex v' , corresponds to the situation in which the player who has been forced to switch his strategy gets the chance to update and switches back to D. At that point, there are no cooperators left in the network, the network Nash equilibrium is reached, and the next perturbation is about to be executed.

To speed up the numerical simulation, instead of randomly picking the vertex w to update itself from the set of all vertices, pick it only among those that haven't been picked yet. This corresponds to putting all vertices into a list l_{rnd} that is randomly shuffled at the beginning of each update round and then picking w from that list $w \leftarrow (l_{\text{rnd}})_1, w \leftarrow (l_{\text{rnd}})_2, \dots$, until $w = v'$. The emerging degree distribution in Figure 3.4 shows a power law with an exponent of $\gamma = 2$ over 4 magnitudes of degree k .

To investigate the influence of the exact update rule, let's investigate two other, but similar rules. Both again tag a random vertex v' at the beginning of an update round and repeatedly let a random vertex w connect to the tagged vertex if they're not yet connected. If an edge has been created, an edge has to be removed from the graph to conserve the total number of edges. It is the selection of this edge, that distinguishes the two variants from the original rule, which removes a random edge from w to one of its neighbors $\mathcal{N}(w)$.

In the first variant, *variant a*, pick another random node w' and remove a random edge $e \in w' \times \mathcal{N}(w')$ from w' to one of its neighbors $\mathcal{N}(w')$. As depicted in Figure 3.4, the emerging degree distribution deviates drastically from the strict power law produced by the original update rule, and shows a Poissonian distribution for the low degrees and a power-law tail with $\gamma = 1$ for the high degrees.

The second modified update rule, *variant b*, does the same as the first, except, that the edge to be removed from the network is picked randomly from the set of all edges $e \in \mathcal{E}(\mathcal{G})$. Although this might seem to be the same at first glance, it isn't. Recall from the description of the scale-free networks introduced by Barabási and Albert [1999] in Section 2.2.2, that following a random edge to its end, the probability to end at a vertex with degree k is proportional to $kp(k)$, while the probability of a randomly picked vertex to be k is $p(k)$. This means, that in the first variant, the degree of one of the vertices that loose a link is distributed according to $p(k)$ while the other follow $kp(k)$. In the second variant both degrees follow a

probability distribution proportional to $kp(k)$. This difference of the update rules has a major impact on the emerging degree distribution of the networks, as can be seen in Figure 3.4, where the second variant results in an increased probability for low degrees, while for the higher degree range, the power law behavior with $\gamma = 2$ is preserved. Although here not too much insight in the causes of the different outcomes of the dynamics of the above network formation processes is offered, the results point out, that the exact choice of an update rule is crucial for the emerging network structure.

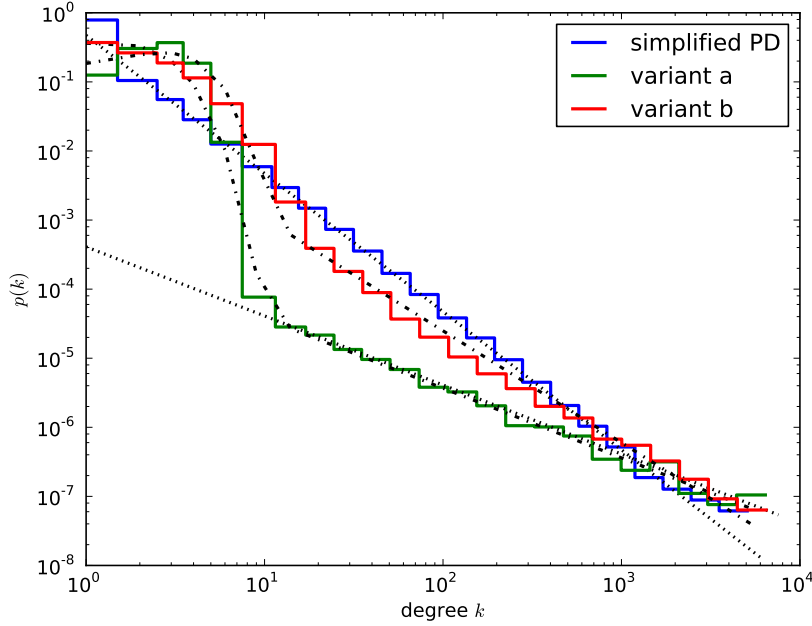


Figure 3.4.: Degree distributions emerging from prisoners' dilemma with topology modifications, simulated through the simplified update rule, and from it's two variants. The graphs have been initialized as Poisson graphs of size $N = 10000$, with an average degree $\langle k \rangle = 6$. The degree distributions shown here are snapshots of the $(\frac{N}{2}\langle k \rangle)^{\text{th}}$ update round, averaged over 40 realizations. The dash-dotted lines show fits of an additive combination of Poisson and power-law distributions $p(k) = \epsilon N_{\text{P}} \frac{\lambda^k}{k!} + (1 - \epsilon) N_{\text{sf}} k^{-\gamma}$ where $N_{\text{P}}, N_{\text{sf}}$ are normalization constants, and λ is the average degree of the Poisson distribution. The contribution of the Poisson distribution amounts to $\epsilon = 0.999$ with $\lambda = 1.8$ and $\gamma = 1$ for variant a, and $\epsilon = 0.925$, $\lambda = 3.3$, and $\gamma = 1.6$ for variant b. To indicate the scale free behavior of the whole range of k for the simplified PD and in the high degree tail of variant a, the dotted lines show power laws $k^{-\gamma}$ with $\gamma = 1$ and 2 , respectively.

4. Iterated prisoners dilemma network game

As has been shown in Section 3.4, network game dynamics are able to reorganize graph structures. Using such update rules to let technological networked systems organize themselves into a sufficiently optimal graph structure is an easy task from the implementer's point of view. Rules, requiring only local information, carried out by the networked devices themselves instead of a centralized instance, have a low computational complexity, are therefore easy to implement, and have moderate hardware demands. The prerequisite for the implementation is of course to find out the set of rules that yield a graph structure that is (close to) optimal for the given application. Finding the corresponding rules is the crux of the matter. As we have seen, minor changes to the update rules of networked game dynamics can result in significant differences of the emerging network structures. For technological applications distributed network engineering algorithms are desirable, however, as applications differ in premises and requirements, update rules will have to be adapted to specific problems. This suggests to find a more systematic way of changing the update rules to allow interpolation between the self organized graph structures, and thereby enable coverage of a broader range of applications.

Trying to find an update rule variant that allows for a smooth interpolation between classes of emergent network structure, is the subject of this chapter. We will refer to update rules as *tunable* update rules, if they allow to interpolate between the emerging structures in a continuous way by means of few, ideally a single, parameter. As we have seen in the previous chapter, the outcome of the prisoner's dilemma, with its unique dominant Nash equilibrium, does not depend on the parameters in the payoff matrix, as long as they obey the inequalities that characterize the prisoner's dilemma. For this reason, here we will use a game with multiple Nash equilibria for the pairwise interaction between the players, the iterated prisoner's dilemma (IPD). The IPD as a two players game and the used neighborhood exploration schemes are described in Section 4.1 and 4.2. The existence of network Nash equilibria for the given game and neighborhood exploration schemes is shown in Section 4.3, followed by numerical simulations to show, that these NNEs are in fact reached by the dynamics. Once more Section 4.4 picks up the concept of repeatedly perturbing network Nash equilibria until stationary states are reached. The emerging network structures are characterized in Section 4.5, and Section 4.5 puts the idea of using the described dynamics to influence the global performance

4. Iterated prisoners dilemma network game

of a network to a test.¹

4.1. Iterated Prisoner's Dilemma (IPD)

Recall from Section 3.1, that the prisoner's dilemma is defined by its payoff matrix \mathcal{P}_{PD} (3.1) based on the strategy choices $\mathcal{S}_{\text{PD}} = \{C, D\}$. The Inequalities (3.2) and (3.3) define the allowed ranges for the entries of \mathcal{P}_{PD} and result in the single Nash equilibrium of defection on both sides. The fact, that the unique Nash equilibrium of the PD, which is carried over to the networked version with the neighborhood modifying update rule, and the dynamics from one NNE to the next, are independent of the parameters in \mathcal{P}_{PD} , makes the networked PD not well suited as a network creation game, as it can not be adapted to a specific task. Although the emerging graph structures are an interesting subject to study, for the application as a network creation game it is important for a dynamic to be tunable, to allow control of the emerging structures. Through repetitive play of the game, the prisoner's dilemma can be turned into such a game, which is the iterated version of the PD, the so called iterated prisoner's dilemma (IPD).

Assume, that two players encounter each other an infinite number of times, playing the prisoner's dilemma, still the Nash equilibrium is to defect. That changes when the ability to memorize the strategy choices of the opponent is introduced. In principle every player could have an arbitrarily large memory, but for simplicity we will assume, following Ebel and Bornholdt [2002a], a memory of size $m = 1$, which enables the player to memorize the opponents last strategy choice. Already this tiny memory allows the player to react to exploitation by the opponent appropriately. Now the player, by means of his memory, can be in three different states: remember being defected by the opponent in the last encounter, remember cooperation, or having no memory of a previous event, as it is the case for the first time the opponent is encountered. In each of these three states, the player can choose from two different actions $\{C, D\} = \mathcal{S}_{\text{PD}}$, resulting in $2^3 = 8$ behavioral patterns. Consequently the behavior of a player is completely described by a triple $(s_0, s_C, s_D) \in \mathcal{S}_{\text{PD}}^3 =: \mathcal{S}_{\text{IPD}}$, the set of these triples is the set \mathcal{S}_{IPD} of strategies of the iterated prisoner's dilemma. The first element of the triple s_0 defines the PD strategy chosen when there is no memory of a previous encounter, i.e. in the first PD game of a round of games, the so called *opening move*. The other two elements s_C and s_D respectively specify which strategy to choose when the opponent has been cooperating or defecting during the last encounter. The 8 triples that define the possible strategies of the IPD are listed in Table 4.1, along with names given to the strategies and, for convenience, an enumeration $1, \dots, 8$, that will be used from now on to specify IPD-strategies.

Consider for example player A choosing the *generous tit-for-tat* strategy ($s_A = 7$), defined by the triple $(s_0^A = C, s_C^A = C, s_D^A = D)$, and its opponent B playing the *always*

¹It should be noted, that to a large extent this chapter's contents culminated in a publication in the *New Journal of Physics* [Scholz and Greiner, 2007].

Table 4.1.: Each of the eight strategies of the IPD game comes with an opening move s_0 as well as the responses s_C and s_D to a previous C and D move of the opponent.

\mathcal{S}	(s_0, s_C, s_D)	name
1	(D,D,D)	always defect
2	(D,D,C)	suspicious anti tit-for-tat
3	(D,C,D)	suspicious tit-for-tat
4	(D,C,C)	suspicious cooperate
5	(C,D,D)	generous defect
6	(C,D,C)	generous anti tit-for-tat
7	(C,C,D)	generous tit-for-tat
8	(C,C,C)	always cooperate

defect strategy ($s_B = 1$), defined by ($s_0^B = D, s_C^B = D, s_D^B = D$). Consequently, in the opening move strategy $s_0^A = C$ meets $s_0^B = D$, resulting in a payoff $\mathcal{P}_{PD}(C,D) = S$ for player A. In the second move, the player A remembers a defecting opponent and therefore chooses $s_D^A = D$, whereas player B chooses $s_C^B = D$. The payoff of A in the second and all subsequent moves is $\mathcal{P}_{PD}(D,D) = P$. The payoff collected by player A during a total number of n PD interactions with B is the sum of these payoffs $\mathcal{P}_{IPD}(7, 1) = S + (n - 1)P$. For simplicity we are interested in the IPD with an infinite number of moves, i.e. $n \rightarrow \infty$, where $\mathcal{P}_{IPD}(s_A, s_B)$ obviously diverges, therefore we define $\mathcal{P}_\infty(s_A, s_B) := \lim_{n \rightarrow \infty} \mathcal{P}_{IPD}(s_A, s_B)/n$, which for the example above is $\mathcal{P}_\infty(7, 1) = P$.

Generally, the IPD's payoff matrix \mathcal{P}_{IPD} is calculated from the PD's payoff matrix \mathcal{P}_{PD} in a recursive manner:

$$\mathcal{P}_{IPD}(s^A, s^B) = \mathcal{P}_{PD}(s_0^A, s_0^B) + \mathcal{P}_{PD}(s_{s_0^B}^A, s_{s_0^A}^B) + \mathcal{P}_{PD}(s_{s_{s_0^A}^B}^A, s_{s_{s_0^B}^A}^B) + \dots \quad (4.1)$$

$$= \mathcal{P}_{PD}(s^A(1), s^B(1)) + \sum_{t=2}^n \mathcal{P}_{PD}(s^A(t), s^B(t)), \quad (4.2)$$

with recursively defined strategy choices of player A and B $s^A(t) = s_{s^B(t-1)}^A$ and $s^B(t) = s_{s^A(t-1)}^B$, anchored at $t = 1$ through the opening moves $s^A(1) = s_0^A$ and $s^B(1) = s_0^B$, respectively. For an infinite number of interactions, the average payoff per interaction is

$$\mathcal{P}_\infty(s^A, s^B) := \lim_{n \rightarrow \infty} \frac{\mathcal{P}_{IPD}(s^A, s^B)}{n}. \quad (4.3)$$

For times $t \geq 2$ the players have the knowledge of the opponent's previous strategy, because of this, from time $t = 2$ on, the two players are in one of the four states of

4. Iterated prisoners dilemma network game

the 2×2 state space $\mathcal{S}_{PD} \times \mathcal{S}_{PD}$. The deterministic behavior of the players assures, that once a state is reached that has been reached before, the sequence of chosen PD strategies will be in a limit cycle. It follows from the finite size of the state space, that it can take at most 4 PD moves to re-reach a previously visited state, so the system is guaranteed to be in the limit cycle at time $t = 2 + 4$. As length of this limit cycle is obviously bounded by the number of states in the state space, the terms in the sum of Equation (4.2) have to repeat with a period length of 4 or less time steps from $t = 6$ or earlier, which comes handy when determining the payoffs analogously to the case of strategy 7 encountering strategy 1 described above.

Collecting the payoff values for the 64 combinations of strategies, we arrive at the full 8×8 average payoff matrix of the iterated prisoner's dilemma:

$$\mathcal{P}_\infty = \begin{pmatrix} P & T & P & T & P & T & P & T \\ S & \frac{P+R}{2} & \frac{P+S+R+T}{4} & T & S & T & \frac{T+P+S+R}{4} & T \\ P & \frac{P+T+R+S}{4} & P & R & P & \frac{T+R+S+P}{4} & \frac{T+S}{2} & R \\ S & S & R & R & S & S & R & R \\ P & T & P & T & P & T & P & T \\ S & S & \frac{S+R+T+P}{4} & T & S & \frac{R+P}{2} & \frac{R+T+P+S}{4} & T \\ P & \frac{S+P+T+R}{4} & \frac{S+T}{2} & R & P & \frac{R+S+P+T}{4} & R & R \\ S & S & R & R & S & S & R & R \end{pmatrix}. \quad (4.4)$$

In the larger payoff matrix of the IPD it's not as obvious as in the PD which strategies are the cooperating, and which are the defecting ones. To identify strategies that deserve to be called cooperative or defective, we determine which strategy of the PD is played more often, once two players with the same IPD strategy have reached the limit cycle. Following this definition, a cooperative strategy s_C yields payoff $\mathcal{P}_\infty(s_C, s_C) = R$ and a defective strategy s_D yields $\mathcal{P}_\infty(s_D, s_D) = P$. From Equation (4.4), we find strategies $\{4, 7, 8\}$ to be cooperative and $\{1, 3, 5\}$ to be defective. For strategies 2 and 6 it's undecided, and these strategies indeed result in alternating C and D moves during the recursion.

The iterated prisoner's dilemma with an infinite number of steps, as characterized by it's payoff matrix \mathcal{P}_∞ , has several combinations of strategies that are Nash equilibria: $(1, 1)$, $(5, 5)$ and $(1, 5)$ consisting of defective, and $(7, 7)$ consisting of cooperative strategies. The derivation of the Nash equilibria is postponed to Section 4.3, where they are found as a byproduct while looking for network Nash equilibria.

Putting the IPD on a network, we proceed in the same way as with the PD in Section 3.2. Players $p_i \in \mathcal{P}$ are identified with vertices $v_i \in \mathcal{V}$ of a graph $\mathcal{G}(\mathcal{V}, \mathcal{E})$. The players connected by the edges \mathcal{E} encounter each other, playing the game $\mathcal{D} := \mathcal{D}(\mathcal{S}_{IPD}, \mathcal{P}_\infty)$ and the payoff of player i is the sum of payoffs $p_i := p_i^*$ resulting from interactions with the neighbors as defined in Equation (3.5). When players update their strategy, we let them choose the best response strategy, given in Equation (3.8).

4.2. Neighborhood Exploration Schemes

Apart from the concrete game that is played on the network, the next crucial constituent of a network game is the way in which the players are allowed to modify the network structure. In principle players may be able to change large portions of the network structure at any time, however, as our main motivation is to find rules that are to a high degree locally confined, we restrict the changes that a player can initiate to changes of his immediate surrounding. The precise rule that players have to adhere is what we will call the *neighborhood exploration scheme*. As we have already seen in Section 3.4, details of these rules can have significant impacts on the properties of the emerging networks. To increase the covered search space, we use four conceptually similar schemes, sharing the common feature of conserving the updating player's degree.

The first aspect that distinguishes the schemes from each other, is the concrete specification of the connectivity update, where we consider two variants. Both variants have the conservation of the total number of edges in the network in common and achieve this by locally conserving the updated vertex's degree. After a player p has added Δk edges, and thereby increased his degree from k to $k' = k + \Delta k$, the player has to remove the same number Δk of edges from his neighborhood. To achieve an optimal outcome for the player, the edges to be removed are selected among the adjacent edges in increasing order of the payoff contributed to p 's payoff, i.e. the edge $e_{p,i}$ with $i = \arg \min_{j \in \mathcal{N}(p)} \mathcal{P}(s_p, s_j)$ is removed first. There is an exception to this rule if the edge to be removed were the last remaining edge of p , then a random edge $e \in \mathcal{E}$ is removed instead. The connectivity update variants' differences lie in the way of choosing the vertices to connect to. Here we distinguish *new vertex exploration* (NVE) and *new edge exploration* (NEE). In new vertex exploration, the updating player p chooses, among all players it is not yet connected to, one player $i = \arg \max_{j \in \mathcal{V} \setminus \mathcal{N}(p)} \mathcal{P}(s_p, s_j)$, that yields the maximal payoff for p . The new edge exploration scheme (NEE) does not consider which vertex may be the best to connect to, but which pair of connected vertices maximizes the players payoff if new edges are created from p to the two vertices connected by an edge $e = \arg \max_{e_{i,j} \in \mathcal{E}} (\mathcal{P}(s_p, s_i) + \mathcal{P}(s_p, s_j))$.

The second aspect of an update scheme determines how updates of the strategy and updates of the neighborhood are interwoven. Again we distinguish two variants, which we denote by respectively prefixing OR or XOR to the scheme's name. The prefixes stem from the analogy to the logic operations OR (inclusive disjunction) and XOR (exclusive disjunction, exclusive or). In the XOR-variants, the strategy and topology updates take place separated from each other: The player first updates his strategy while keeping the connectivity fixed and subsequently the player may, keeping his strategy fixed, try to maximize his payoff by modifying his connectivity. Once the connectivity is updated, the player may again update his strategy. The OR-variants of the update schemes maximize the payoff by adapting strategy and connectivity simultaneously. Note that for the PD on networks, as

4. Iterated prisoners dilemma network game

described in Section 3.3, distinguishing between OR and XOR updating does not make a difference, as, because of the unique Nash equilibrium, the best response strategy does not depend on the neighborhood of the player.

Combining the variants of interweaving of strategy and topology updates (OR and XOR) and the variants of connectivity updates (NVE and NEE), we end up with four schemes, XOR-NVE, OR-NVE, XOR-NEE, and OR-NEE, which we will investigate in the following sections.

4.3. Existence of NNEs

Given a game, a strategy update rule, and a neighborhood exploration scheme, the existence of Network-Nash equilibria (NNEs), as defined by Ebel and Bornholdt [2002b] and described in Section 3.3, is not clear a priori. In this section we show the existence of NNEs for the IPD under the best response strategy update defined by Equation (3.8) and the neighborhood exploration schemes introduced in Section 4.2.

To show that a certain subset $\mathcal{S}_{\text{NNE}} \subseteq \mathcal{S}_{\mathcal{D}}$ of all strategies that are possible in a game \mathcal{D} is a network Nash equilibrium, we first check whether \mathcal{S}_{NNE} qualifies as a Nash equilibrium. If this is the case, we can proceed to check if it is a network Nash equilibrium under the given neighborhood exploration scheme.

A set of strategies comprises a Nash equilibrium, if no single player can increase his payoff by an unilateral change of his strategy $A \in \mathcal{S}_{\text{NNE}}$ to any other available strategy $A' \in \mathcal{S}_{\mathcal{D}}$. This will generally depend on the number of neighbors and their choice of strategies, and on the numerical values of the PD payoffs, as an increase of payoff in one interaction may be compensated by a decrease in another. A situation, where the strategies that are allowed in a Nash equilibrium depend on the topology is shown in Figure 4.1.

To show the existence of Nash equilibria, we consider the sufficient, although not necessary,² case, where none of the payoffs gained from the interaction with any neighbor, with any strategy $B \in \mathcal{S}_{\text{NNE}}$ increases. \mathcal{S}_{NNE} is a Nash equilibrium, if

$$\mathcal{P}(A, B) \geq \mathcal{P}(A', B) \quad \forall \quad A, B \in \mathcal{S}_{\text{NNE}}, A' \in \mathcal{S}_{\mathcal{D}}. \quad (4.5)$$

²Since the notation of *sufficient* and *necessary* conditions is crucial for the present arguments, recall: Let the statement S be true, if the conditions A and B are fulfilled $A \wedge B \rightarrow S$, then for S to be true, both A and B are *necessary* conditions. However, if only one (say A) is fulfilled, S is not true, as A is not a *sufficient* condition. Let, as another example, the statement S be true, if at least one of the conditions A or B are fulfilled $A \vee B \rightarrow S$, then either condition is *sufficient* for S to be fulfilled. But neither A nor B are *necessary* for S , as if for example A is true, then for S to be true it is not necessary that B is true. To sum up, a condition can be *necessary* but not *sufficient* for a statement, and a condition can be *sufficient* for a statement even if it is not *necessary*. If a condition is both *necessary and sufficient* for a statement, the statement is true, *if and only if* (often abbreviated as *iff*) the condition is true. In that case condition and statement are said to be logically equivalent.

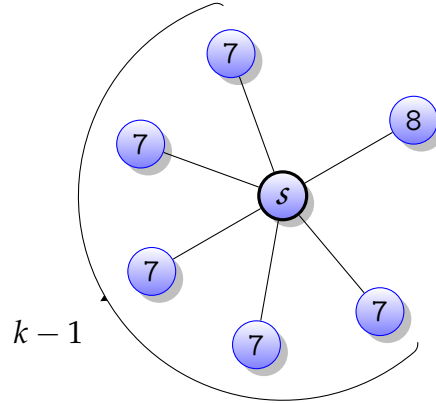


Figure 4.1.: A topology dependent Nash equilibrium of the IPD. Depending on its degree k , the choice of strategy $s = 7$ for the highlighted player, given $k - 1$ neighbors with strategy 7 and one with 8, may or may not be a Nash equilibrium. The highlighted player's payoff is $p^*(s) = (k - 1)\mathcal{P}_\infty(s, 7) + \mathcal{P}_\infty(s, 8)$. This player will switch his strategy s from 7 to 5, if $p^*(7) < p^*(5)$, in which case $s = 7$ is not a Nash equilibrium. Substituting the payoffs in the inequation we get $k(R - P) < T - P$. For $k = 1$, according to Inequation (3.2), this is always fulfilled, i.e. the strategy $s = 7$ is not a Nash equilibrium. For degrees larger than 1, the switch to 5 depends on the values of P , R , and T from the PD's payoff matrix \mathcal{P}_{PD} .

4. Iterated prisoners dilemma network game

Restricting the investigation to the subset of inequations with $A = B \in \mathcal{S}_{\text{NNE}}$ leads to

$$\mathcal{P}(B, B) \geq \mathcal{P}(A', B) \quad \forall \quad B \in \mathcal{S}_{\text{NNE}}, A' \in \mathcal{S}_{\mathcal{D}}, \quad (4.6)$$

which is a necessary condition to fulfill Inequation (4.5). Although (4.6) is obviously not a sufficient condition for (4.5), as the inequations for $A \neq B$ are necessary to be fulfilled as well, it provides a convenient way of ruling out strategies: For a strategy to comprise a topology independent Nash equilibrium in the sense of Inequation (4.5) its entry on the diagonal of the payoff matrix has to be greater than or equal to all payoffs in its column.

Considering the IPD, with its set of strategies $\mathcal{S}_{\mathcal{D}} = \mathcal{S}_{\text{IPD}} = \{1, \dots, 8\}$ as listed in Table 4.1, and its payoff matrix (4.4), it turns out that strategies 3, 4 and 8 fail to satisfy (4.6) because of the constraints given by Inequation (3.2). Strategies 2 and 6 fail because $\frac{P+R}{2} < R$ and $R < T$. The only strategies that satisfy (4.6) are 1, 5 and 7, which is obvious for strategies 1 and 5, as $P > S$. For strategy 7 Inequation (3.3) assures $R \geq \frac{T+S}{2}$ and term wise comparison of

$$\frac{T+S}{4} + \frac{R+P}{4} < \frac{2R}{4} + \frac{R+R}{4} = R$$

shows that R is indeed the largest value in the 7th column. For a strategy set with one member $|\mathcal{S}_{\text{NNE}}| = 1$, A and B of Equation (4.5) are equal by definition, making Equations (4.5) and (4.6) equivalent for those cases. Therefore the strategy sets $\{1\}$, $\{5\}$, and $\{7\}$ comprise Nash equilibria. On top of that, the set $\{1, 5\}$ obeys (4.5), while $\{1, 7\}$ or $\{5, 7\}$ don't, as for example

$$\underbrace{\mathcal{P}(5, 7)}_{=P} \not\geq \underbrace{\mathcal{P}(4, 7)}_{=R},$$

i.e. a player with strategy 5 encountering 7 will switch to strategy 4 (or 7, or 8, as they all result in a payoff of R) to maximize its payoff.

To assure that \mathcal{S}_{NNE} is a network Nash equilibrium with respect to the XOR-NVE scheme, it has to be shown that, apart from Inequation (4.5), a change in neighborhood does not increase the payoff. Regarding the change in payoffs, the neighborhood exploration is equivalent to a change of the opponent's strategy $B \in \mathcal{S}_{\text{NNE}}$ to another strategy $B' \in \mathcal{S}_{\text{NNE}}$ to be found in the network. Formally, \mathcal{S}_{NNE} is a XOR-NVE NNE, if Inequation (4.5) holds and

$$\mathcal{P}(A, B) \geq \mathcal{P}(A, B') \quad \forall \quad A, B, B' \in \mathcal{S}_{\text{NNE}},$$

which is, due to the symmetry in the arguments, equivalent to the equality

$$\mathcal{P}(A, B) = \mathcal{P}(A, B') \quad \forall \quad A, B, B' \in \mathcal{S}_{\text{NNE}}. \quad (4.7)$$

The Equality (4.7) is trivially fulfilled by single element strategy sets $|\mathcal{S}_{\text{NNE}}| = 1$, and, consulting (4.4), by the combination of strategies $\mathcal{S}_{\text{NNE}} = \{1, 5\}$ as well.

Within the OR-NVE scheme, agents explore strategy and neighborhood changes at the same time, to maximize their payoff. Again the increase of payoff in one interaction may generally be compensated by a decrease in other interactions. To proof the mere existence of NNEs it is sufficient to demand that not a single payoff of a player's interactions gets decreased during the exploration. Merging these requirements for strategy and neighborhood we get the sufficient but not necessary conditions for the existence of NNEs in the OR-NVE exploration scheme

$$\mathcal{P}(A, B) \geq \mathcal{P}(A', B') \quad \forall \quad A, B, B' \in \mathcal{S}_{\text{NNE}}, A' \in \mathcal{S}_{\mathcal{D}}. \quad (4.8)$$

The set of strategies explored by the active node A' can be split in $A' \in \mathcal{S}_{\text{NNE}}$ and $A' \in \mathcal{S}_{\mathcal{D}} \setminus \mathcal{S}_{\text{NNE}}$, leading to two expressions

$$\mathcal{P}(A, B) = \mathcal{P}(A', B') \quad \forall \quad A, A', B, B' \in \mathcal{S}_{\text{NNE}}, \quad (4.8a)$$

$$\mathcal{P}(A, B) \geq \mathcal{P}(A', B') \quad \forall \quad A, B, B' \in \mathcal{S}_{\text{NNE}}, A' \in \mathcal{S}_{\mathcal{D}} \setminus \mathcal{S}_{\text{NNE}}. \quad (4.8b)$$

The corresponding conditions for NNEs with respect to the XOR-NVE scheme (4.5) and (4.7) are subsets of (4.8) for $B = B'$ and of (4.8a) for $A = A'$, respectively. Thereby these conditions are necessary prerequisites to fulfill (4.8), starting from the few strategy sets that guarantee XOR-NVE NNEs it is easily seen, that the strategy sets that fulfill the conditions for NNEs for the XOR-NVE scheme, fulfill the conditions for OR-NVE NNEs as well. Analogue argumentation shows, that for both NEE schemes these strategy sets guarantee network Nash equilibria.

The previous paragraphs proof, that indeed network Nash equilibria exist with respect to the investigated strategy updates and neighborhood exploration schemes. However, it is not guaranteed, that, starting from an arbitrary initial network and strategy configuration, the NNEs are indeed reached through repeated application of the update rules, as the system might get stuck in a periodic limit cycle. Extensive numerical, agent based simulations of the update processes show, that the NNEs *are* in fact reached. For the simulations, we fix

$$S = 0, \quad P = 1, \quad R = 3, \quad (4.9)$$

to commonly used values [e.g. [Axelrod and Hamilton, 1981](#), [Ebel and Bornholdt, 2002a](#)] and keep T as a free parameter that we will vary within the bounds $3 < T < 6$ given by Inequation (3.2).

For demonstration, the variant with the XOR-new-vertex-exploration scheme is applied to an initial BA-scale-free network [[Albert and Barabási, 2002](#)], where each vertex has been randomly assigned one out of the eight possible IPD strategies. For the payoff parameter $T = 4$ Figure 4.2a illustrates the degree distribution obtained from the first NNE. It differs significantly from the initial scale-free distribution. A similar finding holds for the strategy distribution. As can be seen in Figure 4.2b it is no longer homogeneous. By far the most frequent strategy is 7, generous tit-for-tat. Two other cooperative strategies occur with small frequency although they are not present in the \mathcal{S}_{NNE} strategy set determined during the proof of the

4. Iterated prisoners dilemma network game

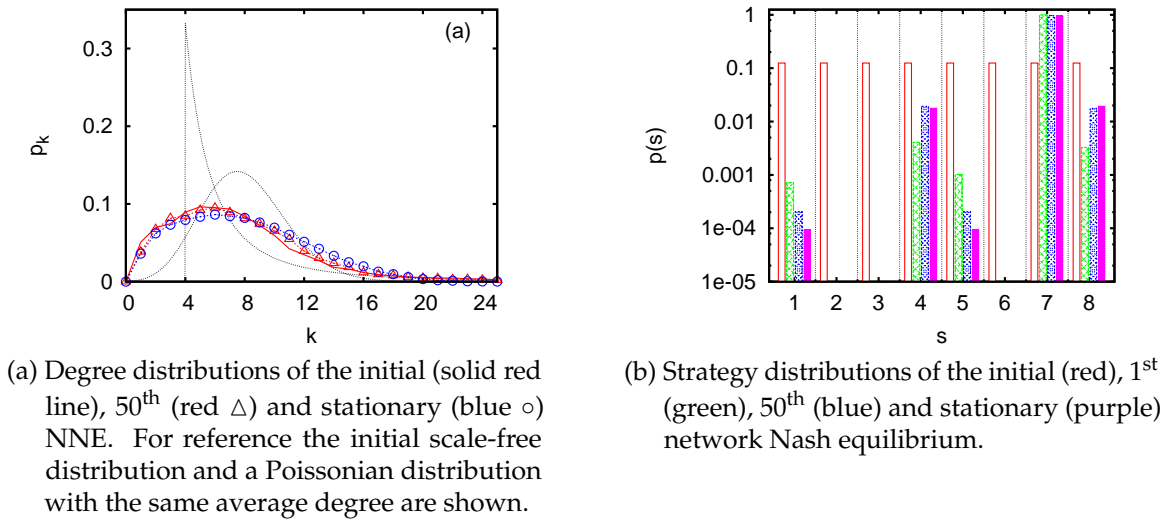


Figure 4.2.: Vertex degree and strategy distributions obtained from the IPD network creation game with the XOR-NVE scheme. The figures show averages of an ensemble of 200 realizations of scale-free graphs of size $N = 100$ with an average degree $\langle k \rangle = 8$, constructed through preferential attachment, as proposed by Barabási and Albert [1999]. Here the payoff parameters are $S = 0$, $P = 1$, $R = 3$, and $T = 4$.

existence of NNEs. This emphasizes the effects of the networks topology on the abundance of strategies, as has been argued in Figure 4.1. Defective strategies are highly suppressed through the generous tit-for-tat strategy’s ability to fight back against the defective strategies and cooperate with the cooperative strategies.

4.4. Perturbation dynamics of NNEs

As shown in Figure 4.2a, applying the update schemes to a graph of connected IPD players, results in a massive reconfiguration of the network structure until a network Nash equilibrium is reached. Once an NNE is reached, the system is by definition in a stable state. Analogous to Section 3.3 let’s now investigate the reactions of the system to perturbations in the form of forcing a player to use a suboptimal strategy.

Following a perturbation, the dynamics of the strategy and topology updates sets in again until eventually the next NNE is reached. We repeat the procedure of perturbation and subsequent stabilization into a NNE convergence over and over and refer to the NNE following the t^{th} perturbation step as the t^{th} NNE, the NNE reached after starting from the initial network structure and strategy distribution is consequently called the 0^{th} , or initial NNE. Apart from the initial NNE, Figure 4.2a

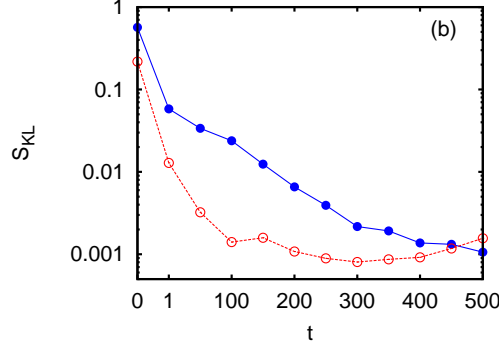


Figure 4.3.: Kullback-Leibler entropy (4.10) of the NNE degree distributions with respect to the stationary NNE degree distribution as a function of the NNE number. As initial distributions a BA scale-free distribution (blue ●) and a Poissonian (red ○) have been chosen.

also shows subsequent NNE. With increasing NNE number t the distributions $p_k(t)$ converge to an asymptotic form $p_k(\infty)$. To quantify the convergence towards the final degree distribution Figure 4.3 shows the difference of the degree distribution $p_k(t)$ at time t to the stationary degree distribution denoted as $p_k(\infty)$. The difference is calculated using the Kullback-Leibler entropy

$$S_{\text{KL}}(p_k(t), p_k(\infty)) = \sum_k p_k(t) \ln \left(\frac{p_k(t)}{p_k(\infty)} \right), \quad (4.10)$$

which is a measure of difference between two probability distributions. The two curves represent different initial network structures, namely a BA scale-free network and a random Poisson network with the same average degree $\langle k \rangle$. Independent of the initial network structure, the asymptotic form $p_k(\infty)$ is reached at approximately $t \approx 500$. We refer to NNEs in this asymptotic regime as the stationary NNEs.

It is interesting to study the dynamics from one stationary NNE to the next one in more detail. We define a strategy-based average Hamming distance

$$H_{\text{strategy}} = \left\langle \sum_{i=1}^N (1 - \delta(s_i(t+1), s_i(t))) \right\rangle_t \quad (4.11)$$

between two subsequent NNEs. H_{strategy} counts the average number of players, whose strategy in the newly reached NNE differs from the one used before the perturbation. It does not consider the number of strategy switches *during* the avalanche of updates.

As shown in Figure 4.4a the strategy-based Hamming distance H_{strategy} appears to be surprisingly small. Despite a weak dependence on the payoff parameter T its values lie around $H_{\text{strategy}} \approx 2$. The reason for this small value becomes clear by looking again at Figure 4.2b. For the stationary NNEs the strategy distribution is

4. Iterated prisoners dilemma network game

almost entirely peaked in the generous tit-for-tat strategy. Consequently, for most subsequent NNEs, almost all vertices use strategy 7 before the perturbation and do so again afterward.

Similar to Equation (4.11) we also define an edge-based Hamming distance

$$H_{\text{structure}} = \left\langle \sum_{i=1}^N \sum_{j=i+1}^N (1 - \delta(a_{ij}(t+1), a_{ij}(t))) \right\rangle_t \quad (4.12)$$

between two subsequent NNEs. It counts the number of edges, that have been removed from or added to the network by the topology updates, by counting the altered entries in the network's adjacency matrix a_{ij} . Note that moving an edge, i.e. deleting an edge between and adding one in a different location, contributes to the edge-based Hamming distance with magnitude 2. Figure 4.4b reveals that the edge-based Hamming distance is significantly larger than its strategy-based counterpart and shows a strong increase with the payoff parameter T .

The two Hamming distances H_{strategy} and $H_{\text{structure}}$ ignore events that take place during the sequence of strategy and topology changes. To investigate the relation of the number of changes during an avalanche, we define the avalanche size as the number of vertices, that either evoke a change of strategy or neighborhood between two consecutive NNEs. Figure 4.4c shows the average avalanche size in dependence of payoff parameter T . The distribution of avalanche sizes shown in Figure 4.5 shows non Gaussian distributions, as have already been observed for strategy avalanches on fixed networks by [Ebel and Bornholdt \[2002a\]](#).

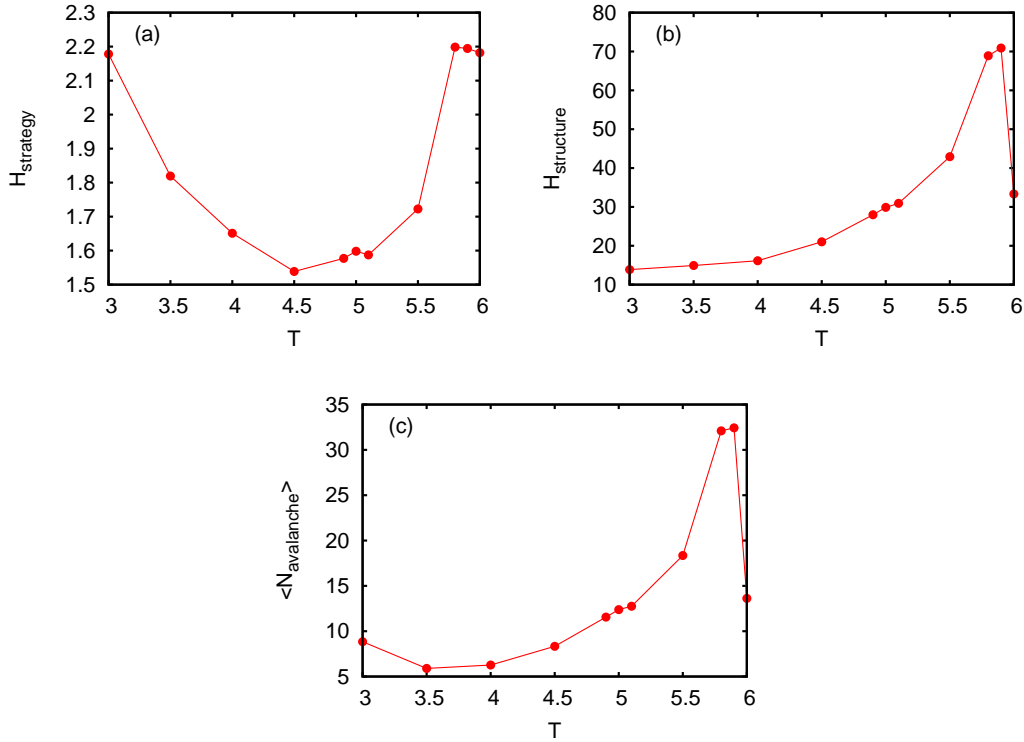


Figure 4.4.: (a) Strategy-based Hamming distance (4.11), (b) edge-based Hamming distance (4.12) and (c) average avalanche size between two consecutive stationary NNEs obtained from the IPD network creation game with the XOR-NVE scheme. Each curve has been sampled over 20 independent realizations. The size of the network has been fixed to $N = 100$ vertices and an average degree of $\langle k \rangle = 8$.

4. Iterated prisoners dilemma network game

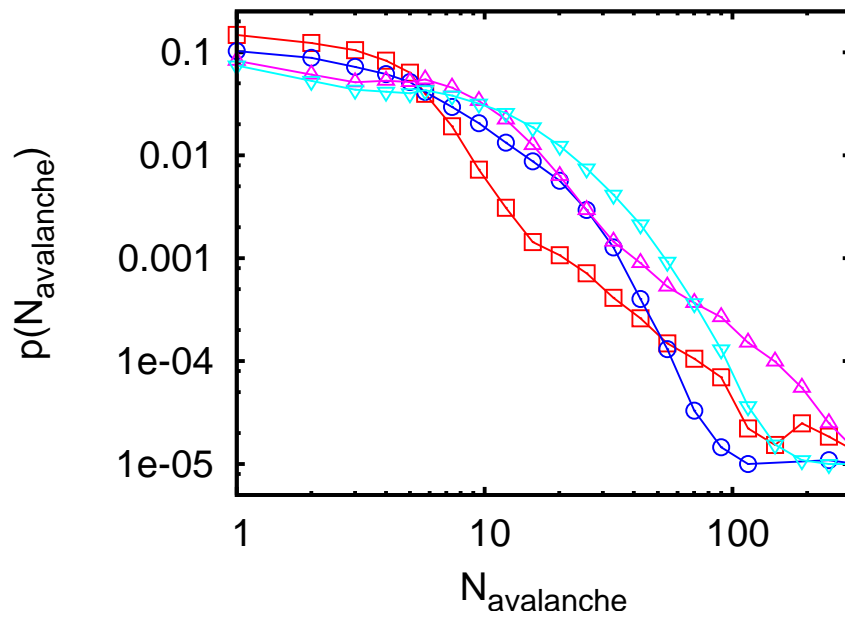


Figure 4.5.: Avalanche size distributions between two consecutive stationary NNEs obtained from the IPD network creation game with the XOR-NVE scheme and $T = 3$ (red \square), $T = 4$ (blue \circ), $T = 5$ (purple \triangle), $T = 6$ (light blue ∇). Each curve has been sampled over 20 independent realizations. The size of the network has been fixed to $N = 100$ vertices and an average degree of $\langle k \rangle = 8$.

4.5. Properties of stationary NNEs

Qualitatively, the results of Section 4.4 also carry over to other payoff parameter values and to the other neighbourhood exploration schemes. We will now examine the quantitative differences of the respective stationary NNEs.

Figure 4.6 depicts the degree distributions. For all neighbourhood exploration schemes they show a dependence on the chosen value for the payoff parameter T . For the XOR-new-vertex-exploration scheme the degree distribution is close to a Poissonian for $T = 3$, becomes broader for larger T and evolves into a two-hump structure for $T = 6$. For the OR-new-vertex-exploration scheme the trend is opposite. For $T = 3$ the distribution is broadest and evolves in direction of a Poissonian for larger T .

The Poissonian has to be viewed as a reference distribution, as it is the stationary result of a local random edge exchange, where a randomly picked vertex builds up an edge to a randomly picked non-neighbour and removes an edge to a randomly picked neighbor [Scholz et al., 2005]. In this respect, the results of Figure 4.6a and b clearly show, that the game component of the IPD network creation game introduces a new quality, which goes beyond restructuring of the network using only a topology update rule without a game.

The degree distributions resulting from the two new-edge-exploration schemes are illustrated in Figure 4.6c and d. The XOR variant produces little variation for most T values. Only close to $T = 6$ a noticeable variation occurs. All distributions come with a pronounced tail towards large degrees, but are not scale-free. A reference distribution is also shown, which results from a pure new-edge randomization, where a randomly picked vertex builds up new edges to the two vertices of a randomly picked edge and removes the same amount of edges to randomly picked old neighbors. Although some small differences are noticeable, this distribution remains close to the XOR distribution in the regime $3 \leq T \leq 5$. In this regime the game component of the IPD network creation game has only a small influence.

The degree distributions resulting from the OR-new-edge-exploration scheme show more variation with T . For values between $T = 3$ and 4 the respective distributions $p_k \sim k^{-\gamma}$ appear to be scale-free with a finite-size cutoff towards very large degrees. The scale-free exponent is approximately $\gamma \approx 1.1$. For larger T values the degree distribution develops half-way in direction of a Poissonian, only to be left in a two-hump structure at $T = 5$.

Another structural property of the stationary NNEs to look at is the average degree-dependent cluster coefficient $\langle \mathbb{C} | k \rangle$, defined in Equation (2.20). The results for the four different neighborhood exploration schemes of the IPD network creation game are shown in Figure 4.7. For the variant with the OR-new-vertex exploration the cluster coefficient does not show a k dependence. However, we notice a dependence on the payoff parameter. The cluster coefficient is a decreasing function with T and for $T \approx 5$ approaches the value $\langle \mathbb{C} \rangle \approx \langle k \rangle / N$ of the reference Poissonian network obtained from a local random edge exchange. This trend is in accordance with the trend observed in the respective degree distribution, which

4. Iterated prisoners dilemma network game

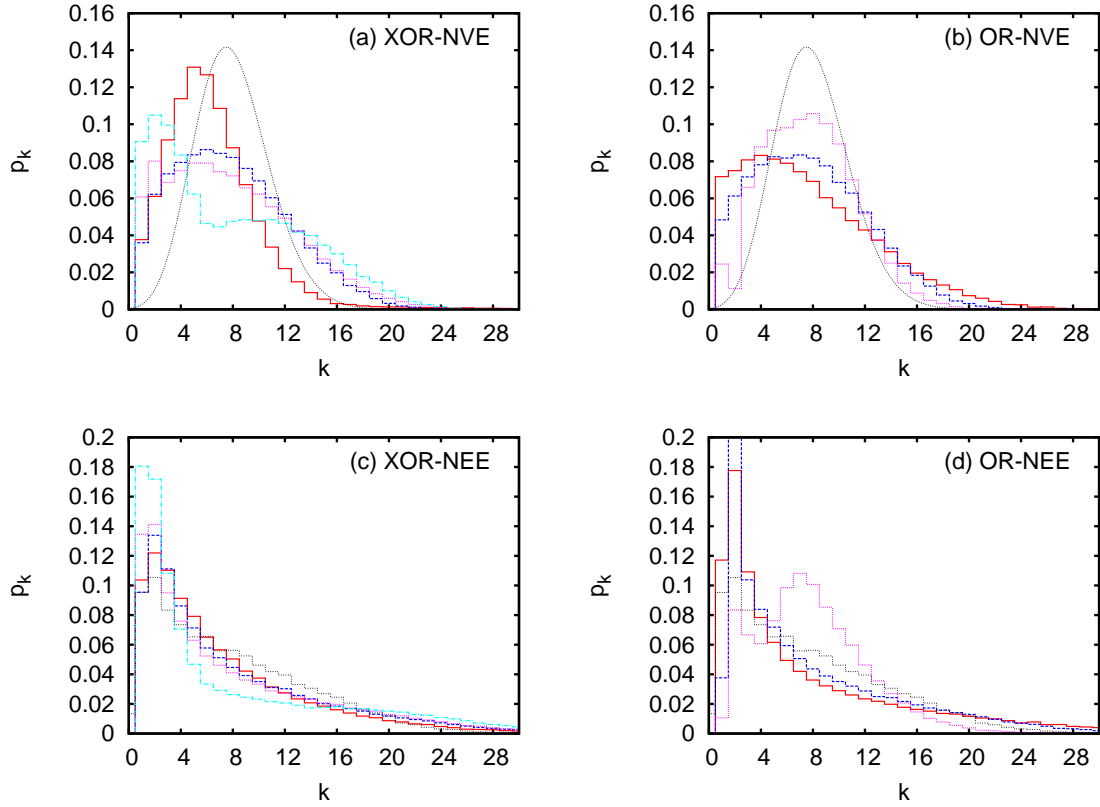


Figure 4.6.: Degree distributions for stationary NNEs obtained from the IPD network creation game with the (a) XOR-NVE, (b) OR-NVE, (c) XOR-NEE and (d) OR-NEE scheme. The T -dependence is shown as $T = 3$ (red —), $T = 4$ (blue - -), $T = 5$ (purple ···), and (for XOR variants) $T=6$ (light blue -·-). Each curve has been sampled over 400 independent realizations. For reference a Poissonian (dotted black) is shown in (a), (b) and the distribution (dotted black) resulting from a new-edge randomization is shown in (c), (d). The size of the network has been fixed to $N = 100$ vertices and an average degree of $\langle k \rangle = 8$.

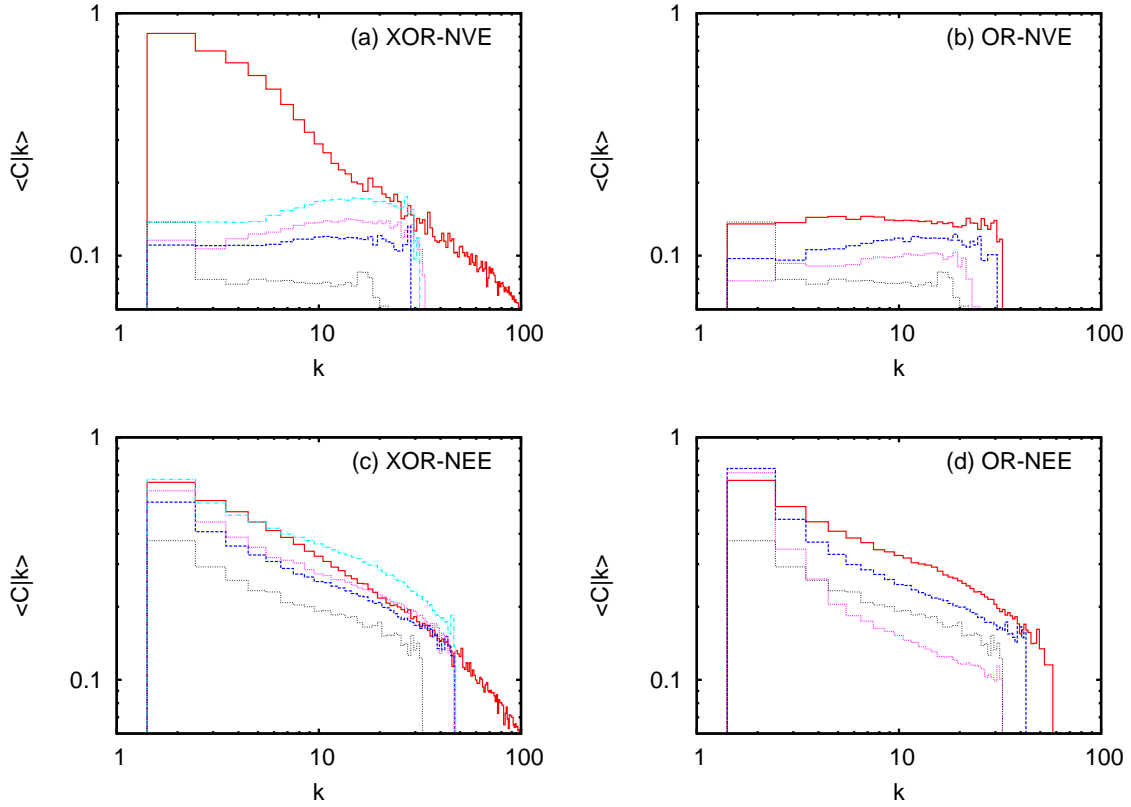


Figure 4.7.: Degree-dependent cluster coefficient $\langle C|k \rangle$ obtained from the IPD network creation game with the (a) XOR-NVE, (b) OR-NVE, (c) XOR-NEE and (d) OR-NEE scheme. The T -dependence is shown as $T = 3$ (red —), $T = 4$ (blue - -), $T = 5$ (purple ···), and (for the XOR variants) $T=6$ (light blue -·-). Each curve has been sampled over 400 independent realizations. In (a), (b) a reference $\langle C|k \rangle$ is shown in black resulting from a random edge exchange; in (c), (d) the reference in black is the outcome of a new-edge randomization. The size of the network has been fixed to $N = 100$ vertices and an average degree of $\langle k \rangle = 8$.

4. Iterated prisoners dilemma network game

has been exemplified in Figure 4.6b.

Except for $T = 3$, an analogous picture arises for the variant with the XOR-new-vertex exploration. The cluster coefficient shows almost no dependence on the vertex degree. It is an increasing function with T . For $T \gtrsim 3$ slightly larger than 3 the cluster coefficient is close to the value $\langle \mathbb{C} \rangle \approx \langle k \rangle / N$ of the reference Poissonian network. Again, this trend is consistent with the trend observed in the respective degree distribution of Figure 4.6a. However, the payoff value $T = 3$ appears to be singular. The cluster coefficient reveals a power-law dependence $\langle \mathbb{C} | k \rangle \sim k^{-\delta}$ with exponent $\delta \approx 0.66$. We have carefully checked by extensive simulations that this power-law is immediately lost once the payoff parameter $T \gtrsim 3$ is chosen just slightly larger than three. We can not offer an explanation for this singular finding.

The cluster coefficients obtained from the new-edge exploration schemes turn out to be much larger than for the new-vertex exploration schemes. This is explained by the fact, that acceptance of a newly explored edge always introduces a new triangle. For all payoff parameters T , although with differing quality, the cluster coefficient turns out to be a power-law function of the vertex degree. The exponent $\delta \approx 0.4$ as well as the order of magnitude of the cluster coefficient is the same as for the pure new-edge randomization, where a randomly picked vertex builds up a pair of new edges to the endvertices of a randomly picked edge and removes the same amount of edges to randomly picked old neighbors. Note however, that for both new-edge exploration schemes the absolute value of the cluster coefficient reveals a noticeable dependence on the payoff parameter T .

As announced in Chapter 3, let's take a brief glance on the use of the IPD network updates as a tool of distributed network optimization. The variant of closeness proposed by [Holme and Ghoshal \[2006\]](#)

$$s_i := \frac{c_i}{k_i} = \sum_{j \in \mathcal{V}(\mathcal{G})} (d(i, j) k_i)^{-1}, \quad (4.13)$$

which has already been given in Equation (2.12), combines two properties that might be desirable for nodes of social or technological networks. First, to be central in the network in a the sense, that other nodes can be reached via short paths as quantified by the closeness c_i . Second, to have low costs or efforts, quantified by the degree k_i . The combination of these properties, assigns a large value to nodes that are central and have a low degree at the same time. Figure 4.8 shows the dependence of the average value $\langle s \rangle$ on the parameter T of the payoff matrix. Compared to reference topologies of Poissonian and BA graphs $\langle s \rangle$ increases significantly for values of T between 3 and 4. Perhaps more important than the mere increase of $\langle s \rangle$ is the pronounced dependency of $\langle s \rangle$ on T . It is this property, that turns the present chapter into a proof of principle for the ability of local topology updates, coupled to game-like rules, to shape a network in a way that (positively) influences non-local properties of its graph structure. Moreover, through the dependency on the parameters of the game, in the present case T , the emerging topology can be specialized to tasks and functions imposed upon the network.

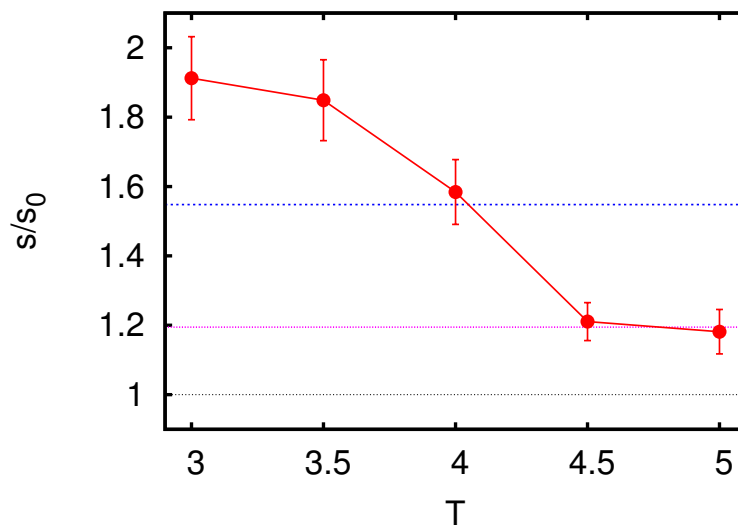


Figure 4.8.: Influence of the OR-NEE dynamic on the network performance measured by $\langle s \rangle$. The scale $\langle s \rangle$ is normalized to value for Poissonian graphs $\langle s \rangle_0$. From top to bottom the horizontal lines show $\langle s \rangle$ for the outcome of new-edge randomization (blue), i.e. just NEE-exploration without evaluation of payoffs, BA-graphs (purple), and Poissonian graphs (black).

5. Incentives for cooperation

The previous chapter showed, that by giving players a short-term memory and letting them play a game repeatedly, cooperation, manifested in the Tit-for-Tat strategy of the IPD, can be brought to the Prisoner's Dilemma on networks. An alternative approach that renders prevailing cooperation possible, pursued among others by [Nowak and May \[1992\]](#) and [Ohtsuki et al. \[2006\]](#), is changing the way players update their strategies from choosing the best response, see Equation (3.8), to imitation of the most successful neighbor, Equation (3.7). This effectively corresponds to less sophisticated players, as a best response player has to be aware of all possible strategies, whereas an imitator has to merely adopt an opponents strategy. While for technical applications the assumption of complete knowledge of strategies may be reasonable, regarding biological or social networks, this information may not be available to the players. In such situations, imitation of the most successful neighbor's strategy might be the best a player can do. An implication of this rule is that strategies may die out. Once the last player employing a certain strategy decides to switch to another strategy, his previous strategy will be gone from the system forever. For the imitating game dynamic, as proposed by [Ohtsuki et al. \[2006\]](#), the present chapter addresses the question whether it is possible to enhance the cooperativeness of the players by giving incentives and, if so, how to distribute the incentives effectively.

5.1. Underlying interaction model

The payoff matrix of the Prisoner's dilemma can be formulated in a way that emphasizes the role of cost c and benefit b for the players [e.g. [Ohtsuki et al., 2006](#)]. In this parametrization

$$\mathcal{P}_{\text{PD}} = \begin{pmatrix} b - c & -c \\ b & 0 \end{pmatrix} \quad (5.1)$$

of the PD payoff matrix, which has been introduced briefly as Equation (3.4), the benefit is the amount a player gets, when encountering a cooperator, in contrast to zero payoff when encountering a defector. On the other hand, the cost corresponds to the invest a cooperator spends when entering the game, while a defector does not invest anything. To fix the absolute magnitude of the payoff we normalize the average payoff

$$(\mathcal{P}(C,C) + \mathcal{P}(C,D) + \mathcal{P}(D,C) + \mathcal{P}(D,D))/4 = 1, \quad (5.2)$$

5. Incentives for cooperation

yielding $b = 2 + c$ as relation between cost and benefit.

The game is played on a network of N players $P = \{p_1, \dots, p_N\}$. Interactions take place between players that are neighbors in the network. The total payoff of a player $p_i \in P$ is the sum of payoffs

$$p(p_i) := p^*(p_i) = \sum_{j \in \mathcal{N}(p_i)} \mathcal{P}(s_i, s_j) \quad (5.3)$$

from interactions with the set of neighbors $\mathcal{N}(p_i)$, where the strategy of player p_i is given by $s_i \in \mathcal{S}_{PD} = \{C, D\}$.

Subject to an asynchronous update, the strategies of the players may change according to a *death-birth process* [Ohtsuki et al., 2006]. In each update step a random player p_i dies, leaving a vacant site i in the network. Now the neighbors $\mathcal{N}(p_i)$ compete to take over the empty site and to propagate their strategy to a new *born* player who will then inhabit site i . This competition for the site i is modeled by a stochastic selection with a probability proportional to the fitness $F(p_x)$ of the neighbors. The probability for a player $p_x \in \mathcal{N}(p_i)$ to win this competition is

$$\text{prob}(p_x) = \frac{F(p_x)}{\sum_{p_j \in \mathcal{N}(p_i)} F(p_j)}. \quad (5.4)$$

Once the winner of this competition p_x is determined, the strategy of the winner is copied to the new born player $s_x \rightarrow s_i$.

The fitness of a player p_x consists of a constant term, the baseline fitness, and the game's payoff:

$$F(p_x) = 1 - w + wp(p_x) = 1 + w(p(p_x) - 1). \quad (5.5)$$

The weighting factor w decides for strong ($w \approx 1$) or weak ($0 < w \ll 1$) selection. Weak selection accounts for the fact, that many factors contribute to the overall fitness of an individual, and that the game is only one of those factors.

To measure the cooperativeness of the PD with stochastic imitation strategy updates, the fixation probability ρ is used, see e.g. Wild and Taylor [2004]. Starting with a network full of defectors, with just one cooperator at a random position, ρ is defined as the probability, that this one cooperator turns all other players into cooperators through successive stochastic strategy updates. A fixation probability of $\rho = \frac{1}{N}$ is said to be neutral. If $\rho > \frac{1}{N}$, then the system favors cooperation. For the case of regular graphs and weak selection Ohtsuki et al. [2006] calculate the critical ratio

$$\frac{b}{c} = \langle k \rangle \quad (5.6)$$

in a mean field approximation and conclude, that for ratios $\frac{b}{c} > \langle k \rangle$ the fixation probability $\rho > \frac{1}{N}$, i.e. cooperation is favored. To ensure comparability we implement weak selection as well and fix $w = 0.01$ for the numerical simulations.

5.2. Incentive model and distribution strategies

From the critical ratio of benefit and cost in Equation (5.6) we see, that lowering the cost increases the fixation probability ρ , i.e. the system gets more cooperative the lower the cost of cooperation is. Here we investigate, whether lowering the cost on an individual basis can be more effective than lowering the cost globally.

To model individual modifications of the cost, we introduce ϕ_i , the incentive given to player p_i . Through this incentive, the cost of the player is reduced from c to $c_i = c - \phi_i$ and we now get an individual payoff matrix for player p_i :

$$\mathcal{P}_i := \begin{pmatrix} b - c_i & -c_i \\ b & 0 \end{pmatrix}. \quad (5.7)$$

As the players encounter costs for each interaction with their neighbors, the total amount of incentives Φ is given by the weighted sum of incentives:

$$\Phi = \sum_{p_i \in \mathcal{P}} \phi_i k_i. \quad (5.8)$$

Putting the sum of incentives in relation to the total sum of costs, we define the fraction f of incentives ϕ_i to costs c :

$$f := \frac{\sum_{p_i \in \mathcal{P}} \phi_i k_i}{\sum_{p_i \in \mathcal{P}} c k_i} = \frac{\Phi}{c \langle k \rangle N}. \quad (5.9)$$

To investigate the effect of the distribution of incentives among the players, we propose the following incentive distribution strategies that may be employed to assign the individual incentives ϕ_i to the players:

- Uniform distribution: $\phi_i = \frac{\Phi}{\sum_{j \in \mathcal{P}} k_j} = \frac{\Phi}{N \langle k \rangle}$ for all players.
- Distribution proportional to a centrality measure $C(i)$, see Section 2.1, resulting in incentives $\phi_i = \frac{\Phi}{\sum_{j \in \mathcal{P}} C(j) k_j} C(i)$.
- Selection of a percentage x (1%) of players $\mathcal{P}_{\text{top}} \subset \mathcal{P}$ that rank highest with respect to a centrality and distribute the incentives $\phi_i = \frac{\Phi}{\sum_{j \in \mathcal{P}_{\text{top}}} k_j}$ uniformly among those $n = |\mathcal{P}_{\text{top}}|$ players and $\phi_i = 0$ for those that are not in the top- x percent.

Centralities we investigate are the *degree centrality* ($C_d(i) = k_i$) as defined in Equation (2.2), where players are more central the more neighbors they have, and the *betweenness centrality* ($C_b(i) = b(i)$), see Equation (2.13).

5.3. Comparison of incentive distribution strategies

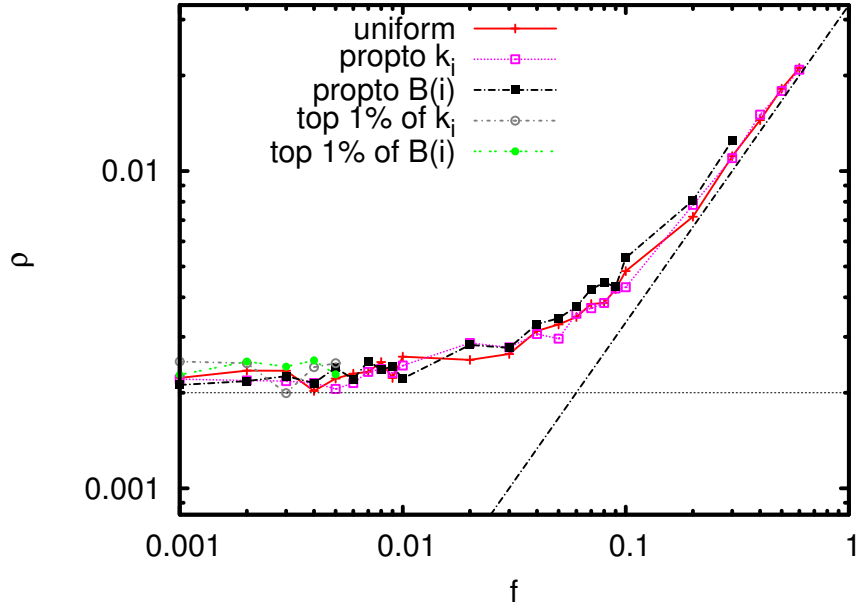
To compare the efficacy of the various incentive distribution strategies, we determine $\rho(f)$, the fixation probability's dependence on the factor f defined in Equation (5.9), numerically for square grids and BA scale-free networks. Square grids approximate regular graphs, except for the players located at the borders, very well and should therefore reproduce the fixation probability expected from the mean field calculations [Ohtsuki et al., 2006]. BA-networks on the other hand are a much better approximation to real social networks as they emerge from a growth process and exhibit a scale-free degree distribution, see Section 2.2.2. We fix the global parameters b and c according to the critical ratio $\frac{b}{c} = \langle k \rangle$ and the normalization of Equation (5.2). This assures, that in the mean field approximation for regular graphs the fixation probability is $\rho = \frac{1}{N}$, i.e. the system is neutral, it favors neither cooperation, nor defection.

The numerical determination of the fixation probability is done by injecting a cooperator at a random position in a network full of defectors and applying the stochastic update rule until all agents either cooperate or defect. This is done 10^3 times for each realization and repeated for 100 realizations, the fixation ρ is then determined by averaging over the ensemble. The used networks consist of $N = 484$ players for the square grid and $N = 500$ for BA-networks, both with an average degree $\langle k \rangle \approx 4$.

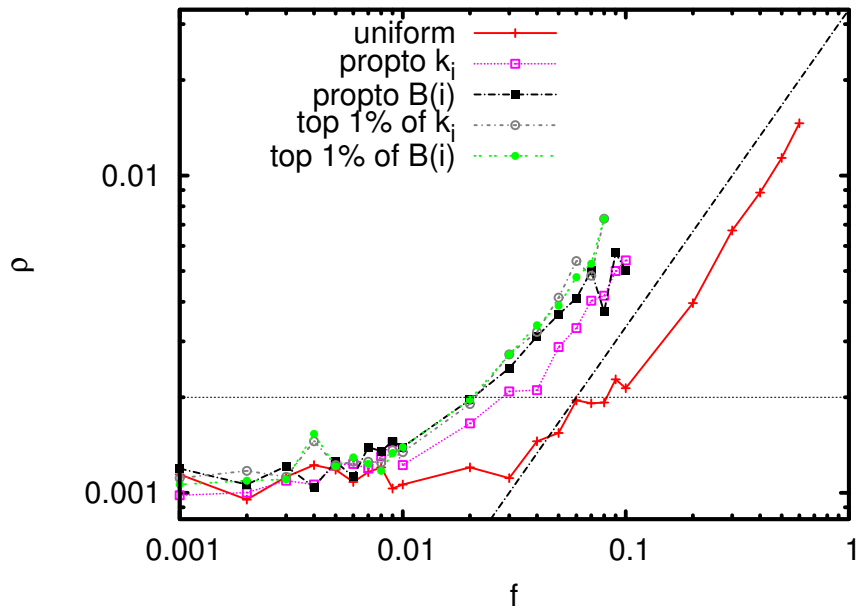
Figure 5.1 shows the numerically determined fixation probability ρ as a function of f , the ratio of the total incentives Φ to the total costs, as defined in Equation (5.9). It compares the effectiveness of the different incentive distribution strategies, by showing the different increases in ρ they result in. On the square grid the mean field fixation probability $\rho = \frac{1}{N}$ is reproduced very well by the numerical calculations, as can be seen in the low incentives $f \ll 1$ part of Figure 5.1a. With increasing incentives the fixation probability is increasing, first sublinearly, and from $f \gtrsim 0.1$ linearly. On the grid networks neither the choice of policy nor centrality has a big influence on the cooperation in the network. For this very homogeneous kind of networks what matters is the sum that invested, not how it is distributed.

With social networks in mind, scale-free BA networks, although still idealized, are much more interesting than the highly regular grids. Figure 5.1b shows the influence of incentive distribution strategies and the used centralities on the fixation probability ρ on BA networks. Here the fixation probability for very small incentives is well below the mean field estimation, as already observed by Ohtsuki et al. [2006]. Similar to the grid graphs, for increasing incentives a transition from sublinear increase to linear increase of ρ is observed. However, unlike for grid graphs, in the case of BA-networks, the choice of the incentive distribution strategy does make a difference: The top-1% policies, both for degree centrality and betweenness centrality, and the distribution proportional to the betweenness centrality result in a linear increase of ρ that is approximately a factor of 5 steeper, i.e. the same increase of cooperativeness can be achieved with a fifth of the investment. Distributing the incentives proportional to the degree is also a lot more effective than uniform

5.3. Comparison of incentive distribution strategies



(a) 22×22 chess board like grids with $N = 484$



(b) Scale-free BA-networks with $N = 500$

Figure 5.1.: Fixation probability ρ as function of the factor f of incentive sum to total costs, see Equation (5.9). The fixation probability is shown for regular grids with $N = 484$ vertices and scale-free BA-networks with $N = 500$, both with an average degree $\langle k \rangle = 4$. The dotted horizontal line marks the mean field fixation probability $\rho = \frac{1}{N}$ for regular graphs. As a reference, the dash-dotted line shows a linear proportionality $\rho \sim f$. Note, that the maximal possible value of f for a policy is determined by the constraint $c_i = c - \phi_i > 0$ for the personalized costs.

5. Incentives for cooperation

distribution, but falls slightly behind the other policies.

As demonstrated by [Ohtsuki et al. \[2006\]](#), prevailing cooperation is possible in the prisoner's dilemma on graphs with imitation of the best scoring neighbor as update rule, and that the cooperativeness can be enhanced by lowering the costs. Their results, however, hold only for the case of identical payoff matrices for all players. We show, by introducing incentives given to the players, which results in individualized payoff matrices, that on scale-free graphs the cooperation can be enhanced in a much more effective way, using the proposed incentive distribution strategies.

6. Communication throughput of networks

The transport process considered in the following chapters models the flow of data packets in communication networks. Communication networks are set apart from other transport processes on networks, for example electrons in electric resistor networks that follow Kirchhoff's law [Kirchhoff, 1847] and traded commodities, which are traditionally a subject of various maximal flow algorithms [Hu, 1969], by the fact, that the transported quantities are distinguishable. Every data packet has definite origin and target. A data packet that does not arrive at its target is of little use. To study the spacio-temporal dynamics of communication networks cellular automata like models of communication networks are used [e.g. Fukš and Lawniczak, 1999, Lawniczak et al., 2004]. In these and similar models, phase transitions from a free flowing phase to a jammed or congested phase are found for example by Solé and Valverde [2001] and Guimera et al. [2002]. Tadić et al. [2007] study the underlying graph topology's influence on the dynamic of the cellular automata's dynamic.

After the introduction of the used traffic model and the derivation of an analytic expression of the transport capacity of this model of communication networks, with Section 6.3 the present chapter highlights the influence of the clustering coefficient on the transport capacity.

As already apparent from this sections title and the previous paragraphs, in the context of communication networks it is common practice to talk of *networks* instead of graphs, *nodes* instead of vertices, and *links* instead of edges. For the purpose of the present work these can be considered synonyms and the following chapters generally try to adopt the network/node/link terminology.

6.1. Data Traffic Model and Load

To investigate the performance of a communication network with a topology given by a connected graph $\mathcal{G}(\mathcal{V}, \mathcal{E})$, consider a traffic model of data packets that can be moved along the links \mathcal{E} of the network. To map the transport process on a mathematical and numerical treatable description, we consider a model working in discrete time steps. In each time step, at nodes $s \in \mathcal{V}$ packages with destination $t \in \mathcal{V}$ are created with rates determined by the traffic matrix μ_{st} . The node s at which a packet is created is its *source*, the destination t is the *target*. At every time step the data packets can be transported from nodes to their neighbors, given the

6. Communication throughput of networks

bandwidth of the corresponding link is not yet exceeded. The bandwidth Ξ_{ij} of a link $e_{ij} \in \mathcal{E}$ determines the amount of traffic, approximated by the number of data packets, that the link e_{ij} can carry from i to j and, assuming symmetric links, from j to i in a single time step.¹ In the standard notation of queuing models, suggested by Kendall [1953], this queuing model is denoted as the M/M/k model.

To reach their destination the packets are routed along shortest paths, as defined in Equation (2.8). Multiple shortest paths $|\text{spaths}(s, t)| > 1$ may exist from the source s of a packet to its target t . In this case, a path $\mathcal{P} \in \text{spaths}(s, t)$ out of the set of shortest paths is selected randomly when the packet is created.

The amount of traffic a link $e \in \mathcal{E}$ has to carry is called its *load* L_e . The load on the link e resulting from packets with source i and target j is

$$L_e^{ij} = \frac{|\{\mathcal{P} \in \text{spaths}(i, j) : e \in \mathcal{E}(\mathcal{P})\}|}{|\text{spaths}(i, j)|} \mu_{ij}. \quad (6.1)$$

The total load of e is the sum over all vertex pairs

$$L_e = \sum_{i, j \in \mathcal{V}} \frac{|\{\mathcal{P} \in \text{spaths}(i, j) : e \in \mathcal{E}(\mathcal{P})\}|}{|\text{spaths}(i, j)|} \mu_{ij} \quad (6.2)$$

To further calculate the load, specification of the packet generation rates by means of the traffic matrix μ_{ij} is necessary. Unfortunately, for this observable no reliable data of a representative portion of the Internet is available and probably won't be available in the near future, because, as Krioukov et al. [2007] put it, measuring these quantities is "notoriously difficult". To get qualitative results, for the time being we assume uniform packet generation rates $\forall i, j \in \mathcal{V} : \mu_{ij} = \frac{\mu}{N-1}$, with $\mu_{ii} = 0$, such that the rate of packet creation at a node v_i is $\mu_i = \sum_{j \in \mathcal{V}} \mu_{ij} = \mu$ and the total packet generation rate of the whole network is $N\mu$. With the assumption of uniform μ_{ij} , i.e. on average every node sends the same number of packets to every other node, Equation (6.2) factorizes to

$$L_e = \frac{\mu}{N-1} \sum_{i, j \in \mathcal{V}} \frac{|\{\mathcal{P} \in \text{spaths}(i, j) : e \in \mathcal{E}(\mathcal{P})\}|}{|\text{spaths}(i, j)|}. \quad (6.3)$$

The terms in the sum correspond to the probability, for a packet with source i and destination j , to be routed over e . We identify the sum with the betweenness centrality b_e of the edge, introduced by Freeman [1977] and given in Equation (2.14), and abbreviate

$$L_e = \frac{\mu}{N-1} b_e. \quad (6.4)$$

¹In principle a bandwidth should be assigned to the nodes as well, accounting for example for limited computing power. However, today's network technology generally operates in full-duplex mode, i.e. data may be transmitted and received on all links simultaneously, which renders the links the limiting elements. Especially as the upgrade of a node with insufficient computing power is much less costly than installing additional network connections, this idealization of unlimited node bandwidth is plausible.

6.2. Derivation of Throughput Capacity T_{e2e}

The networks end-to-end throughput performance T_{e2e} is defined as the maximal number of packets that can be created across the whole network within a single time step without overloading any link. To calculate T_{e2e} , consider the links' loads L_e in relation to their bandwidths Ξ_e . As mentioned before, the bandwidth Ξ_e of a link $e \in \mathcal{E}$ determines the maximal number of packets it is able to carry per time step. The link's load L_e , on the other hand, specifies the number of packets that have to be carried by the link. In this model, as long as for all edges $e \in \mathcal{E}$ the load is less than the bandwidth

$$L_e = \frac{\mu}{N-1} b_e \leq \Xi_e \quad (6.5)$$

the network is in the *free flow* regime. For a sufficiently small packet generation rate μ this is clearly the case, however with increasing μ , for $\mu = \mu_{\text{crit}}$, there exists at least one edge e_{BN} , the *bottleneck*, for which

$$\frac{\mu_{\text{crit}}}{N-1} b_{e_{\text{BN}}} = \Xi_{e_{\text{BN}}}. \quad (6.6)$$

At the critical value of $\mu > \mu_{\text{crit}}$ traffic congestion will occur.

$$\mu_{\text{crit}} = (N-1) \frac{\Xi_{e_{\text{BN}}}}{b_{e_{\text{BN}}}}. \quad (6.7)$$

The bottleneck link e_{BN} is given by

$$e_{\text{BN}} = \underset{e \in \mathcal{E}}{\text{arg min}} \frac{\Xi_e}{b_e} \quad (6.8)$$

and the value of μ_{crit} is accordingly

$$\mu_{\text{crit}} = (N-1) \min_{e \in \mathcal{E}} \frac{\Xi_e}{b_e} = (N-1) \frac{\Xi_{e_{\text{BN}}}}{b_{e_{\text{BN}}}}. \quad (6.9)$$

Similar to the traffic matrix, measured data of the link bandwidths Ξ_e is not available, which makes us resort to assuming uniform bandwidths $\forall e \in \mathcal{E} : \Xi_e = \Xi$. Without further loss of generality, let $\Xi = 1$. With this approximation

$$\mu_{\text{crit}} = (N-1) \frac{\Xi}{\max_{e \in \mathcal{E}} b_e} = (N-1) \frac{\Xi_{e_{\text{BN}}}}{b_{e_{\text{BN}}}} \quad (6.10)$$

$$= \frac{N-1}{\max_{e \in \mathcal{E}} b_e} = \frac{N-1}{b_{e_{\text{BN}}}} \quad (6.11)$$

6. Communication throughput of networks

As μ_{crit} is the maximal packet creation rate that can be handled by the network without overloading the bottleneck, the throughput capacity T_{e2e} is defined as

$$T_{e2e} = N\mu_{\text{crit}} = \frac{N(N-1)}{\max_{e \in \mathcal{E}} b_e}, \quad (6.12)$$

which is the maximal number of packages that may be created per time step without traffic congestion, see [Scholz et al. \[2008\]](#).

For the dual case of limited node bandwidths and unlimited link bandwidths, the M/M/1 model in [Kendall's](#) notation, the corresponding throughput capacity has been derived and numerically verified by [Guimerà et al. \[2002\]](#) and [Krause et al. \[2004\]](#).

Compared to determining the transport capacity via an agent based simulation on a packet-by-packet basis, the pure graph theoretic expression for T_{e2e} is inevitable for a numerically feasible determination of a network structure's performance. Without such an approximation, further explorations of the influence of topology changes or link weights (see [Chapter 7](#)) wouldn't be possible within reasonable computational expenses.

6.3. Influence of network structure on data throughput

As an example of the dependence of T_{e2e} on the network structure, consider three simple networks, with betweenness centralities that are easy to calculate: A complete network, a star, and a double star. In a complete network, every node is connected directly to every other node, $\forall i, j \in \mathcal{V}(\mathcal{G}), i \neq j : \exists e_{ij} \in \mathcal{E}(\mathcal{G})$. The shortest path between two nodes i and j in such a network is trivial, $\text{spath}(i, j) = e_{ij}$, and contains just the edge that directly connects source and target. Accordingly the number of shortest paths that contain an edge e is 1, the betweenness centrality is $b_e = 1$, resulting in a throughput capacity $T_{e2e} = N(N-1) \approx N^2$, for large N . A star network, with one central node c and $N-1$ nodes connected to it, $\mathcal{E}(\mathcal{G}) = \{e_{ci} : i \in \mathcal{V}(\mathcal{G}) \setminus c\}$, has a betweenness centrality of $b_e = N-1$ for all edges. The throughput capacity of a star is therefore given by $T_{e2e} = N$. For a double star network, constructed by adding an edge e_c between the central nodes of two stars with the same number of vertices $\frac{N}{2}$, the betweenness centrality is slightly harder to calculate. Here from every node in the first star, $\frac{N}{2}$ shortest path to the nodes in the other star cross e_c . This results in $b_{e_c} = (\frac{N}{2})^2$ and $T_{e2e} = 4(N-1)\frac{1}{N} \approx 4$ for large N . Note the different scaling behaviors $T_{e2e} \sim N^\gamma$ of the three exemplified networks with scaling exponents $\gamma = 2, 1$, and 0 , respectively.

The computational complexity of naively determining the betweenness centralities (Equations [\(2.13\)](#) and [\(2.14\)](#)) is on the order of $\mathcal{O}(N^3)$. With the algorithm proposed by [Brandes \[2001\]](#), the complexity is lowered to $\mathcal{O}(NM)$, which makes

6.3. Influence of network structure on data throughput

the computation of the betweenness centrality, and hence the computation of T_{e2e} , for arbitrary network structures with $N \gtrsim 10000$ numerically feasible.

Figure 2.4 illustrates, that one of the most basic observables, the average $\langle \mathbb{C} \rangle$ of the clustering coefficient, as defined by Equation (2.10), sets AS Internet scans apart from the idealized models, represented by the BA-model and the configuration model. Using the geometric- p model, proposed in Section 2.3, that allows for tuning of $\langle \mathbb{C} \rangle$, the present section investigates the influence of the network structure on the throughput capacity T_{e2e} , putting an emphasis on clustering.

As exemplified above for the three archetypal topologies (complete graph, star, and double star) the scaling behavior of T_{e2e} with respect to the number of nodes N , depends strongly on the network structure. Figure 6.1 shows the dependency of T_{e2e} on the number of vertices N in the geometric- p network. Independent of the parameter p , the throughput capacity T_{e2e} scales with N as a power law $T_{e2e}(N) \sim N^\beta$ with $\beta \approx 0.5$. For BA networks Scholz et al. [2008] find the corresponding exponent $\beta \approx 0.3$, compare Figure 7.5b. With respect to this finding, the geometric- p model with a scale-free degree distribution characterized by $\gamma = 2.3$ and the BA model get located between the double star ($\beta = 0$) and the single star ($\beta = 1$).

Apart from the scaling of T_{e2e} with the system size, a clear dependence of T_{e2e} on the parameter p of the geometric- p model is visible in Figure 6.1. With increasing values of p , the throughput capacity T_{e2e} is decreasing. Recalling the relation of \mathbb{C} and p shown in Figure 2.6, we find that for the given scale-free degree distribution, networks generated by the geometric- p model have an increasing T_{e2e} for decreasing $\langle \mathbb{C} \rangle$. The throughput capacity is reduced roughly by a factor of 3 due to the transition from $p = 0$ to $p = 1$, which corresponds to a change of $\langle \mathbb{C} \rangle \approx 0.05$ to $\langle \mathbb{C} \rangle \approx 0.6$. This behavior can be explained by the fact, that in the geometric- p model the total number of links is implicitly given by the degree distribution, and is therefore independent of p . In the parameter regime of high clustering, nodes form small, densely interconnected local groups with a high redundancy of connections. Due to the fixed total number of edges in the network, the number of edges that connect geometrically separated regions is comparatively small, resulting in a high burden of load to be handled by these few edges.

6. Communication throughput of networks

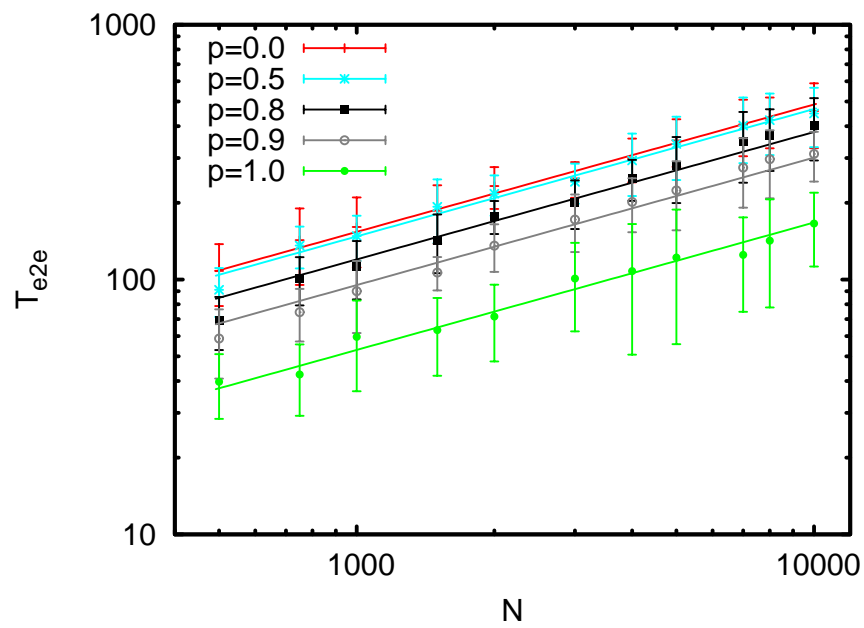


Figure 6.1.: Transport capacity T_{e2e} as a function of the number of vertices N for scale-free geometric- p networks with $\gamma = 2.3$ and varying values of p . The averages are each obtained from an ensemble of ten network realizations, the error bars show the standard deviation of the mean.

7. Advanced routing

Today's society relies heavily on communication networks, with their most prominent example being the Internet. Because of the ubiquitous permeation of everyday life in our modern world optimization of the traffic flow, resulting in more efficient and reliable utilization of communication networks in general and the Internet in particular, is of obvious interest. As demonstrated in the previous chapter, the underlying graph structure of a communication network has tremendous influence on its performance, measured by the throughput capacity. Attempts to optimize the throughput capacity T_{e2e} by changing the network structure include [Ferrer and Solé \[2003\]](#) and [Krause, Scholz, and Greiner \[2006\]](#).

There is, however, another approach to optimization of traffic throughput: Employing a routing metric and determination of the shortest paths with respect to the metric, with the intention of relieving the high loaded links of some of their load. Current Internet routing protocols [[Doyle, 1998](#)] can use various different metrics based on hop-count, bandwidth, actual load and round-trip time, reliability as well as cost. The drawback of current routing protocols like RIP (Routing Information Protocol), EIGRP (Enhanced Interior Gateway Routing Protocol), and OSPF (Open Shortest Path First), see [Malkin \[1998\]](#), [Cisco Systems, Inc. \[2005\]](#), and [Fortz and Thorup \[2000\]](#) respectively, is that these protocols are confined to the intra-AS level. The routing protocol used to select routes for traffic from one AS to the other is the Border Gateway Protocol (BGP) [[Rekhter and Li, 1995](#)]. The BGP allows to assign weights to routes, however this requires manual configuration, detailed knowledge of the network structure, and is implementation dependent. For a carefully configured router, selecting the shortest possible path is among the most important criteria for route selection, for routers in the default configuration it is even more so. For details of the implementation of the perhaps most prominent manufacturer of Internet routers, see [Cisco Systems, Inc. \[2006\]](#).

It is the goal of the present chapter to determine the potential of using appropriate metrics on the AS-level, as well as proposing candidates for such a metric.

We want to discuss various link-based weight assignments and find out which of them are most efficient with respect to the transport capacity of Internet-related networks. In [Section 7.2](#) we list several routing weight assignments for links, which are straightforward generalizations of their node-based precursors [[Yan et al., 2006](#), [Krause et al., 2006](#), [Schäfer et al., 2006](#), [Danila et al., 2006b](#)]. [Section 7.3](#) focuses on synthetic scale-free networks and discusses first consequences like load distributions and decorrelation effects between loads and degrees. Based on an analytic expression for the transport capacity of the network, the different routing weight assignments are rated according to their efficiency. [Section 7.5](#) sends a clear

7. Advanced routing

warning when trying to carry over the previously obtained results to synthetic Internet topologies at the AS level, and forces us to improve on the routing weight assignments. Real AS-level Internet topologies are discussed in Section 7.5 and it is shown that compared to BGP-like shortest-hop routing the most efficient new routing weight assignments are able to improve the overall transport capacity by a factor of about five.

7.1. Weights and metrics

As can be seen from the definition of T_{e2e} in Equation (6.12), the performance of a network is determined by the one link with the highest load, the so called bottleneck link. The aim of routing weights is to change the paths that are used to route a packet from its source to its destination in such a way, that bottlenecks are avoided. This can be achieved, by assigning weights to nodes and/or links and defining a weighted length of a path which is then used to determine the shortest paths.

The most general form of weights is a combination of node weights $\omega_i > 0$, $i \in \mathcal{V}(\mathcal{G})$ and link weights $w_e > 0$, $e \in \mathcal{E}(\mathcal{G})$. Equations (2.7) to (2.9) define path length, shortest paths, and distance for the unweighted case. With respect to node and link weights, the length of a path is

$$\text{length}(\mathcal{P}; \omega, w) := \sum_{v \in \mathcal{V}(\mathcal{P})} \omega_v + \sum_{e \in \mathcal{E}(\mathcal{P})} w_e. \quad (7.1)$$

The corresponding set of *shortest paths* is denoted as

$$\text{spaths}(s, t; \omega, w) := \underset{\mathcal{P} \in \text{paths}(s, t)}{\text{arg min}} (\text{length}(\mathcal{P}; \omega, w)). \quad (7.2)$$

The distance of two nodes is not simply the length of the shortest path connecting the nodes, but instead

$$d(s, t; \omega, w) := \min_{\mathcal{P} \in \text{spaths}(s, t; \omega, w)} |\mathcal{E}(\mathcal{P})|, \quad (7.3)$$

the number of edges in the shortest path. Which amounts to the number of hops it takes to get from s to t when the shortest path is determined with respect to the weights ω and w . Note, that every combination of node and link weights ω and w can be replaced by link weights W , constructed according to

$$W_{e_{ij}} = \frac{\omega_i}{2} + \frac{\omega_j}{2} + w_{e_{ij}}, \quad (7.4)$$

and node weights set to 0, without any effect on the shortest paths:

$$\text{spaths}(s, t; \omega, w) = \arg \min_{\mathcal{P} \in \text{paths}(s, t)} (\text{length}(\mathcal{P}; \omega, w)) \quad (7.5)$$

$$= \arg \min_{\mathcal{P} \in \text{paths}(s, t)} (\text{length}(\mathcal{P}; 0, W) + \frac{\omega_s}{2} + \frac{\omega_t}{2}), \quad (7.6)$$

$$= \arg \min_{\mathcal{P} \in \text{paths}(s, t)} (\text{length}(\mathcal{P}; 0, W)). \quad (7.7)$$

The equality of (7.6) and (7.7) holds, because the terms $\frac{\omega_s}{2}$ and $\frac{\omega_t}{2}$ are identical for all paths $\mathcal{P} \in \text{paths}(s, t)$ and therefore have no influence on the minimization. Ergo

$$\text{spaths}(s, t; \omega, w) = \text{spaths}(s, t; 0, W). \quad (7.8)$$

This asserts, that any configuration of node weights can be replaced by link weights constructed according to Equation (7.4), for the opposite direction this is not the case, as can be shown by a simple counterexample: Consider the graph $\mathcal{G}(\mathcal{V}, \mathcal{E})$ consisting of a single triangle, with vertices $\mathcal{V} = \{a, b, c\}$ and edges $\mathcal{E} = \{e_{ab}, e_{bc}, e_{ca}\}$. Let the edges be weighted such, that $w_{ab} + w_{bc} < w_{ca}$. The shortest path from a to c will then be the 2-hop path going over b . The length of the direct connection is $l_{ac} = \omega_a + \omega_c$ and the length of the connection including b is $l_{abc} = \omega_a + \omega_b + \omega_c$. For any choice ω of positive node weights, $l_{abc} > l_{ac}$ the direct connection will be the shorter, i.e. to get the considered path containing b as a shortest path between a and c is not possible using node weights. From this and Equation (7.8) we conclude, that the shortest paths accessible via node weights are a strict subset of those accessible with edge weights. For this reason, the remainder of this work will only consider the more general edge weights and we define:

$$\text{length}(\mathcal{P}; w) := \text{length}(\mathcal{P}; 0, w), \quad (7.9)$$

$$\text{spaths}(s, t; w) := \text{spaths}(s, t; 0, w), \quad (7.10)$$

$$d(s, t; w) := d(s, t; 0, w). \quad (7.11)$$

For positive weights $w_i > 0$, the distance $d(s, t; w)$ satisfies the characteristic conditions of a metric.¹ Although in the rigorous mathematical sense the weight vector w is not a metric, it is common to use the terms *metric* and *weight* synonymously, as the weights, through the definition of shortest paths define the distance and hence the metric.

Other graph theoretical observables like closeness, betweenness centrality, and throughput capacity are generally straight forward to convert to the case of shortest paths that are influenced by weights. In the possibility of ambiguity of weighted and unweighted quantities, the weighted ones will be labeled with the weight's identifier, as for example in T_{e2e}^w . However, if it is clear from the context, these labels will be omitted.

¹A metric has to satisfy the following conditions for all $i, j, x \in \mathcal{V}$: non-negativity: $d(i, j; w) \geq 0$, zero distance only for identical vertices: $d(i, j; w) = 0 \iff i = j$, symmetry: $d(i, j; w) = d(j, i; w)$, and the triangle inequality: $d(i, j; w) \geq d(i, x; w) + d(x, j; w)$.

7.2. Routing weight assignments

Recently the idea of using weights to influence the paths used in networks has been put to a test by several studies, e.g. [Yan et al. \[2006\]](#), [Krause, Scholz, and Greiner \[2006\]](#), [Schäfer, Scholz, and Greiner \[2006\]](#) and [Danila et al. \[2006b\]](#). These studies, however, confined themselves to the realm of node weights and did not take into consideration to associate weights with the links. As shown by the proof of Equation (7.8), the metrics that are accessible by using node weights are a subset of the metrics accessible by putting weights on edges. After briefly reviewing previously presented routing metrics and reformulating them to use the more appropriate link weights, the present section sheds some light on how these metrics influence shortest paths and the transport capacity T_{e2e} .

Hop metric The simplest of all metrics is the hop metric. It assigns the same value to all edge weights, without loss of generality this value is set to 1 and the hop metric is defined by

$$\forall e \in \mathcal{E} : w_e^{\text{hop}} = 1. \quad (7.12)$$

Using this metric, packets will be routed along those paths that result in the least number of node-to-node hops. Compare the definitions for unweighted and weighted path lengths (Equations (2.7) and (7.1)) to find, that Chapter 6, dealing with unweighted networks, implicitly makes use of the hop metric.

Degree metric As reported by [Goh et al. \[2001\]](#), [Barthélemy \[2003, 2004\]](#), the betweenness centrality of nodes in scale-free networks is positively correlated with their degree. Because of this connection of betweenness centrality and throughput capacity [Yan et al. \[2006\]](#) propose to use node weights proportional to the node degrees k :

$$\forall v \in \mathcal{V} : \omega_v^{\text{deg}} = k_v. \quad (7.13)$$

Using Equation (7.4) we get the corresponding edge weights

$$\forall e_{ij} \in \mathcal{E} : w_{e_{ij}}^{\text{deg}} = \frac{k_i}{2} + \frac{k_j}{2}. \quad (7.14)$$

Extremal metric [Danila et al. \[2006b\]](#) have proposed an extremal-optimization algorithm which explicitly strives for minimization of the maximal node betweenness. It does so, by iteratively adding weight to the node with the maximal betweenness centrality. The adaptation of this scheme to link weights leads to the link weights w_e^{extr} , which we refer to as the *extremal metric*. The iteration scheme is laid out in Algorithm 1.

A tremendous drawback of the extremal metric is its computational complexity, which is “extremal” as well. Calculating the betweenness centrality with weights

Algorithm 1 Extremal Link Load Metric

Initialize the link weights using the hop metric.

$$w_e \leftarrow w_e^{\text{hop}}$$

for $t = 1$ to T_{extr} **do**

Calculate all links' traffic load with respect to the weights, given by the betweenness centrality b_e^w .

$$L_e = b_e^w$$

Determine the highest loaded link $e_{\text{max}} = \arg \max_{e \in \mathcal{E}} L_e$ and increase its weight by one unit.

$$w_{e_{\text{max}}} \leftarrow w_{e_{\text{max}}} + 1$$

end for

The weights w_e after T_{extr} iterations are the weights of the extremal metric.

$$w_e^{\text{extr}} \leftarrow w_e$$

using the optimized algorithm proposed by [Brandes, 2001] requires a computation effort that scales roughly like $\mathcal{O}(N^2 \log N)$ for a fixed average degree $\langle k \rangle = \frac{2M}{N}$. Applying the algorithm $T_{\text{extr}} = M = |\mathcal{E}|$ times as suggested by Danila et al. [2006b] therefore yields a complexity $\mathcal{O}(N^3 \log N)$. This numerical complexity renders the extremal metric practically unusable for networks beyond $N > 3000$.

Smoothing metric Schäfer, Scholz, and Greiner [2006] propose to use the node betweenness centrality itself as node weights and use this weight assignment in the context of cascading failures in networks [Motter and Lai, 2002]. Like the extremal metric, this requires an iterative approach because the weights determine, by means of the shortest paths, the betweenness and the betweenness in turn determines the weights. Schäfer et al. [2006] observe a homogenization of the node betweenness, i.e. paths tend to get shifted from high betweenness nodes to low betweenness nodes. From this observation, the use as a routing metric in communication networks suggests itself. Carrying the scheme over into link betweenness and link weights, we arrive at the iteration described in Algorithm 2. Note, that weights from previous iteration steps are taken into account by the weight updating step to guarantee convergence of the weights, which will be discussed in detail in Section 7.4. The direct assignment $w(l; t + 1) = L(l; t)$ would lead to route flapping and no convergence. Schäfer et al. [2006] observe no major changes of the weights after the 10th iteration step, and consequently set $T_{\text{smoothing}} = 10$.

7. Advanced routing

Algorithm 2 Smoothing Link Load Metric

Initialize the link weights with the value of the average betweenness centrality

$$\langle b \rangle = \frac{1}{M} \sum_{e \in \mathcal{E}} b_e.$$

$$w_e \leftarrow \langle b \rangle$$

for $t = 0$ to $T_{\text{smoothing}}$ **do**

Calculate all links' traffic load, given by the betweenness centrality b_e^w .

$$L_e(t) = b_e^w$$

Update all link weights according to

$$w_e(t+1) = \frac{L_e(t) + tw_e(t)}{t+1}$$

end for

Use the weights of the last iteration $w_e(T_{\text{smoothing}})$ as weights of the smoothing metric.

$$w_e^{\text{smoothing}} \leftarrow w_e(T_{\text{smoothing}})$$

The small and constant number of iteration steps $T_{\text{smoothing}}$ of the smoothing metric results in a significant reduction of its numerical complexity compared with the extremal metric. The smoothing metrics complexity is given by the complexity of calculating the betweenness centrality $\mathcal{O}(N^2 \log N)$. As a consequence, applying the smoothing metric to networks with $N \gtrsim 10000$, e.g. graphs of the Internet on AS-level, is possible with reasonable computational resources.

7.3. Effects of metrics on distances and loads

To discuss some general consequences of the various routing weight assignments, we focus on scale-free networks of the BA-type [Barabási and Albert, 1999]. The average node degree is set to $\langle k \rangle = 6$, which roughly corresponds to the value observed in the AS-level Internet.

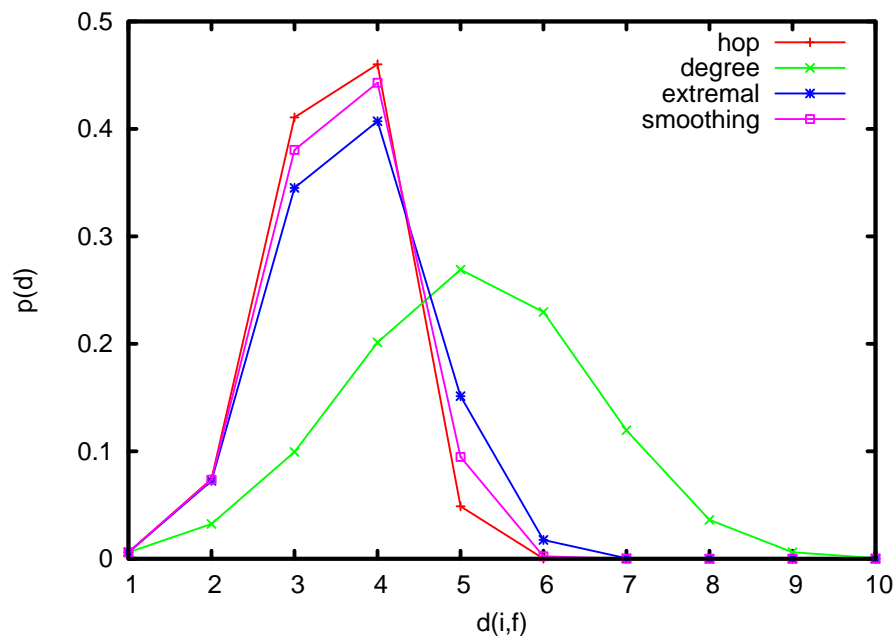
By definition, the minimal distance $d(i, j; w)$ between a pair of nodes $i, j \in \mathcal{V}$, see Equation (7.11), is the distance when shortest paths are determined with respect to the hop metric w^{hop} . For any other weight assignment $w \neq w^{\text{hop}}$ the distance is at least as long $d(i, j; w^{\text{hop}}) \leq d(i, j; w)$. The amount of increase, however, and the probability distribution of distances depends on the weight assignments, as shown in Figure 7.1a. In case of the degree metric w^{degree} the increase of distances compared with the hop metric is very pronounced. Respective routes avoid the high-degree nodes and detour into the periphery of the network. Comparatively small effects are observed for the extremal and smoothing metric.

The link load distributions are illustrated in Figure 7.1b. The hop metric leads to a fat-tailed distribution, a well-known result for scale-free networks [Goh et al., 2001, Barthélemy, 2003, 2004]. The load distribution resulting from the degree metric results in a pronounced increase for small link loads. Large link loads are overrepresented, compared to the hop metric, although the maximal load value is slightly smaller than the maximal value for the hop metric. As intended, the extremal metric removes load from the high loaded links and redistributes it to the other links. This leads to a distinct narrowing of the distribution towards the medium load regime. A similar result is found for the smoothing metric, justifying its name that stems from its ability of smoothing the loads across the network. The respective distribution is even slightly narrower, but the maximal load value is a little larger than for the extremal metric, however, it is still much smaller than for the hop and degree metrics. The attention paid to the maximal load value stems from its importance for the throughput capacity of networks, which is discussed thoroughly in Section 7.5.

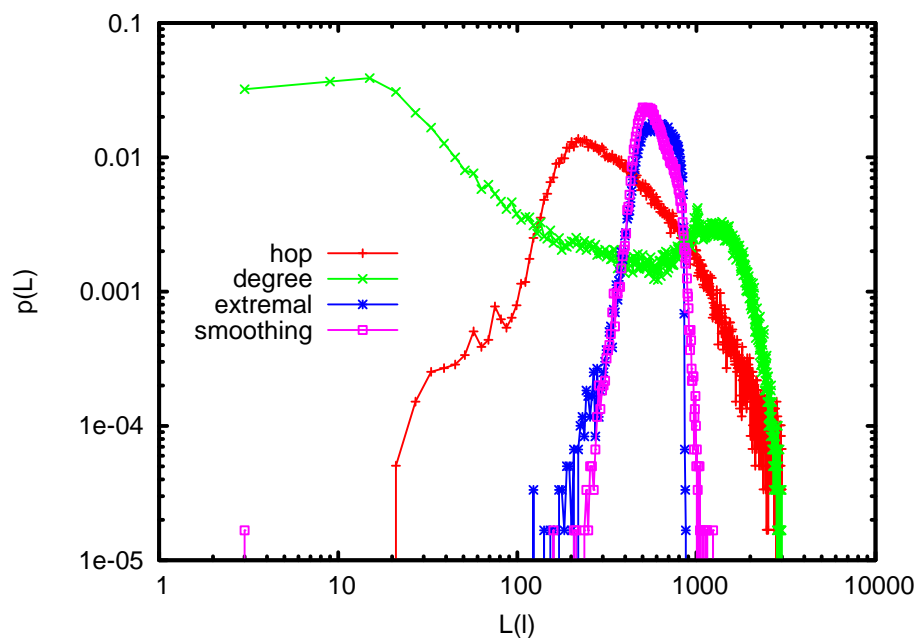
The results on the route lengths and load distributions are closely related to correlation effects between loading on the network and structure of the network. A measure for the correlation between load $L(n)$ and degree k_n of a node $n \in \mathcal{V}$ is the conditional moment

$$L(k) := \langle L_n | k_n = k \rangle \sim k^\beta. \quad (7.15)$$

7. Advanced routing



(a) Probability distribution of distances $p(d(i,j;w))$, with $i, j \in \mathcal{V}$.



(b) Probability distribution of link loads $p(L)$, with $L(l) = b_l^w$ and $l \in \mathcal{E}$.

Figure 7.1.: Probability distribution of hop distances (a) and link loads (b) for the metrics w^{hop} (hop), w^{degree} (degree), w^{extremal} (extremal), $w^{\text{smoothing}}$ (smoothing). An ensemble of 20 BA scale-free network realizations with $N = 1000$ nodes and an average degree $\langle k \rangle = 6$ has been used.

7.3. Effects of metrics on distances and loads

For a link the respective moment is conditioned on the product $\kappa = k_{n_1}k_{n_2}$ of degrees of adjacent nodes $n_1, n_2 \in \mathcal{V}$

$$L(\kappa) := \langle L_{n_1 n_2} | k_{n_1} k_{n_2} = \kappa \rangle \sim (k_{n_1} k_{n_2})^\Theta, \quad (7.16)$$

where k_{n_1} and k_{n_2} are the degrees of the two nodes connected by the link $e_{n_1 n_2} \in \mathcal{E}$. Figure 7.2 illustrates the two conditional moments resulting from the four link weight assignments w^{hop} , w^{degree} , w^{extremal} , and $w^{\text{smoothing}}$. Except for $L(k)$ and the degree metric, both moments show the power-law scaling indicated in Equations (7.15) and (7.16). The fitted exponents β and Θ are listed in Table 7.1.

To better understand the power-law scaling in Figure 7.2b, assume L_{ij} to be uncorrelated to k_i (and for symmetry not to k_j as well), then the conditioned average $L(\kappa)$ is independent of κ , hence $\Theta = 0$ for the uncorrelated case.

To understand the power-law scaling in Figure 7.2a, we need the approximate sum rule

$$L_i \approx \frac{1}{2} \sum_{j \in \mathcal{N}(i)} L_{ij}, \quad (7.17)$$

that relates the node load to the edge load. The rule holds, because any path that contains a node $i \in \mathcal{V}$ will contain two of the links adjacent to i , except for those paths that start or end at i and therefore contain only one of the links. Assume again, the link load to be uncorrelated to the node degrees, then the sum rule is reduced to $L_i \approx \frac{1}{2} k_i \langle L_{ij} \rangle$ and Equation (7.15) is approximated by

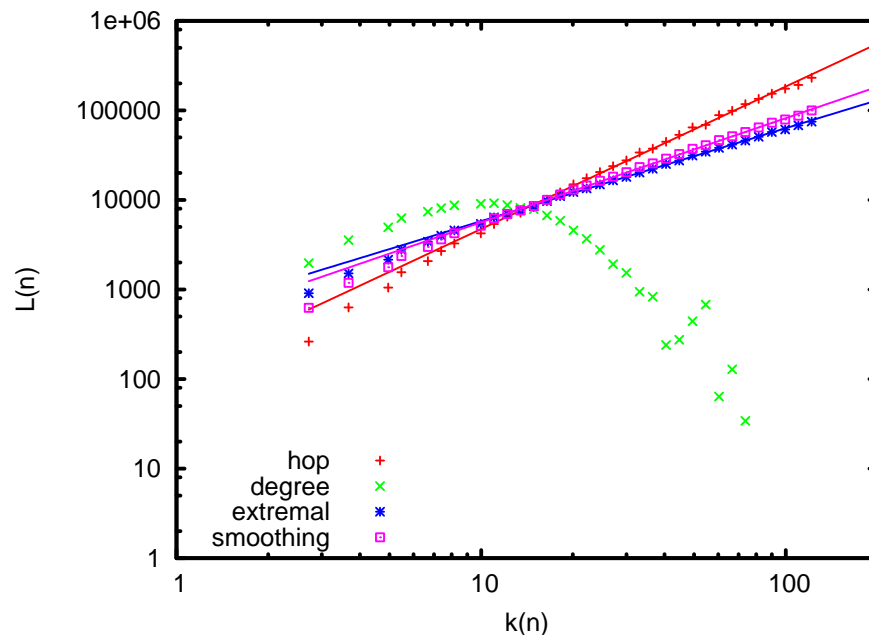
$$L(k) \approx \langle \frac{1}{2} k_i \langle L_{ij} \rangle | k_i = k \rangle \sim k^\beta, \quad (7.18)$$

with $\beta = 1$. Deviations from $\beta = 1$, $\Theta = 0$ indicate the existence of correlations between the load and the local network structure, as represented by the node degrees. For the hop weights these correlations are positive, expressing the fact that high-degree nodes and links have to carry exceptionally large loads when compared to low-degree nodes and links. For the degree weights these correlations turn out to be mostly negative. From low-degree to high-degree nodes there is a transition from positive to negative correlation. For links the correlations are continuously negative.

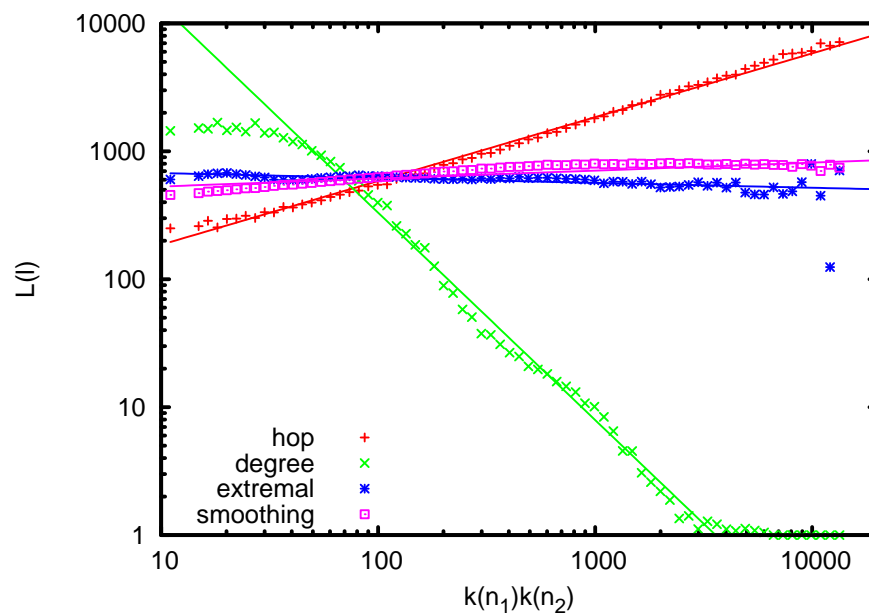
link weight	β	Θ
hop	1.59	0.50
degree	—	-1.62
extremal	1.03	-0.04
smoothing	1.16	0.06

Table 7.1.: Scaling exponents β and Θ of Eqs. (7.15) and (7.16) as fitted to the simulation data shown in Fig. 7.2.

7. Advanced routing



(a) Conditional moment $L(k)$, defined in Equation (7.15)



(b) Conditional moment $L(k_{n_1}k_{n_2})$, defined in Equation (7.16)

Figure 7.2.: Conditional moments $L(k)$, part (a), and $L(k_{n_1}k_{n_2})$, part (b), for the metrics w^{hop} (hop), w^{degree} (degree), w^{extremal} (extremal), and $w^{\text{smoothing}}$ (smoothing). An ensemble of 20 BA scale-free network realizations with $N = 1000$ nodes and an average degree of $\langle k \rangle = 6$ has been used. The straight lines are fits with scaling exponents listed in Table 7.1.

The two iterative weight assignments, the extremal and the smoothing metric, do not exaggerate like the degree weight assignment, but result in loads, that are to a large extent decorrelated from the node degrees, as reflected by the exponents $\beta \approx 1$ and $\Theta \approx 0$. All nodes and links are then about equally loaded, consult again Figure 7.1b. This leaves us with a speculation: those routing weight assignments which are able to decorrelate the network loading from the network structure will increase the transport capacity of the network the most. Sections 7.4 and 7.5 support this speculation.

7.4. Hybrid metric

The present section proposes a further metric, that we construct by a combination of the smoothing metric, originating in Schäfer, Scholz, and Greiner [2006], and the extremal metric proposed by Danila et al. [2006b], both in the variants adapted to link weights as described in Algorithms 1 and 2 of Section 7.2. This combination is motivated by Figure 7.3a, which shows the strengths of the two metrics and antedates the successful combination of the two to form, what we denote as the *hybrid metric*, see Scholz et al. [2008].

Figure 7.3a shows the dependency of the throughput capacity T_{e2e} , as introduced by Equation (6.12), during the iteration steps of Algorithms 1 and 2. The first thing to notice in the figure, is the leap of T_{e2e} during the first few iteration steps of the smoothing metric. This steep increase is followed by a saturation and indeed, like observed by Schäfer et al. [2006], approximately from the 10th iteration step on, no big changes occur anymore. On the other hand, the extremal metric shows a slow, but steady increase of T_{e2e} until around iteration $t = 1000$ the throughput performance of the smoothing metric is reached and T_{e2e} further improved upon. As the computational complexity for a single iteration step of smoothing and extremal metric is practically identical, the figure reveals, that the extremal metric requires about a hundred times more computational resources to achieve the throughput performance of the smoothing metric. To create an iteration scheme, that combines the fast computability of the smoothing metric and the superior T_{e2e} result of the extremal metric, the first guess would be, to initialize the weights according to the smoothing metric before starting the iterations of the extremal metric. However, this combination, which we may call the *additive hybrid metric*, is not successful.

A combination, that turns out to be very successful and results in a metric that is computationally feasible for networks with 10000 and more nodes, is very similar to the additive hybrid metric. The weights are initialized according to the smoothing metric at its 10th iteration step, followed by an iteration identical to the extremal metric, except that the weight of the highest loaded link $e_{\max} = \arg \max_{e \in \mathcal{E}} L_e$ is not increased by adding a constant value, but instead it is increased multiplicatively according to $w_{e_{\max}} \leftarrow 1.1 \cdot w_{e_{\max}}$. The iteration scheme of this metric, the *hybrid metric*, is detailed in Algorithm 3.

To further characterize what happens in the course of the three presented iterative

7. Advanced routing

Algorithm 3 Hybrid Metric

Assign link weights according to the smoothing metric (see Algorithm 2).

$$w_e \leftarrow w_e^{\text{smoothing}}$$

for $t = T_{\text{smoothing}} + 1$ to T_{hybrid} **do**

Calculate all links' traffic load with respect to the weights, given by the betweenness centrality b_e^w .

$$L_e = b_e^w$$

Determine the highest loaded link $e_{\max} = \arg \max_{e \in \mathcal{E}} L_e$ and increase its weight by 10%.

$$w_{e_{\max}} \leftarrow 1.1 \cdot w_{e_{\max}}$$

end for

The weights w_e after T_{hybrid} iterations are the weights of the hybrid metric.

$$w_e^{\text{hybrid}} \leftarrow w_e$$

metrics, we investigate the changes occurring to the routing matrix during the iterations. The routing matrix R determines, for every node $a \in \mathcal{V}$, which of its neighbors $v \in \mathcal{N}(a)$ is suitable as the next step for a packet with destination b . The elements R_{ab} of the routing matrix are sets of nodes

$$R_{ab}^w := \{v_1(\mathcal{P}) : \mathcal{P} \in \text{spaths}(a, b; w)\}, \quad (7.19)$$

where $v_1(\mathcal{P})$ is the node of a path \mathcal{P} which is adjacent to its initial vertex. To quantify the changes of the routing matrix caused by the change in weights from the previous iteration time step $t - 1$ to the current t , we count the changes of entries in the routing table according to:

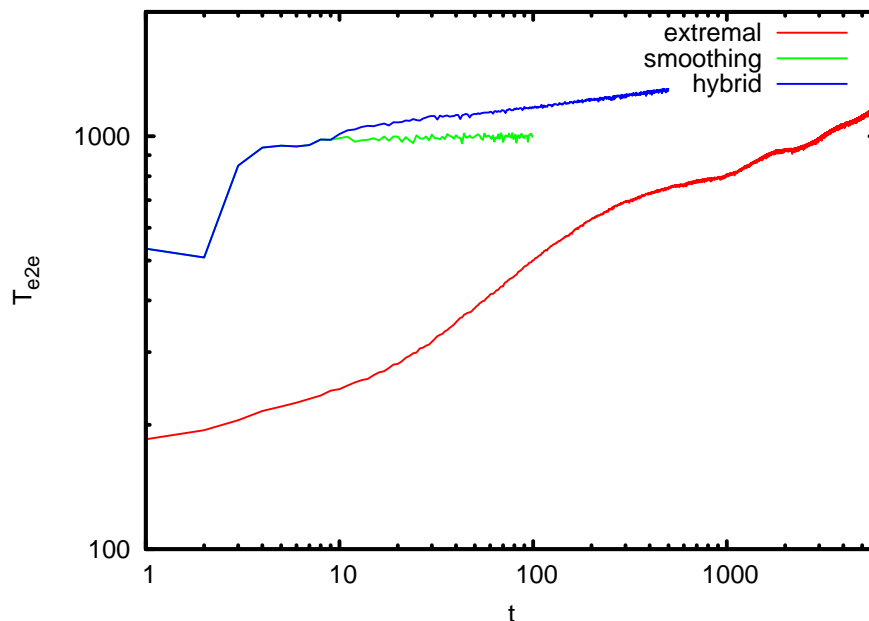
$$f(t) = \sum_{a, b \in \mathcal{V}} \left(\left| R_{ab}^{w(t-1)} \cup R_{ab}^{w(t)} \right| - \left| R_{ab}^{w(t-1)} \cap R_{ab}^{w(t)} \right| \right). \quad (7.20)$$

Figure 7.3b illustrates the number of changes in the routing matrix during the iterations of the metrics on an ensemble of 20 BA networks with $N = 1000$ nodes. For the extremal metric the fraction of changed entries decreases slowly with the number of iteration steps. Even at the chosen iteration cutoff $T_{\text{extr}} = 2M$ it has not reached convergence. The transport capacity (6.12), which is shown in Fig. 7.3a, reveals a similar non-convergence behaviour with the number of iteration steps. For the smoothing metric a saturation of both T_{e2e} and the number of routing matrix changes is apparent from $t \approx 10$ iteration steps. Compared to the fraction of changed entries in the routing tables, the transport capacity converges even faster. Although from iteration time $t = 10$ on, the hybrid metric results by far in the fewest changes to the routing matrix, it steadily improves the throughput supplied by the smoothing metric, and at $t \approx 100$ it achieves a throughput as high as the extremal metric's throughput at $t = T_{\text{extr}}$. Thorough testing with various network sizes have shown, that $T_{\text{hybrid}} = 500$ is a good compromise of computational effort and achieved T_{e2e} .

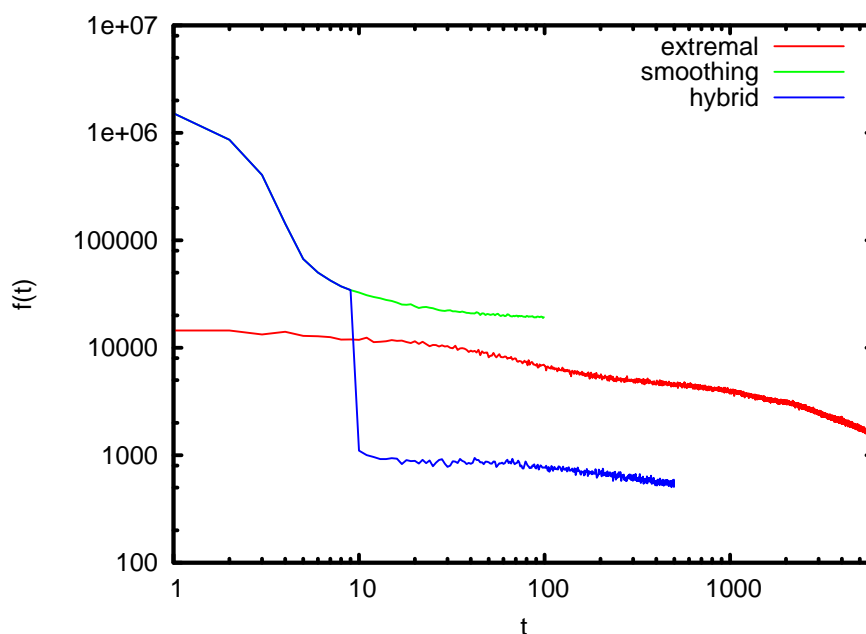
As the number of necessary iterations T_{hybrid} of the hybrid metric appears to be independent of the number of nodes, its computational complexity $\mathcal{O}(N^2 \log N)$ scales in the same way as the smoothing metric's. This allows to determine efficient weight assignments for networks of a size comparable with Internet AS-scans within reasonable amounts of time using current PC hardware.

Figure 7.4 once more compares the development of T_{e2e} during the metrics' iterations, this time for one instance of a PFP network, see Section 2.2.2. In addition to the smoothing and hybrid metric, also the additive hybrid metric is shown here, to demonstrate that it is not able to raise the throughput capacity as fast as the (multiplicative) hybrid metric. Drawing the attention to the smoothing and hybrid metric, we observe much stronger fluctuations of T_{e2e} during the iterations, than for the BA networks shown in Figure 7.3b. This is not only due to the averaging over 20 realizations in Figure 7.3b, but also to the less idealized network model. Especially the hybrid metric shows collapses during the iteration, although most of the time it recovers quickly onto a relatively smooth envelope. For this reason, we

7. Advanced routing



(a) Transport capacity T_{e2e}^w as function of metric iteration steps t .



(b) Changes of shortest paths as function of metric iteration steps t .

Figure 7.3.: Dependence of (a) the transport capacity and (b) the fraction of changed entries in the routing tables (7.20) on the number of iteration steps of the metrics w^{extremal} (extremal), $w^{\text{smoothing}}$ (smoothing), and w^{hybrid} (hybrid). Note the discontinuities in the plots of the hybrid metric at $t = 10$, where the switch from the smoothing metric's update to the multiplicative extremal update occurs. An ensemble of 20 BA scale-free network realizations with $N = 1000$ nodes and an average degree $\langle k \rangle = 6$ has been used.

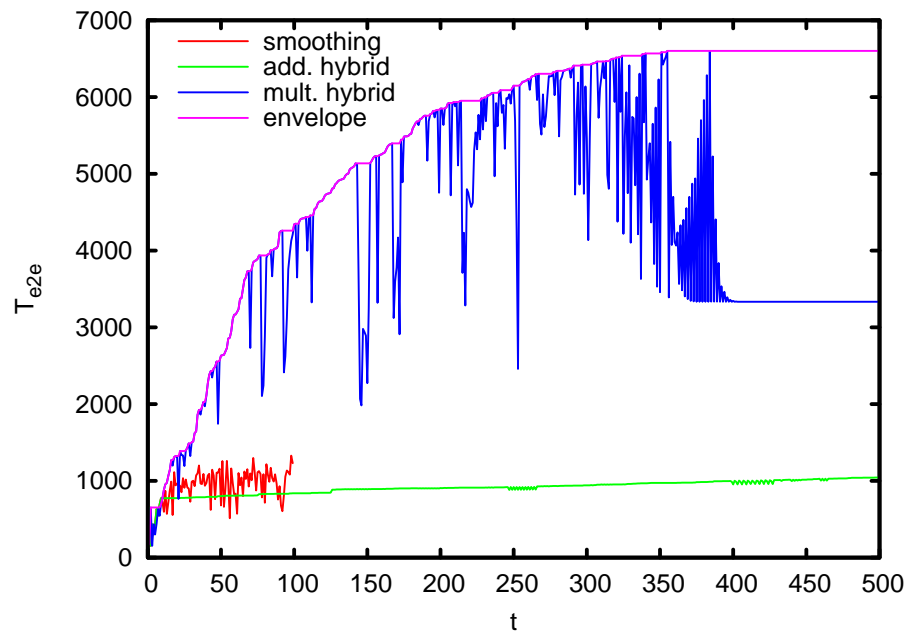


Figure 7.4.: Convergence of the transport capacity (6.12) of one typical realization of an $N_n = 10000$ PFP network with the number of iteration steps for the link weight assignments smoothing (Alg. 2), additive hybrid, and multiplicative hybrid (Alg. 3). Also shown is the envelope to the multiplicative hybrid curve.

7. Advanced routing

extend the definition of the hybrid metric to adopt, at the end of the iterations, the weight assignment

$$w_{\max} = \underset{w=w^{\text{hybrid}}(t):1 < t < T_{\text{hybrid}}}{\operatorname{arg\,max}} T_{e2e}^w \quad (7.21)$$

that resulted in the highest value of T_{e2e} during the iteration. The value of the envelope is depicted as the purple line in Figure 7.4.

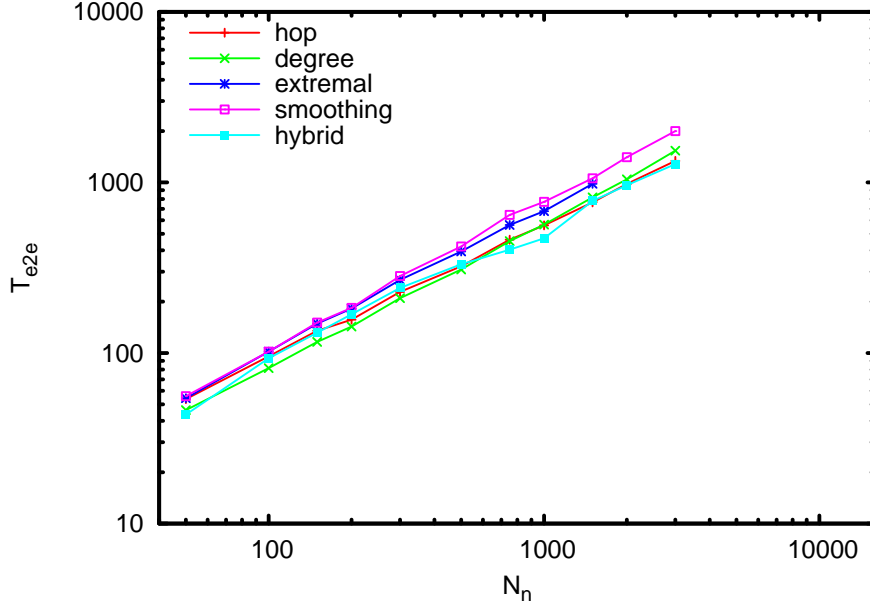
7.5. Comparing T_{e2e} -scaling of the metrics

After introduction and adaptation to the case of link weights of the previously proposed hop metric [Yan et al., 2006], smoothing metric [Schäfer, Scholz, and Greiner, 2006], and extremal metric [Danila et al., 2006b] in Section 7.2, followed by proposing our own iterative metric, the hybrid metric in Section 7.4, see also Scholz et al. [2008], the present section puts all these metrics to the test and thoroughly investigates the achieved throughput capacities. Following the example of Figure 6.1 in Section 6.3, we present the dependence of the throughput capacity T_{e2e}^w , as defined in Equation (6.12), on the number of nodes N , for the presented metrics and various network structures.

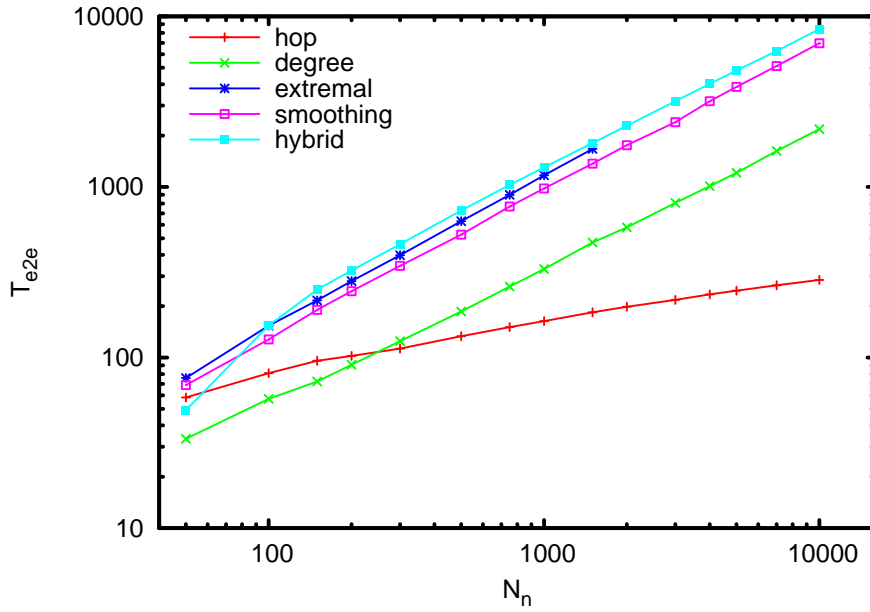
Poissonian graphs Figure 7.5a illustrates the throughput capacity for Poissonian graphs with an average degree $\langle k \rangle = 6$. For all metrics a power law scaling of the form $T_{e2e}^w(N) \sim N^\beta$, with $\beta \approx 0.8$. Only a minor dependency on the chosen metric is observed. The reason for this is that Poissonian graphs are very tree like, i.e. they contain few circles. This is also expressed by the vanishing clustering coefficient $\lim_{N \rightarrow \infty} \langle \mathbb{C} \rangle = 0$ of Poissonian graphs, see Equation (2.24). In a tree \mathcal{T} however, for every pair of nodes $a, b \in \mathcal{V}(\mathcal{T})$ there is only a single path connecting the two, $|\text{paths}(a, b)| = 1$, hence the routing cannot be influenced by a metric.

BA networks In Figure 7.5b the transport capacity of BA networks is shown as a function of the size of these scale-free networks. As expected from the probability distribution of loads shown in Figure 7.1b, the maximal betweenness centrality is reduced significantly for the extremal and the smoothing metric, resulting in enhanced throughput capacities. The hybrid metric performs even slightly better than the extremal metric. The last data point calculated for the extremal metric is at $N = 1500$ because of the increasing computational effort for large N . Notably, the degree metric performs worse than the hop metric for networks smaller than $N \approx 300$, and better for larger networks. Except for the hop metric a power law scaling of the form $T_{e2e}^w(N) \sim N^\beta$, with $\beta \approx 0.8$ to $\beta \approx 0.9$ is observed. Although the degree metric's scaling with the system size is similar to the scaling of the extremal, smoothing, and hybrid metric, its absolute T_{e2e} -values are smaller by a factor of ≈ 3 .

7.5. Comparing T_{e2e} -scaling of the metrics



(a) $T_{e2e}^w(N_n)$ for connected Poisson networks



(b) $T_{e2e}^w(N_n)$ for BA networks

Figure 7.5.: Transport capacity $T_{e2e}^w(N_n)$ as a function of the number of vertices N_n for the metrics w^{hop} (hop), w^{degree} (degree), w^{extremal} (extremal), $w^{\text{smoothing}}$ (smoothing), and w^{hybrid} (hybrid). For each data point an ensemble of (a) 20 random (but connected) Poisson network realizations and (b) 20 BA scale-free network realizations with average degree $\langle k \rangle = 6$ has been used.

7. Advanced routing

PFP model of AS-level Internet topologies The PFP model proposed by [Zhou and Mondragon \[2004\]](#) allows to produce an ensemble of network topologies, that reproduce many statistical properties of AS-level Internet topologies. Having an ensemble of topologies allows to investigate for example mean values, which may help to uncover systematic trends, that might be hidden in noise when only single topologies are investigated. Using the PFP model we are able to create ensembles of Internet-like networks of varying size N . Although the model is based on a growth process, the growth process is not designed to model the growth of the Internet, but merely to grow in a way that reproduces statistical properties of an AS-level snapshot of the Internet with $N \approx 11000$. With these words of caution in mind, [Figure 7.6](#) shows the dependence of the transport capacity on the network size for the different routing weight assignments discussed above. For smaller networks ($N_n \lesssim 2000$) the results are almost as expected from the previous results on BA-networks. The extremal and smoothing metric perform best, for networks smaller than $N \approx 2000$. For larger networks, the smoothing metric experiences a saturation of T_{e2e} , even followed by a descent. This is not an issue of an insufficient number of iterations as one might guess. Increasing the iteration cutoff time $T_{\text{smoothing}}$ has been tested and did not show a change of this behavior. The extremal metric appears to continue to be the best metric available with respect to T_{e2e} , however for $N > 3000$ it is computationally infeasible. The hybrid metric performs very well, and for $N = 10000$ it outperforms the degree metric by a factor of ≈ 7 and the hop metric by a factor of ≈ 20 . Apart from the hop metric and the smoothing metric for $N \gtrsim 2000$, the throughput capacity once more follows a power-law scaling $T_{e2e}^w(N) \sim N^\beta$ with $\beta \approx 0.9$. The respective scaling exponents corresponding to [Figures 7.5](#) and [7.6](#) are summarized in [Table 7.2](#).

link weight	Poisson	BA	PFP
hop	0.78	0.30	—
degree	0.85	0.78	0.58
extremal	0.85	0.90	0.91
smoothing	0.88	0.87	0.85
hybrid	0.81	0.91	0.92

Table 7.2.: Scaling exponent β of the transport capacity $T_{e2e}^w(N) \sim N^\beta$ as fitted to the simulation data shown in [Figures 7.5a, b](#), and [7.6](#). For the PFP networks the scaling exponents for the smoothing link weight assignment has been extracted from $N \leq 2000$ only.

To sum up, the results of [Fig. 7.5](#) demonstrate that in comparison to shortest-hop routing the three iterative routing weight assignments are all able to increase the transport capacity by an impressive factor. This holds for heterogeneous networks like scale-free networks. On the contrary, for homogeneous networks like random Poisson networks the different routing weight assignments do lead to almost

identical results. For PFP networks, which are a much better approximation of the real Internet structure on the AS-level than either Poissonian or BA networks, the conveyed picture is rather different. As shown in Figure 7.6, in the regime of networks with 10000 or more nodes, which corresponds to the size of the current Internet topology on the AS-level, only the hybrid metric, is available to increase the throughput capacity significantly. The extremal metric is ruled out because of its enormous computational demands, and the smoothing metric fails to increase the throughput performance relative to the degree metric.

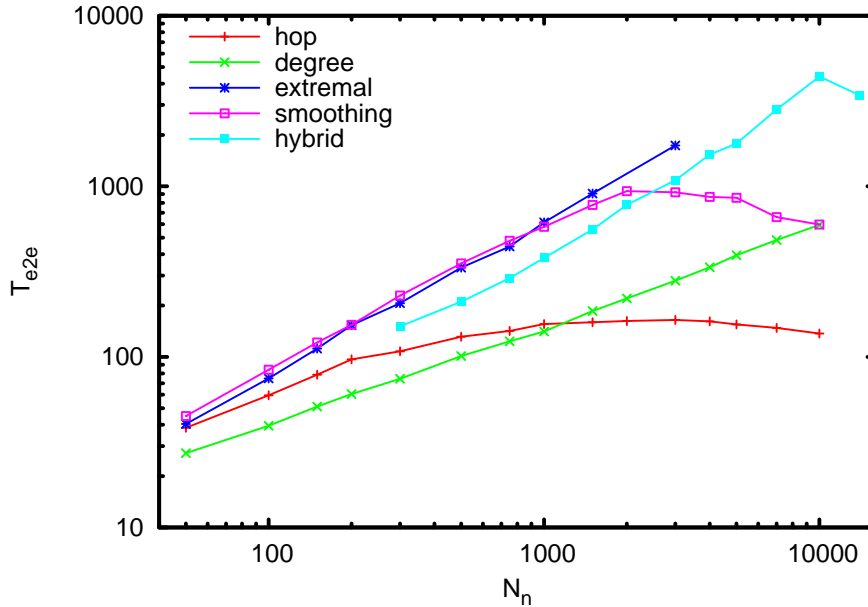


Figure 7.6.: Transport capacity $T_{e2e}^w(N_n)$ as a function of the PFP network size N_n for the metrics w^{hop} (hop), w^{degree} (degree), w^{extremal} (extremal), $w^{\text{smoothing}}$ (smoothing), and w^{hybrid} (hybrid). An ensemble of 20 PFP network realizations has been used to determine the average values.

Empirical AS-level Internet topologies The main application for the discussed routing weight assignments are large scale communication networks. The ultimate test for the weight assignments are Internet topologies on the AS-level. We use the adjacency information of the Internet on the AS-level provided by several Internet mapping projects, as described in Section 2.2. For our analysis we use the giant component of the network, apply the previously discussed metrics, and determine the corresponding throughput capacities.

Figure 7.7 illustrates the transport capacity T_{e2e}^w of the selected Internet scans for the hop, degree, smoothing, and hybrid metric. For all scans, the hop, degree and smoothing metric result in throughput capacities of roughly the same magnitude.

7. Advanced routing

Unlike for the model networks we investigated before, among these three metrics there is no clear winner. The hybrid metric, however, is confirmed to be the best choice among the presented metrics. We denote the factor of throughput increase, given by the ratio of

$$g = \frac{T_{e2e}^{w^{\text{hybrid}}}}{T_{e2e}^{w^{\text{hop}}}}, \quad (7.22)$$

as the gain ratio. The numerical values of properties of the empirical network structures, like size of the giant component, average degree, the resulting T_{e2e} -values, and the gain factor are available in Table A.1 of the Appendix. For the investigated network structures provided by ROUTEVIEWS and NETDIMES, the average gain ratio is $\langle g \rangle \approx 4$, for the data provided by CAIDA it is $\langle g \rangle \approx 7$. For standard deviation, minimal, and maximal value of the gain factor, see Table A.1.

Geometric p -network and $T_{e2e}^w(\mathcal{C})$ As noted in Section 2.2.2, one of the most basic properties that distinguishes the Internet scans from the idealized network models, represented by the configuration model and the BA model, is the pronounced clustering of the empirical data. Following the spirit of Section 6.3, here the influence of the clustering on the efficacy of routing metrics is investigated. For this purpose, the geometric- p model, proposed in Section 2.3, is utilized once more. Most of the AS-level Internet scans of the CAIDA project [CAIDA Macroscopic Topology Project Team, 2000–2006] are of size $N = 8000 \pm 500$, with a clustering coefficient $C \approx 0.45$; consult again Figure 2.4. Consequently we fix $N = 8000$ for the geometric- p networks, and note, that the average cluster coefficient of the CAIDA data is reproduced by the geometric- p model with $p \approx 0.8$, see Figure 2.6. Nevertheless, we keep $0 \leq p \leq 1$ as free parameter to tune the clustering coefficient.

Figure 7.8 compares the transport capacity $T_{e2e}^w(\langle \mathcal{C} \rangle, N)$ obtained from the three routing metrics sketched in the last two paragraphs with T_{e2e} obtained from the hop metric. The parameter p of the scale-free geometric- p networks has been converted into the clustering coefficient according to Figure 2.6. For all routing metrics a strong decrease of transport capacity with increasing clustering coefficient is revealed. The trend of decreasing T_{e2e} for increasing clustering $\langle \mathcal{C} \rangle$, as already observed for the hop metric w^{hop} in Section 6.3, can not be compensated by the advanced metrics introduced in the earlier sections of the present chapter.

The performance of the degree metric w^{degree} is of roughly the same order as for the hop metric, with a minor performance increase for low-clustered networks. For the networks with $\langle \mathcal{C} \rangle > 0.4$, which includes the clustering of the empirical data, the degree metric performs worse than the hop metric.

Compared to the hop and degree metric, the two metrics $w^{\text{smoothing}}$ and w^{hybrid} do much better. Note however, that the gain ratio reduces from about 6 for small clustering coefficients to about 3 for large clustering coefficients.

Figure 7.9 compares the transport capacity T_{e2e} of the Internet scans provided by CAIDA with the scale-free geometric p networks with $p = 0, 0.8$ and 1 . From

7.5. Comparing T_{e2e} -scaling of the metrics

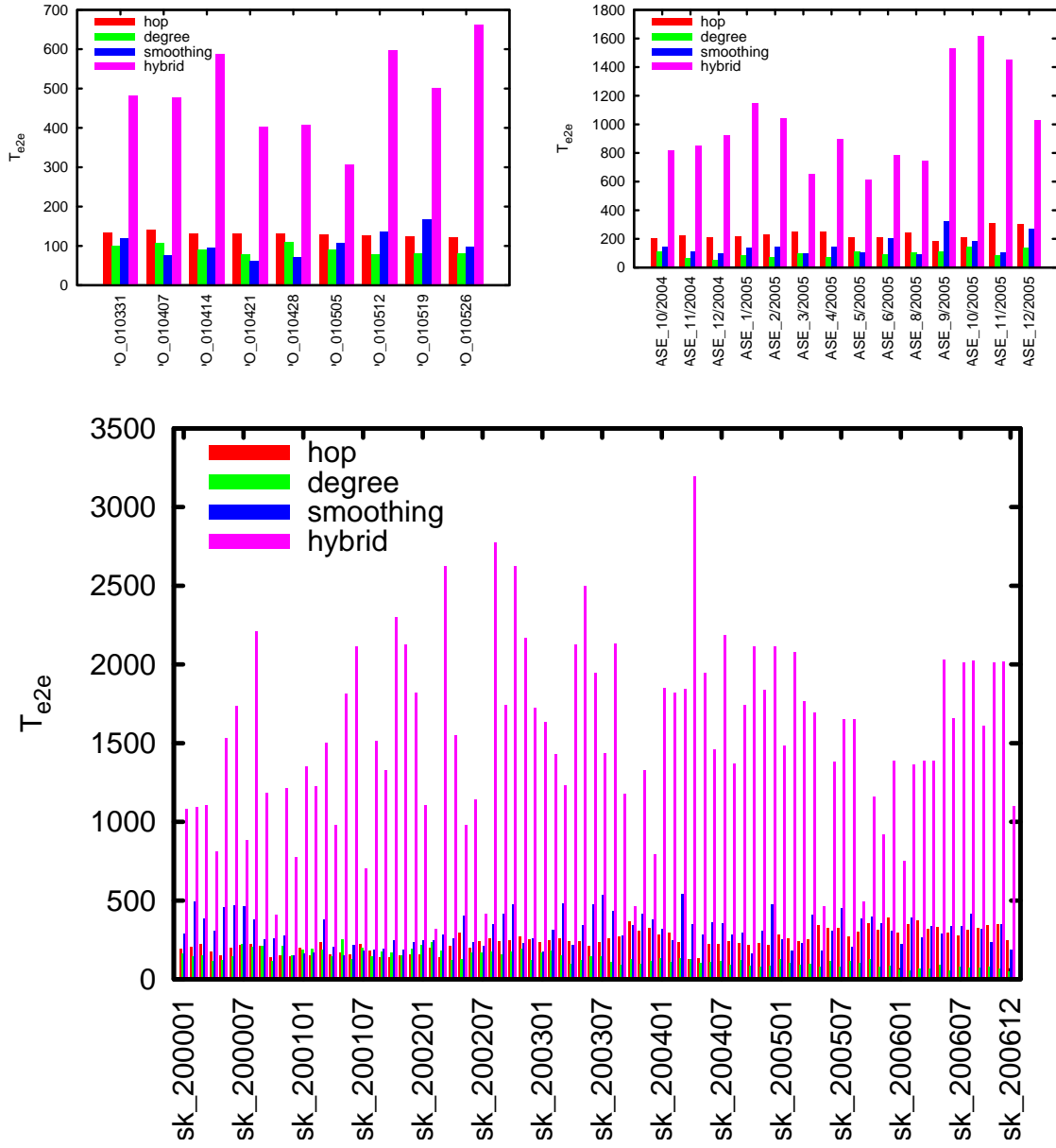


Figure 7.7.: Transport capacities of Internet scans from (a) ROUTEViews [University of Oregon, 2001], (b) NETDIMES [Shavitt and Shir, 2005], and (c) CAIDA [CAIDA Macroscopic Topology Project Team, 2000–2006] for the metrics w^{hop} (hop), w^{degree} (degree), $w^{\text{smoothing}}$ (smoothing), and w^{hybrid} (hybrid).

7. Advanced routing

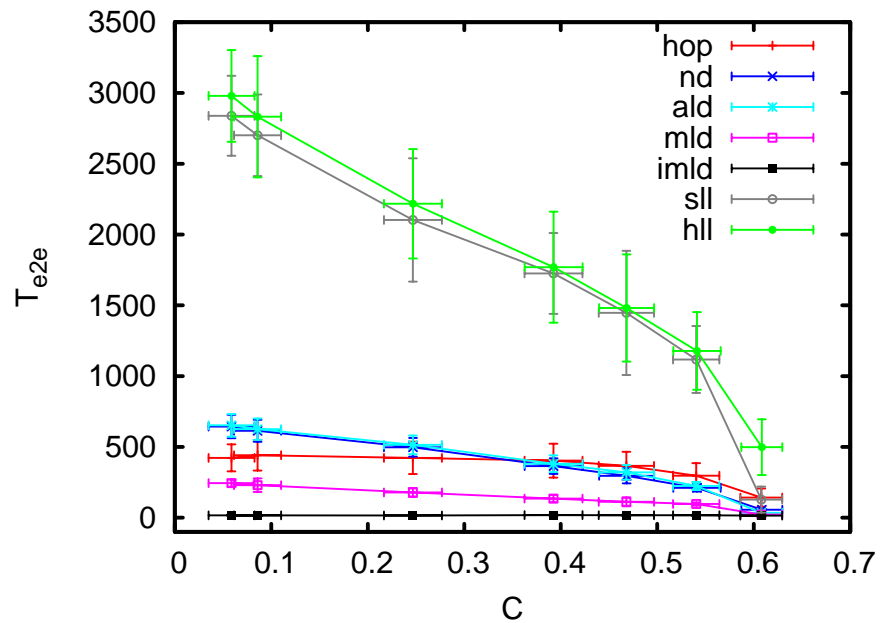


Figure 7.8.: Transport capacity T_{e2e} as a function of clustering coefficient $C = \langle \mathcal{C} \rangle$ for scale-free geometric- p networks with $\gamma = 2.3$ and $N = 8000$. The routing metrics are w^{hop} , w^{degree} , $w^{\text{smoothing}}$, and w^{hybrid} . Each symbolized error cross is obtained from ten equivalent network realizations. They correspond to $p = 0.0, 0.2, 0.5, 0.7, 0.8, 0.9, 1.0$ (from left to right) for each metric.

all data sets, only those with $7500 \leq N \leq 8500$ have been used here to enhance comparability with the geometric- p networks of size $N = 8000$.

For the hop, degree, and smoothing link load metrics the transport capacity of the Internet scans fall between the $p = 0.8$ and $p = 1$ values. For the hybrid link load metric it falls between the $p = 0$ and $p = 0.8$ values. This demonstrates that the scale-free geometric p networks with $p \approx 0.8$ catch the transport-capacity features of the Internet scans and may well serve as simple topology generators. Compared with the PFP model, the deviations from the throughput capacity of the Internet scans are on the same order of magnitude. This clearly points out that neither model is accurately reproducing the Internet's topology, but that both have to be considered as idealized models.

Figure 7.9 also points out the sensitivity of the smoothing and hybrid metric to the clustering. This can be considered as a downside of these metrics in the context of changing network topologies, caused for example by topology updates similar to the ones discussed in Chapters 3 and 4. In case a network, that employs the hybrid metric changes towards a more clustered topology, the performance will be reduced significantly.

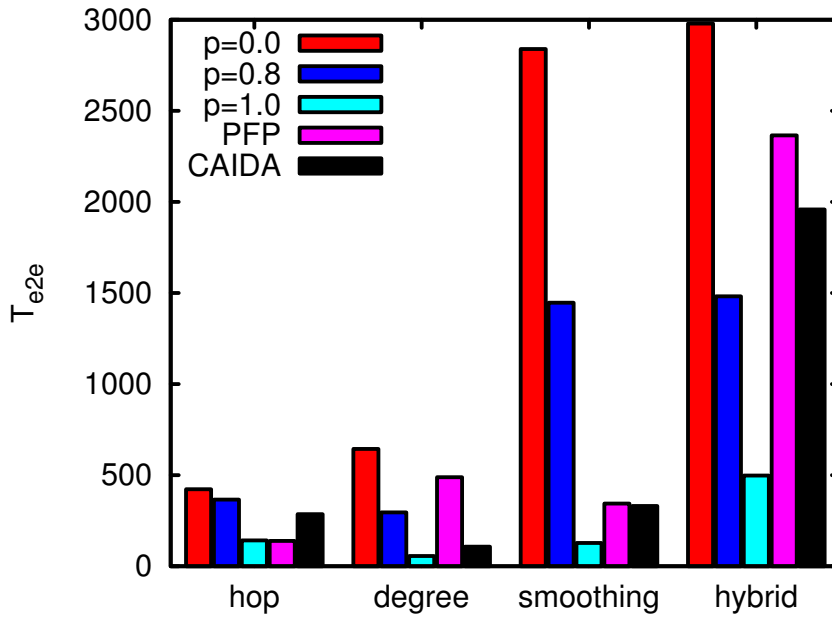


Figure 7.9.: Transport capacity T_{e2e} for scale-free geometric p networks ($p = 0, 0.8, 1; \gamma = 2.3, N = 8000$), PFP networks ($N = 8000$), and $N = 8000 \pm 500$ Internet scans from CAIDA. The routing metrics w^{hop} , w^{degree} , $w^{\text{smoothing}}$, and w^{hybrid} are shown.

7.6. Self-organizing (SO) metric

Previous work [Yan et al., 2006, Krause et al., 2006, Schäfer et al., 2006, Danila et al., 2006b, Scholz et al., 2008] has found smart metrics that are able to increase the transport capacity T_{e2e} , depending on the underlying network structure by a factor of 5–10. However, these metrics are rather hard to obtain, requiring numerical calculations that scale with the number of vertices N approximately like $\mathcal{O}(N^2 \log N)$ [Scholz et al., 2008] or worse $\mathcal{O}(N^3 \log N)$ [Danila et al., 2006b]. In an attempt to find numerically less expensive metrics with similar performance increases, we investigate local, self organizing weight assignments and find a stunningly simple and effective weight assignment.

The gist of the most successful previously proposed metrics, the extremal metric by Danila et al. [2006b], and the hybrid metric, proposed in Chapter 7.4 and Scholz et al. [2008], is to find the highest loaded link of the network, the bottleneck e_{BN} , defined in Equation (6.8), and to increase its weight, $w_{e_{\text{BN}}}$, either additively or multiplicatively. As the optimization applies only to the maximally loaded link, it is a form of extremal optimization [Danila et al., 2006a]. Because the weight influences the shortest paths, which in turn determine the bottleneck, the procedure has to be iterated. As successful as the application of extremal optimization is, it is also a weak point of the metrics. In every iteration step, only a single weight is adjusted, which necessitates a relatively large number of steps, compared for example with the smoothing metric, which updates all link weights in every iteration.

Looking for a way to reduce the number of needed iterations, we introduce a rule, that every node can apply by itself, in concert with its neighbors, using information as local as possible, e.g. it must not be necessary to determine a global maximum of the load. Additionally, we demand that the weights are conserved by the local rule. Weights shall not be created or destroyed, but only moved from one link to another. The rule for a stepwise update of the link weights w we propose and which we call the self organizing (SO) metric, is the following:

$$w_i(t+1) = \frac{1}{2} \sum_{j \in \mathcal{L}(i)} \left(\frac{w_i}{\ell_i} + \frac{w_j}{\ell_j} \right) + \frac{\epsilon}{2} \sum_{j \in \mathcal{L}(i)} \left(\frac{w_i}{\ell_i} + \frac{w_j}{\ell_j} \right) \text{sign}(L_i - L_j), \quad (7.23)$$

where $\mathcal{L}(i)$ is the edge neighborhood of an edge i and ℓ_i is its edge degree, as defined in Equations (2.3) and (2.4), and $\text{sign}(x)$ is the signum function.² For brevity, the indication of the iteration time t as an argument to w and L is not written out. The intention of the first sum in Equation (7.23) is to average the weights in the (edge) neighborhood, while the second sum results in weights that are shifted from edges with a relatively low load to neighbors that are relatively high loaded. The influence of the second sum in relation to the first is controlled by parameter ϵ , which may take values $0 \leq \epsilon < 1$. As a change of the edge weights results in different packet routing, the edge loads L_e have to be recalculated after the weight update.

²The signum function is defined as $\text{sign}(x) = -1$ for $x < 0$, $\text{sign}(x) = 0$ for $x = 0$, and $\text{sign}(x) = 1$ for $x > 0$.

The demand of weight conservation is fulfilled by the SO metric, as can easily be verified by calculating $\sum_{i \in \mathcal{E}} w_i(t+1)$. The contributions of the first sum in Equation (7.23) sums up to $\sum_i w_i$, and the second sum vanishes, as for every instance of the signum function, another one with the negative argument exists. From this $\sum_{i \in \mathcal{E}} w_i(t+1) = \sum_{i \in \mathcal{E}} w_i(t)$ follows.

For the case of $\epsilon = 0$ we can determine the resulting edge weights in the limit $t \rightarrow \infty$ by interpreting Equation (7.23) as a difference equation, and introducing Δt , which had been implicitly set to 1 before, we get

$$\frac{w_i(t+1) - w_i(t)}{\Delta t} = -\frac{1}{2}w_i + \frac{1}{2} \sum_{j \in \mathcal{L}(i)} \frac{w_j}{\ell_j}. \quad (7.24)$$

Using matrix notation and going to infinitesimal time steps, this can be written as

$$\frac{\partial w(t)}{\partial t} = -\frac{1}{2} \left(\mathbf{I} - \mathbf{A} \mathbf{D}^{-1} \right) w(t), \quad (7.25)$$

where \mathbf{I} is the identity matrix, \mathbf{A} is the adjacency matrix of the line graph $\widehat{\mathcal{G}}(\mathcal{G})$ of \mathcal{G} , and \mathbf{D} is the diagonal matrix of the edge degrees ℓ . Abbreviating $\frac{1}{2} (\mathbf{I} - \mathbf{A} \mathbf{D}^{-1}) = \tilde{\Lambda}$ the differential equation is solved by

$$w(t) = \exp(-\tilde{\Lambda}t)w_0. \quad (7.26)$$

As, through the similarity transform $D^{\frac{1}{2}}$, the linear operator $\tilde{\Lambda}$ is similar to the normalized graph Laplacian

$$\Lambda = \mathbf{I} - D^{-\frac{1}{2}} \mathbf{A} D^{-\frac{1}{2}} \quad (7.27)$$

as defined by Chung [1997], we know that for connected graphs the eigenvalues λ_i of $\tilde{\Lambda}$ are all positive, except $\lambda_0 = 0$. For $t \rightarrow \infty$ all eigenvectors will be damped out, except \tilde{v}_0 corresponding to λ_0 . With the help of the similarity transform $D^{\frac{1}{2}}$, we get \tilde{v}_0 in terms of the v_0 , the zeroth eigenvector of the normalized Laplacian

$$\tilde{v}_0 = D^{\frac{1}{2}} v_0. \quad (7.28)$$

The normalized Laplacian's eigenvector v_0 is given by $v_0 = D^{\frac{1}{2}} \mathbf{1}$, [Chung, 1997], therefore, for $\epsilon = 0$

$$\lim_{t \rightarrow \infty} w_i^{\text{SO}} = \ell_i \quad (7.29)$$

Starting from initial weights set to 1 for every edge, Figure 7.10 shows the development of the end to end throughput T_{e2e} of an AS-level Internet snapshot [CAIDA

7. Advanced routing

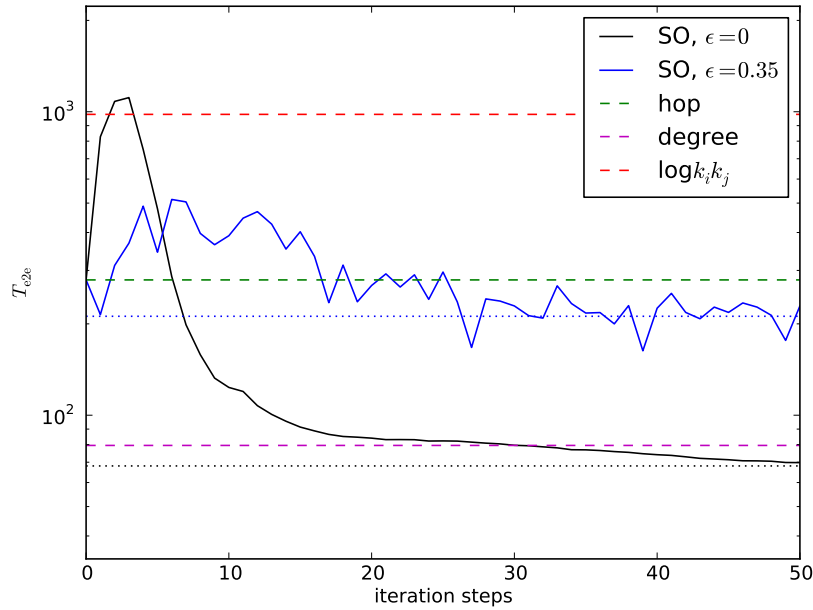


Figure 7.10.: Evolution of the T_{e2e} performance during iteration of the SO metric with $\epsilon = 0$ and $\epsilon = 0.35$. The dotted horizontal lines indicate the performance in the steady state of the iteration, determined by averaging the values from step 80 to 100. Dashed horizontal lines show the performance achieved by the hop, degree, and $\log(k_i k_j)$ metric. The network topology used here is an AS-scan [CAIDA Macroscopic Topology Project Team, 2000–2006] from June 2006, with 8111 nodes and 22370 edges.

Macroscopic Topology Project Team, 2000–2006], during the iteration of the update rules. After a sufficient number of iteration steps, the networks performance gets stationary around a mean value. For $\epsilon = 0$ the weight $w_i = \ell_i$ is reached, as predicted by Equation (7.29). The throughput performance in this stationary state depends on the parameter ϵ , we numerically determine that the best T_{e2e} performance in this stationary state is achieved by $\epsilon \approx 0.35$. Unfortunately, in the case of the depicted AS-scan, the T_{e2e} performance of the SO-metric is worse than the one of the hop metric. However, for small ϵ , especially for the depicted $\epsilon = 0$ the T_{e2e} performance exhibits a surprisingly high peak around the 2nd to 3rd step.

To further investigate the peculiar performance peak of the SO metric for $\epsilon = 0$, Figure 7.11 compares the distribution of weights at the peak with the distribution in the steady state for $\epsilon = 0.35$. While in the weight distribution of the steady state in Figure 7.11b no particularly clean structure is visible, Figure 7.11a shows a pronounced relation of the product of node degrees to the weights assigned at

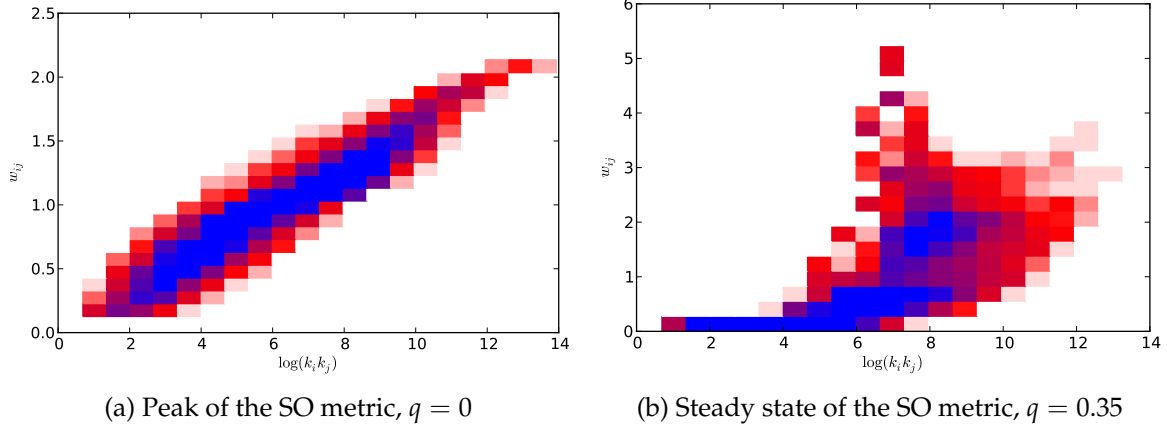


Figure 7.11.: Density of link weights produced by the SO metric for $\epsilon = 0$ (a) at the greatest performance reached during iteration, and in the steady state for $\epsilon = 0.35$ (b). The topology is the same as in Figure 7.10.

the performance peak of the SO metric. Here a rough functional dependence of the weight on the node-degrees is found:

$$w_{ij} \sim \log(k_i k_j). \quad (7.30)$$

7.7. The $\log(k_i k_j)$ -metric

The impressively clean relation between the weight of a link $e_{ij} \in \mathcal{E}$ to the logarithm of the product $k_i k_j$ of its adjacent vertices degrees, which occurs at the peak of *tete* performance reached during the iteration of the SO-metric, inspires another, amazingly simple weight assignment. We acknowledge the observation of Equation (7.30) and in a straightforward fashion turn it into a metric, by letting

$$\forall e_{ij} \in \mathcal{E} : w_{ij}^{\log k_i k_j} := \log(k_i k_j) \quad (7.31)$$

be the weight assignment of the metric we name $\log k_i k_j$ metric. Figure 7.12 shows the T_{e2e} performance of this metric compared to the hop metric, the smoothing metric, and most notably the hybrid metric, as proposed in Section 7.4. The hybrid metric continues to be the best of the tested metrics, but the performance of the $\log(k_i k_j)$ metric is in the same order of magnitude. Relative to the hop metric it results in a gain ratio (see Equation (7.22)) $g \approx 5$ which compares very well with $g \approx 7$ for the hybrid metric. This huge increase of performance is especially impressive, if we compare the computational complexity of the two metrics. As

7. Advanced routing

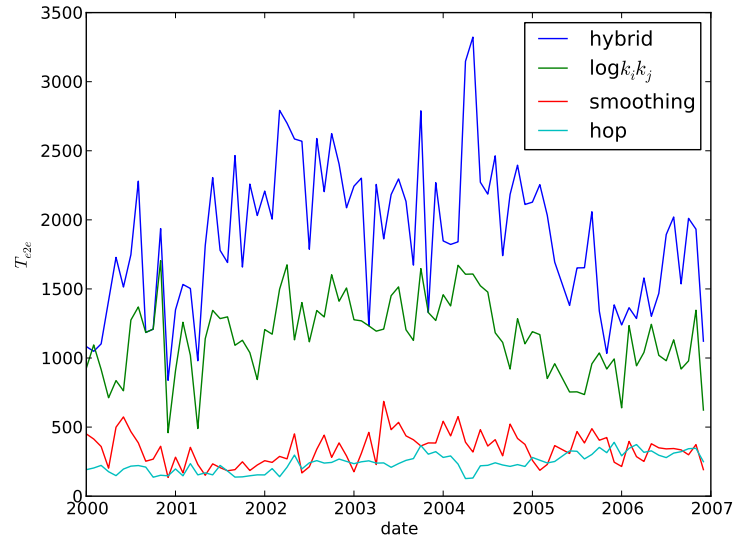


Figure 7.12.: Comparison of the throughput capacity T_{e2e} achieved by the $\log(k_i k_j)$ metric and other metrics on monthly Internet snapshots by the CAIDA project. The $\log(k_i k_j)$ -metric is compared with the w^{hop} (hop), $w^{\text{smoothing}}$ (smoothing), and w^{hybrid} (hybrid) metric. The degree metric and the link degree metric (steady state of the SO-metric, see Equation (7.29)), generally perform similar to the hop metric or worse, but are left out, to avoid cluttering the figure.

given in Section 7.4, the computational complexity of iterating the hybrid metric is $\mathcal{O}(N^2 \log N)$. The $\log(k_i k_j)$ metric however does not need to be iterated, it merely determines the degrees of vertices and calculates the logarithm for every node, hence the complexity is $\mathcal{O}(N)$. Assuming the calculation is done by every node itself, it is trivial to parallelize, in which case the complexity reduces to $\mathcal{O}(1)$.

The increase of throughput capacity by the $\log(k_i k_j)$ metric is shown by Figure 7.12 to be robust in the sense, that the increase is comparable with the increase of the hybrid metric for all tested CAIDA Internet scans. However, the applicability of this metric has to be taken with a grain of salt, as the present work assumes networks with a homogeneous traffic matrix and a uniform bandwidth, as stated in Sections 6.1 and 6.2. Should data on the traffic matrix and bandwidths, or plausible models of this data, get available, a metric like the hybrid metric, which is explicitly based on the traffic load in the network, is straightforward to adapt with the definitions of L_e in Equation (6.2) and e_{BN} in Equation (6.8), which already include the full traffic matrix and link bandwidths. With these modifications, which are beyond the scope of the present work, the extremal optimization is expected to work in a similar satisfying manner, and will probably result in optimization of

7.7. The $\log(k_i k_j)$ -metric

the throughput capacity. For a metric like the $\log(k_i k_j)$ metric, an immediately generalization is not apparent, as it relies completely on information, like the node degree, that is unrelated to the actual traffic flow.

8. Conclusion

The present work demonstrates mechanisms that are able to shape the structure of networked systems and influence the dynamics of processes taking place on the network.

The common ground of the proposed approaches is not only the desire to understand the emergence of macroscopic structural and dynamical pattern, the innate desire of statistical physics, but also the attempt to point out and explicitly investigate the applicability of the proposed approaches. The motivation for application of the presented methods is the possible optimization of real world systems with respect to graph theoretical observables, which are closely coupled to performance measures of real instances of complex systems. The endeavor is divided in three pieces, joined by the common ground of employing the formalism of graph theory as a tool to handle the generalized discrete topologies of the discussed complex systems. Moreover, the first two pieces are joined by the use of game theory, the paradigm of locally optimizing, selfish agents, to describe the microscopic scale and its influences on emergent macroscopic behavior. To prepare the ground for the forthcoming chapters, introductory reviews of graph theory and game theory are given in Chapters 2 and 3.

The first approach to investigate and optimize global properties of a network arising from interactions on the node scale is presented in Chapter 4. It employs a game, the iterated prisoners' dilemma (IPD), to let nodes of the network decide microscopically which of their neighbors to keep, which to decouple from, and which other nodes are good candidates to have as new neighbors. The dynamics arising from the rules, specified as a game, and the complex networked structures, that emerge from the rules, are characterized with respect to graph theoretical observables. A local rule is found, which, depending on a parameter, allows for the optimization of the emergent structure in a way, that results in networks, where each node is able to reach other nodes by short paths. This demonstrates a self organized optimization of the network structure.

The second approach, pursued in Chapter 5, puts the focus on fixed network structures, and elaborates on the emergence of cooperation among intrinsically selfish agents, the behavior of which is again modeled by game theory. The aspect of optimization is resumed by exploring strategies of distributing a given amount of incentives to increase the chance of emergence of cooperation. Compared to the naive strategy of uniform distribution, the cooperativeness of the system can be increased by a factor of 5 by using one of the proposed strategies.

The third approach is covered in Chapters 6 and 7 and investigates how the maximal throughput of a communication network is influenced by the structure of

8. Conclusion

the network and by weights that are applied to the network's links. To illuminate the effects of network structure, a geometrical generalization of the classical configuration model of graphs is proposed. This model is used for the investigation how clustering in the underlying topology influences the transport process on the network. The in-depth examination of the effects of metrics, defined by link weights, on the transport capacity, culminates in the proposal of two metrics that are able to radically increase the performance of the network. The first proposed metric results in an increase of a factor 7 with respect to unweighted networks, but demands considerable computational effort to be calculated. The second proposed metric, found as a spin-off of the investigation of self organizing metrics, achieves a less pronounced increase of a factor of 5, but results in a practically vanishing numerical effort.

The three approaches to characterization and optimization of networked systems consider highly idealized versions of systems found in nature. However, this does not result in a loss of generality. Instead, the abstraction eases the transfer of the found insights to other applications.

Take the game theoretic parts. Already the language of game theory, which identifies nodes of a network with players, suggests the association with social networks. Although social networks indeed gave the inspiration for the present studies, many other systems can benefit from the suggested mechanisms. Consider metabolic or gene expression networks inside of living cells, where the vertices are proteins that interact according to the rules of biochemistry. If these rules are changed in a systematic way, for example by unspecific drugs, similar to the tuning of a parameter in Chapter 4, or by targeted drugs, comparable to the incentive distribution strategies presented in Chapter 5, the emergent behavior of the system will change. To determine which proteins should be targeted by drugs, approaches like the ones described here may well be suitable after adaptation of the very abstract model to the given real network.

Similar arguments hold for the generality of the part that considers optimizing metrics. Although the numerical studies conducted in this work used the transportation of data packets on a network, with the Internet as an example, this does not confine the insights to the transport of data packets alone. In principle the considerations are valid for all kinds of transportation processes of distinguishable quantities that have to be transported from specific origins to specific destinations, and may be applied to logistic problems in general. An example is highway traffic, where weights may be realized through traffic lights, speed limits, or software of navigation systems.

That said, the investigation of more detailed and realistic models are nevertheless of great interest, as the quality of the optimizations will certainly differ with respect to implementation details. However the formalism and mechanisms developed in the present work will provide a convenient framework for those tasks.

Many interesting continuations and extensions of the work presented in this thesis can be thought of. To name but a few, consider a concrete implementation of the game theoretic parts to use games that are less abstract and describe real systems

more closely. An example may be economical systems, where the payoffs of the game directly represents financial gains or losses, and the played game would be a game of imperfect information. Another interesting aspect to pursue is the effect of weights and metrics on properties besides the throughput capacity. As the metrics work by distributing the load on the network evenly, the approach qualifies to enhance the robustness of networks, for example with respect to cascading failures, while enhancing the transport capacity at the same time. An exceptionally well suited candidate for such approaches is the $\log(k_i k_j)$ metric, as it can be calculated very fast and therefore almost instant reactions to failure of network components. A further extension may be the generalization to transport processes of indistinguishable entities, occurring for example in electrical networks, where the load of links given by Kirchhoffs laws instead of the betweenness centrality.

A. AS-level data table

Table A.1.: Properties of the three families of Internet scans ROUTEViews [University of Oregon, 2001], NETDIMES [Shavitt and Shir, 2005], and CAIDA [CAIDA Macroscopic Topology Project Team, 2000–2006]. Listed are the number of vertices N and the average degree $\langle k \rangle$ of the giant component, and the transport capacities T_{e2e}^w defined by Equation (6.12) for the hop, degree, smoothing, and hybrid metric. The last column shows the hybrid-to-hop gain ratio defined as $g = T_{e2e}(\text{hybrid})/T_{e2e}(\text{hop})$. The average of g ($\langle g \rangle$), its standard deviation (σ_g), minimum (g_{\min}), and maximum (g_{\max}) are given for each group of Internet scans separately.

id	N	$\langle k \rangle$	$T_{e2e}(\text{hop})$	$T_{e2e}(\text{degree})$	$T_{e2e}(\text{smoothing})$	$T_{e2e}(\text{hybrid})$	gain ratio
ROUTEViews weekly snapshots, Mar–May 2001							
PO_010331	10900	5.72	134.2	99.6	117.9	481.7	3.59
PO_010407	10981	5.62	140.7	106.3	75.6	477.0	3.39
PO_010414	11019	5.76	130.9	90.1	93.7	586.6	4.48
PO_010421	11080	5.69	130.5	78.4	60.6	402.4	3.08
PO_010428	11113	5.66	130.7	108.2	71.8	406.2	3.11
PO_010505	11157	5.55	127.6	90.2	106.7	307.1	2.41
PO_010512	11260	5.56	126.1	78.2	134.3	597.2	4.74
PO_010519	11375	5.68	124.6	79.5	166.2	501.1	4.02
PO_010526	11461	5.71	120.1	80.3	96.2	660.9	5.50
		$\langle g \rangle = 3.81$		$\sigma_g = 0.91$	$g_{\min} = 2.41$	$g_{\max} = 5.50$	
NETDIMES monthly snapshots, Oct 2004–Dec 2005							
ASE_10/2004	13374	3.69	200.4	110.8	144.2	812.9	4.06
ASE_11/2004	13547	4.10	225.0	63.7	109.0	846.0	3.76
ASE_12/2004	13649	4.12	210.7	53.9	97.1	922.2	4.38
ASE_1/2005	13844	4.33	215.4	82.2	137.9	1144.7	5.31
ASE_2/2005	13683	4.41	231.5	72.8	139.9	1040.8	4.50
ASE_3/2005	13646	4.68	247.0	99.1	93.5	650.8	2.63
ASE_4/2005	13696	4.69	250.3	71.8	143.8	898.3	3.59
ASE_5/2005	14048	4.66	207.4	112.6	102.9	611.7	2.95
ASE_6/2005	12017	4.64	211.4	91.6	200.5	780.3	3.69
ASE_8/2005	14116	5.22	244.2	102.5	87.0	743.6	3.05
ASE_9/2005	14147	5.57	183.8	107.5	321.7	1531.0	8.33
ASE_10/2005	17704	5.37	210.4	140.4	179.4	1615.8	7.68
ASE_11/2005	16695	4.89	307.7	83.2	100.8	1450.4	4.71
ASE_12/2005	14197	4.75	298.3	136.3	267.2	1026.0	3.44
		$\langle g \rangle = 4.43$		$\sigma_g = 1.62$	$g_{\min} = 2.63$	$g_{\max} = 8.33$	
CAIDA monthly snapshots, 2000–2006							
sk_200001	3247	5.89	191.8	159.8	288.4	1083.0	5.65
sk_200002	3282	6.08	203.9	147.0	495.1	1094.7	5.37
sk_200003	3305	5.78	222.8	152.6	386.6	1102.3	4.95
sk_200004	4041	5.15	176.9	116.6	307.9	809.0	4.57
sk_200005	4131	5.34	148.5	121.3	457.6	1529.9	10.30

continued on next page

A. AS-level data table

Table A.1, continued from previous page

id	N	$\langle k \rangle$	T_{e2e} (hop)	T_{e2e} (degree)	T_{e2e} (smoothing)	T_{e2e} (hybrid)	gain ratio
sk_200006	4216	5.63	196.2	145.5	467.7	1735.4	8.84
sk_200007	5278	5.69	217.3	223.3	460.3	880.5	4.05
sk_200008	5408	6.17	221.6	202.5	380.5	2208.2	9.96
sk_200009	5921	6.30	210.5	210.9	250.1	1185.0	5.63
sk_200010	6041	6.25	137.2	112.5	260.3	406.8	2.97
sk_200011	6063	7.85	151.4	208.1	275.7	1213.4	8.01
sk_200012	5567	4.16	147.1	151.5	149.0	777.1	5.28
sk_200101	5392	5.40	196.9	188.6	160.9	1348.8	6.85
sk_200102	6126	5.88	147.4	193.9	168.9	1226.0	8.32
sk_200103	6010	5.48	235.6	188.3	376.7	1503.2	6.38
sk_200104	5875	4.84	154.1	142.6	206.8	980.0	6.36
sk_200105	7254	6.39	168.7	253.9	152.9	1814.2	10.76
sk_200106	7407	6.62	154.3	126.5	216.2	2114.2	13.70
sk_200107	7299	6.75	222.5	200.1	178.1	701.0	3.15
sk_200108	7333	6.84	182.0	142.6	186.5	1511.3	8.30
sk_200109	7277	6.43	138.0	173.2	192.7	1327.8	9.62
sk_200110	7313	6.42	139.8	166.3	247.7	2297.6	16.43
sk_200111	7200	6.69	147.6	153.2	185.9	2126.7	14.41
sk_200112	7138	6.59	154.2	189.8	232.6	1821.1	11.81
sk_200201	7167	6.49	153.8	216.7	243.9	1103.8	7.18
sk_200202	8079	6.22	199.7	234.6	245.4	317.4	1.59
sk_200203	8366	6.52	140.8	178.6	282.1	2622.3	18.62
sk_200204	8117	6.57	209.4	123.1	260.0	1547.1	7.39
sk_200205	7918	6.25	297.5	129.3	402.3	979.5	3.29
sk_200206	8063	6.53	197.1	168.7	233.8	1140.3	5.78
sk_200207	7999	6.19	241.5	169.1	211.8	412.9	1.71
sk_200208	8161	6.36	257.2	176.6	350.0	2776.1	10.79
sk_200209	7821	5.85	239.6	157.7	416.1	1743.5	7.28
sk_200210	7871	6.31	244.2	177.2	475.9	2624.3	10.74
sk_200211	7857	6.25	268.6	191.0	229.2	2167.7	8.07
sk_200212	8477	5.95	251.6	122.4	258.2	1724.9	6.86
sk_200301	9100	6.02	235.1	168.3	175.3	1630.9	6.94
sk_200302	9062	5.95	248.7	181.7	313.6	1430.9	5.75
sk_200303	8624	5.96	255.8	147.6	484.0	1232.9	4.82
sk_200304	8638	5.85	239.3	99.0	214.5	2123.8	8.87
sk_200305	8566	5.83	240.6	121.3	343.5	2497.6	10.38
sk_200306	8662	6.24	208.9	141.6	477.3	1943.7	9.31
sk_200307	8696	6.40	235.8	146.3	537.0	1432.7	6.08
sk_200308	8529	5.87	259.1	109.7	432.3	2133.0	8.23
sk_200309	8215	5.77	272.0	90.0	274.2	1174.4	4.32
sk_200310	8159	6.47	366.6	129.3	340.7	462.3	1.26
sk_200311	7971	5.82	303.6	93.6	415.6	1329.3	4.38
sk_200312	7883	5.74	322.2	114.2	376.3	793.6	2.46
sk_200401	9234	5.52	280.4	132.3	315.8	1847.6	6.59
sk_200402	9106	5.66	291.3	106.4	243.3	1822.0	6.26
sk_200403	9200	6.29	232.3	132.2	539.9	1840.8	7.92
sk_200404	9143	6.41	127.3	124.8	349.7	3193.2	25.08
sk_200405	9064	6.53	131.3	101.9	283.2	1946.4	14.83
sk_200406	9047	6.17	219.9	106.4	360.0	1458.1	6.63
sk_200407	8741	6.29	223.3	113.3	356.8	2186.0	9.79
sk_200408	8714	6.36	241.6	92.0	282.2	1371.9	5.68
sk_200409	8700	6.05	225.7	119.9	293.3	1740.8	7.71
sk_200410	8552	5.64	215.6	81.6	160.9	2113.8	9.81
sk_200411	8480	5.86	228.5	79.5	309.1	1837.5	8.04
sk_200412	8442	5.64	214.9	85.8	472.2	2111.2	9.82
sk_200501	8509	6.21	280.3	127.0	252.3	1482.7	5.29
sk_200502	8468	5.99	260.1	103.4	178.6	2075.3	7.98
sk_200503	8498	5.97	240.5	92.0	227.9	1764.8	7.34

continued on next page

Table A.1, continued from previous page

id	N	$\langle k \rangle$	T_{e2e} (hop)	T_{e2e} (degree)	T_{e2e} (smoothing)	T_{e2e} (hybrid)	gain ratio
sk_200504	8467	6.00	251.0	98.4	409.3	1694.2	6.75
sk_200505	8351	5.69	345.5	75.8	183.3	464.9	1.35
sk_200506	8278	5.49	327.7	114.5	307.9	1380.5	4.21
sk_200507	8257	5.49	324.9	79.2	451.7	1652.2	5.09
sk_200508	8262	5.66	269.5	112.0	207.3	1653.2	6.14
sk_200509	8231	5.66	301.8	102.0	386.1	490.7	1.63
sk_200510	8246	5.66	353.3	128.6	396.0	1159.7	3.28
sk_200511	8260	5.60	314.7	80.1	355.9	918.7	2.92
sk_200512	8304	5.86	389.7	82.8	305.9	1384.8	3.55
sk_200601	8259	5.76	292.0	62.6	220.7	751.7	2.57
sk_200602	8180	5.43	346.1	56.3	393.7	1364.2	3.94
sk_200603	8220	5.58	373.8	67.6	263.7	1389.3	3.72
sk_200604	8159	5.63	317.2	66.6	338.5	1389.0	4.38
sk_200605	8124	5.63	327.9	91.2	286.3	2031.8	6.20
sk_200606	8111	5.52	296.3	54.7	333.6	1656.8	5.59
sk_200607	8082	5.38	279.2	79.5	337.1	2008.6	7.20
sk_200608	8080	5.54	311.8	73.5	412.5	2020.8	6.48
sk_200609	8049	5.32	322.0	74.1	318.2	1610.6	5.00
sk_200610	8041	5.40	343.5	79.5	232.5	2011.0	5.85
sk_200611	8062	5.46	346.4	65.5	348.2	2016.2	5.82
sk_200612	7707	4.61	249.6	49.6	188.4	1101.9	4.41
		$\langle g \rangle = 7.01$		$\sigma_g = 3.86$	$g_{\min} = 1.26$		$g_{\max} = 25.08$

B. Coauthored publications

Parts of the Chapters 4 and 7 were published as peer reviewed articles [Scholz and Greiner \[2007\]](#), and [Scholz, Krause, and Greiner \[2008\]](#). During the preparation of the present thesis, the author also contributed to [Schäfer, Scholz, and Greiner \[2006\]](#) and [Krause, Scholz, and Greiner \[2006\]](#), although not as the main author. For completeness these publications are included facsimile here.

Proactive Robustness Control of Heterogeneously Loaded Networks

Mirko Schäfer,^{1,*} Jan Scholz,^{2,†} and Martin Greiner^{3,‡}

¹*Institut für Theoretische Physik, Justus Liebig Universität, Heinrich-Buff-Ring 16, D-35392 Gießen, Germany*

²*Frankfurt Institute for Advanced Studies and Frankfurt International Graduate School for Science, Johann Wolfgang Goethe Universität, Max-von-Laue-Straße 1, D-60438 Frankfurt am Main, Germany*

³*Corporate Technology, Information & Communications, Siemens AG, D-81730 München, Germany*
(Received 15 September 2005; published 14 March 2006)

A proactive measure to increase the robustness of heterogeneously loaded networks against cascades of overload failures is proposed. It is based on load-dependent weights. Compared to simple hop weights, respective shortest flow paths turn a previously heterogeneous load distribution into a more homogeneous one for the nodes and links of the network. The use of these flow paths increases the networks robustness and at the same time reduces the investment costs into the networks capacity layout. These findings are of relevance for critical infrastructures like communication and transportation networks.

DOI: [10.1103/PhysRevLett.96.108701](https://doi.org/10.1103/PhysRevLett.96.108701)

PACS numbers: 89.75.Hc, 05.90.+m

Modern human societies very much depend on the functioning of critical-infrastructure networks like power grids, telecommunication, and transportation. Such networks work reliably in everyday life. However, as some rare occurrences in the past have shown, they are still vulnerable to major outages. In order to avoid or at least reduce such failures, new robustness- and security-design concepts are needed.

The statistical mechanics of complex networks [1–3] has already started to address this issue. The structural analysis of error and attack tolerance focuses on the fragmentation of synthetic as well as real-world networks upon random and intentional removal of nodes and links [4–11]. In general, a large fraction of randomly broken components is required to lead to network disintegration. However, in case of an intentional attack the removal of only a few, most-important nodes or links are needed. Besides these static failures, also dynamical failures have been discussed [12–17]. The flow of, for example, electrical power or communication packets are characteristic for critical-infrastructure networks. The failure of components leads to a redistribution of flow. After redistribution, some of the remaining nodes and links are loaded with a larger flow than before. If this new load exceeds their capacity, the respective components will also fail, giving rise to more flow redistribution and possibly more failure. For heterogeneous networks, like scale-free networks, such overload avalanches might already be triggered by the failure of only one of the most-loaded nodes or links [12].

In order to avoid such network-wide avalanche outages, a simple reactive defense control has been proposed [13]: after occurrence of a single component failure, the intentional further shutdown of selected lowly (highly) loaded nodes (links) severely limits the spreading of the overload avalanche. However, the time scale needed to react may be relatively short and may not be operationally feasible for some specific situations.

In this Letter we propose a proactive measure to significantly reduce the chance of an overload avalanche and to limit its size in case of occurrence. The key to this control are load weights, a concept which is already implemented in current congestion-aware Internet routing protocols [18]. It determines the load-based lengths of the flow paths. Upon picking only those flow paths with the smallest load-based lengths, a previously heterogeneous load distribution turns into a more homogeneous one for the nodes and links of the network. This proactive control does not only increase the robustness of the network, but also lowers the investment costs into the networks capacity layout. Furthermore, this reduces the need of shutting off nodes and links to stop an avalanche.

We adopt the model presented in Refs. [12,13]. Although it applies only to communication and transportation networks, but not to power grids, it well serves the purpose to demonstrate the new proactive control. Within this model, every node provides (receives) flow to (from) every other node of the network with an equal share. After generation at node i , the flow to destination node f is transmitted along the shortest-hop path $[i \rightarrow f]_{\text{hop}}$. Out of all $N(N-1)$ paths $[i \rightarrow f]_{\text{hop}}$ [19], the betweenness centrality

$$L_n = \frac{1}{N(N-1)} \sum_{i \neq f=1}^N \text{path}([i \rightarrow f]_{\text{hop}}; n) \quad (1)$$

counts all shortest-hop paths which go over the picked node n and defines its load during normal network operation. The index function $\text{path}([i \rightarrow f]_{\text{hop}}; n)$ is equal to one if $n \in \{i, f\}$ belongs to the shortest-hop path $[i \rightarrow f]_{\text{hop}}$, and is zero else [20].

The sum of all loads

$$\text{invest}_0 = \frac{1}{N} \sum_{n=1}^N L_n \quad (2)$$

represents a measure for the minimum investment costs into the network. The lowest curve of Fig. 1 shows only little variation for several independent realizations of random scale-free networks. This curve serves as reference for other curves to come. Because of the heterogeneous network structure, a very heterogeneous load distribution emerges [21]; see also Fig. 2. A few nodes have to carry an exceptionally large load. If some of them fail, or have been the target of an attack, it comes to a network-wide load redistribution. The shortest flow paths, which were going via the failed nodes, are readjusting and are using then other nodes. As a consequence of this readjustment, some nodes have to carry a larger load than before. If this new load exceeds its capacity, then the respective node will also fail, triggering a new load redistribution with possible, subsequent overload failures of other nodes.

In order to reduce the possible occurrence of such a cascading failure, a contingency ($N - 1$) analysis is evoked. One of the N nodes, say m , is virtually removed from the network. The shortest-hop flow paths of the reduced ($N - 1$) network are recalculated, which then according to (1) determine the readjusted loads $L_n(m)$ of the remaining $N - 1$ nodes. This procedure is repeated for every possible single-node removal $1 \leq m \leq N$. The minimum capacity of node n is then defined as

$$C_n = \max_{0 \leq m \leq N} L_n(m), \quad (3)$$

where $L_n(0)$ represents the load resulting from the full

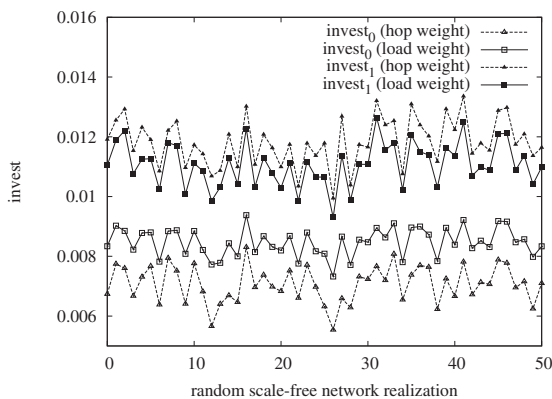


FIG. 1. Various investment costs for 50 independent random scale-free network realizations: invest_0 of Eq. (2) resulting from the hop weights (dashed curve with open triangles) and from the load-dependent weights (solid curve with open squares), and invest_1 of Eq. (4) resulting from the hop weights (dashed curve with full triangles) and from the load-dependent weights (solid curve with full squares). The parameters of the employed random scale-free network are the scale-free exponent $\gamma = 3$, the minimum node degree $k \geq 2$, and the number $N = 1000$ of nodes. This fixes the average node degree to $\langle k \rangle = 2.61 \pm 0.06$ and the network diameter to $\langle d \rangle = 7.98$. It also guarantees network connectivity almost surely.

network with all N nodes. This assignment guarantees that the network remains robust against a one-node failure, i.e., no overload failures of other nodes and no network-wide cascading failure. A consequence of this gain in network robustness is the increase of investment costs. The uppermost curve of Fig. 1 represents the sum

$$\text{invest}_1 = \frac{1}{N} \sum_{n=1}^N C_n. \quad (4)$$

For the example shown, the investment costs have increased from about 0.007 to about 0.012 units.

So far the flow paths have been based on the hop count. Now we introduce load-dependent weights. The basic idea is the following: a load-based path length is introduced as

$$d_{i \rightarrow f} = \sum_{n=1}^N \text{path}(i \rightarrow f; n) L_n. \quad (5)$$

Its minimum defines the load-based shortest path $[i \rightarrow f]_{\text{load}}$ between nodes i and f . Such paths have the tendency to avoid the most-loaded nodes and links, and help to relax the load of the latter.

For the proper determination of the load-based flow paths the minimization of (5) is not yet complete. The paths $[i \rightarrow f]_{\text{load}}$ are not only determined by the loads L_n of the nodes, the former themselves also determine the latter via

$$L_n = \sum_{i \neq f=1}^N \text{path}([i \rightarrow f]_{\text{load}}; n). \quad (6)$$

In order to find a consistent solution of (5) and (6), these equations have to be treated iteratively.

The beginning ($t = 1$) of the iteration is provided by the shortest-hop paths $[i \rightarrow f]_{\text{hop}}$ and the respective node-based loads $L_n(t = 1)$ of (1). This defines also the auxil-

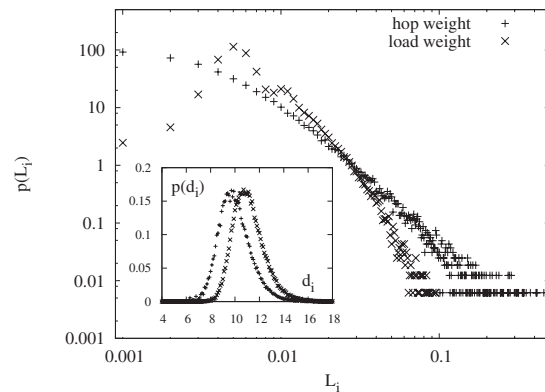


FIG. 2. Distributions of load and (inset) centrality distance following from the hop weights (crosses) and the load-dependent weights (rotated crosses). Parameters for the sample of 50 independent random scale-free networks are as quoted in Fig. 1.

ary, initial node-based weight $W_n(t=1) = \text{invest}_0$. An iteration step $t \rightarrow t+1$ then begins with the updates

$$W_n(t+1) = \frac{1}{t+1}L_n(t) + \frac{t}{t+1}W_n(t) \quad (7)$$

of the weights for all nodes $1 \leq n \leq N$. This update consists of two contributions, i.e., the load and the weight from the previous iteration round. Of course, also other combinations are possible. However, the first-guess update $W_n(t+1) = L_n(t)$ leads to oscillations and no convergence. Another update variant is $W_n(t+1) = \nu L_n(t) + (1-\nu)W_n(t)$, but as our simulations reveal is not able to improve on the choice (7). The weight update (7) also explains the introduction of the auxiliary, initial weight $W_n(t=1)$, which is of the same order of magnitude as the initial loads $L_n(t=1)$. The iteration step $t \rightarrow t+1$ is continued with the insertion of the updated weights (7) into (5), where of course L_n is replaced by $W_n(t+1)$. A subsequent minimization of $d_{i \rightarrow f}$ leads to the updated shortest load-flow paths $[i \rightarrow f]_{t+1}$ for all combinations $1 \leq i \neq f \leq N$. At last, the updated flow paths determine the updated node-based loads $L_n(t+1)$ through Eq. (6). This completes the iteration step $t \rightarrow t+1$.

Figure 3 shows the total network load (2) as a function of the iteration round t . Already after five steps, this sum has practically converged to a constant value of about 0.0084 units. This value is larger than the respective investment cost (2) based on shortest-hop paths. See also the second-lowest curve of Fig. 1, where invest_0 based on load-flow paths obtained with the load-dependent weights at $t=10$ is shown for various independent random scale-free network realizations. For the remainder, we will adopt the value $t=10$ for all results based on the load-dependent weights.

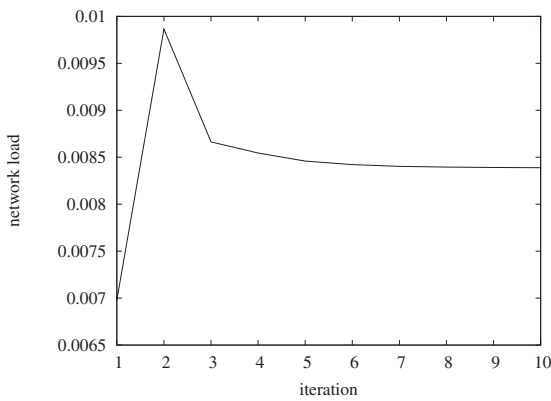


FIG. 3. Total network load $\sum_{n=1}^N L_n(t)/N$ as a function of the iteration round t . The load has been averaged over 50 independent realizations of random scale-free networks with parameters as quoted in Fig. 1.

Because of the sum rule

$$\sum_{n=1}^N L_n = \sum_{i,f=1}^N d_{i \rightarrow f}, \quad (8)$$

the relative increase of the investment cost (2) also implies an increase of the average path length (in hop units) by the same amount. This relative increase is also directly observed in the two respective distributions of the centrality distance $d_i = \sum_{f=1}^N d_{i \rightarrow f}/(N-1)$, which appear to map onto each other by a mere shift; consult inset of Fig. 2. Since the shift remains rather small, the length (in hop units) of each single flow path does not increase much. Note, that if the weights had not been chosen according to the load, but randomly, the length of the respective shortest flow paths might increase more dramatically [22].

A first benefit of the load-dependent weights becomes visible in Fig. 2. Those nodes which had a high hop-based load experience a significant load decrease upon application of the load-dependent weights. Other nodes which had a small load before acquire a little larger load. As expected, the load-dependent weights turn a heterogeneous load distribution into a more homogeneous one.

Networks with flow paths based on the load-dependent weights are less expensive to establish robustness against one-node-induced cascading failure. An $(N-1)$ analysis analogous to (3) and (4) leads to the curve with filled squares of Fig. 1. For all network realizations it is below the investment costs of its hop-counterpart with the filled triangles.

Even more benefit shows up with the two-nodes-removal analysis. The $(N-1)$ analysis does not guarantee network robustness against a failure of two or more nodes. A further increase of capacity beyond (3) is needed:

$$C_n(\alpha) = (1 + \alpha)C_n. \quad (9)$$

The tolerance parameter α is assumed to be the same for every node. The larger α , the larger network robustness will be against a two-node-induced failure, but also the larger the further investment costs $\text{invest}_2 = (1 + \alpha)\text{invest}_1$ will be.

Only a fraction of the nodes is still functioning after such a cascading failure; i.e., their loads are still smaller than their capacities (9). This fraction does not necessarily form a connected network. Usually these nodes cluster into nonconnected subnetworks. The largest of these subnetworks, i.e., the one containing the largest number N_{gc} of nodes, is called the giant component. Figure 4 shows the relative size N_{gc}/N of the giant component belonging to the surviving random scale-free network, obtained after removal of the two most-loaded nodes. As expected, it is almost close to zero for very small additional investment costs. For larger investment costs the size of the giant component very much depends on the chosen weights. At $\text{invest}_2 \approx 0.018$ the relative size is only about 0.75 for the

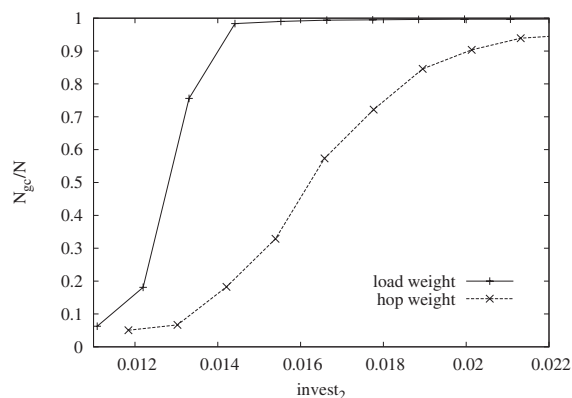


FIG. 4. Relative size of the giant network component, which survives a cascading failure after removal of the two most-loaded nodes, as a function of the investment costs for the hop/load-dependent weights (dashed/solid curves), respectively. Each curve has been averaged over 50 independent realizations of random scale-free networks with parameters as quoted in Fig. 1. Note, that due to $\text{invest}_1(\text{load weight}) < \text{invest}_1(\text{hop weight})$ (see Fig. 1) the two curves start at different absolute invest_2 .

hop weights. For the load-dependent weights the same relative size is already obtained at $\text{invest}_2 \approx 0.013$, and at $\text{invest}_2 \approx 0.018$ it is above 0.99. Compared to the respective hop-weight result, this outcome represents an impressive improvement. Qualitatively similar results have been obtained for other coordinated two-node removals. Consequently, the investment costs to establish network robustness beyond one-node failure are also smaller upon application of the load-dependent weights than for the hop count.

All results presented so far are not restricted to scale-free networks. Other types of networks, like those with a Poisson or exponential degree distribution, have also been studied. Together with a further investigation of a model extension to include link removals and link capacities, this has confirmed our main conclusions from before: the introduction of load-dependent weights increases the robustness of networks against cascades of overload failures and also proactively reduces respective investment costs. These are important findings for critical-infrastructure networks.

More findings are to be expected from several follow-up extensions of this work. So far the load-dependent weights have been assigned proactively to gain robustness against one- and two-node failure. In case of a failure of several nodes and links, a reactive reassignment of these weights could reroute the network flow in such a way that the subsequent overload cascade is avoided. Other topics of interest include, for example, discussions on other forms of

network flows and other-than-load-based weight assignments.

*Electronic address: mirko.schaefer@theo.physik.uni-giessen.de

†Electronic address: scholz@figss.uni-frankfurt.de

‡Electronic address: martin.greiner@siemens.com

- [1] R. Albert and A.-L. Barabási, *Rev. Mod. Phys.* **74**, 47 (2002).
- [2] S. N. Dorogovtsev and J. F. F. Mendes, *Evolution of Networks—From Biological Nets to the Internet and WWW* (Oxford University Press, New York, 2003).
- [3] M. E. J. Newman, *SIAM Rev.* **45**, 167 (2003).
- [4] R. Albert, H. Jeong, and A.-L. Barabási, *Nature (London)* **406**, 378 (2000).
- [5] R. Cohen, K. Erez, D. ben-Avraham, and S. Havlin, *Phys. Rev. Lett.* **85**, 4626 (2000).
- [6] D. S. Callaway, M. E. J. Newman, S. H. Strogatz, and D. J. Watts, *Phys. Rev. Lett.* **85**, 5468 (2000).
- [7] R. Cohen, K. Erez, D. ben-Avraham, and S. Havlin, *Phys. Rev. Lett.* **86**, 3682 (2001).
- [8] A. Motter, T. Nishikawa, and Y. C. Lai, *Phys. Rev. E* **66**, 065103(R) (2002).
- [9] P. Crucitti, V. Latora, M. Marchiori, and A. Rapisarda, *Physica (Amsterdam)* **320A**, 622 (2003).
- [10] R. Albert, I. Albert, and G. L. Nakarado, *Phys. Rev. E* **69**, 025103(R) (2004).
- [11] L. K. Gallos, R. Cohen, P. Argyrakis, A. Bunde, and S. Havlin, *Phys. Rev. Lett.* **94**, 188701 (2005).
- [12] A. Motter and Y. C. Lai, *Phys. Rev. E* **66**, 065102(R) (2002).
- [13] A. Motter, *Phys. Rev. Lett.* **93**, 098701 (2004).
- [14] P. Crucitti, V. Latora, and M. Marchiori, *Phys. Rev. E* **69**, 045104(R) (2004).
- [15] P. Crucitti, V. Latora, and M. Marchiori, *Physica (Amsterdam)* **338A**, 92 (2004).
- [16] R. Kinney, P. Crucitti, R. Albert, and V. Latora, *cond-mat/0410318*.
- [17] E. J. Lee, K. I. Goh, B. Kahng, and D. Kim, *Phys. Rev. E* **71**, 056108 (2005).
- [18] See, for example, J. Doyle, <http://www.ciscopress.com/articles/article.asp?p=24090&rl=1>.
- [19] Because of the symmetry of the network, the shortest paths $[i \rightarrow f]_{\text{hop}}$ and $[f \rightarrow i]_{\text{hop}}$ are identical. Equality also holds for the load-based shortest paths $[i \rightarrow f]_{\text{load}}$ and $[f \rightarrow i]_{\text{load}}$.
- [20] In case of shortest-path degeneracy, the index function is reduced by a factor depending on the degrees and depths of the branching points of the degenerated paths.
- [21] K.-I. Goh, B. Kahng, and D. Kim, *Phys. Rev. Lett.* **87**, 278701 (2001).
- [22] L. Braunstein, S. Buldyrev, R. Cohen, S. Havlin, and E. Stanley, *Phys. Rev. Lett.* **91**, 168701 (2003).



Available online at www.sciencedirect.com

SCIENCE @ DIRECT®

Physica A 361 (2006) 707–723

PHYSICA A

www.elsevier.com/locate/physa

Optimized network structure and routing metric in wireless multihop ad hoc communication

Wolfram Krause^{a,b,*}, Jan Scholz^c, Martin Greiner^a

^aCorporate Technology, Information and Communications, Siemens AG, D-81730 München, Germany

^bFrankfurt Institute for Advanced Studies and Frankfurt International Graduate School for Science, Johann Wolfgang Goethe Universität, Postfach 11 19 32, D-60054 Frankfurt am Main, Germany

^cInstitut für Theoretische Physik, Justus Liebig Universität, Heinrich-Buff-Ring 16, D-35392 Giessen, Germany

Received 21 February 2005; received in revised form 10 June 2005

Available online 2 August 2005

Abstract

Inspired by the Statistical Physics of complex networks, wireless multihop ad hoc communication networks are considered in abstracted form. Since such engineered networks are able to modify their structure via topology control, we search for optimized network structures, which maximize the end-to-end throughput performance. A modified version of betweenness centrality is introduced and shown to be very relevant for the respective modeling. The calculated optimized network structures lead to a significant increase of the end-to-end throughput. The discussion of the resulting structural properties reveals that it will be almost impossible to construct these optimized topologies in a technologically efficient distributive manner. However, the modified betweenness centrality also allows to propose a new routing metric for the end-to-end communication traffic. This approach leads to an even larger increase of throughput capacity and is easily implementable in a technologically relevant manner.

© 2005 Elsevier B.V. All rights reserved.

Keywords: Structure of and dynamics on complex networks; Information and communication networks; Wireless multihop ad hoc communication; Packet traffic

*Corresponding author. Frankfurt Institute for Advanced Studies and Frankfurt International Graduate School for Science, Johann Wolfgang Goethe Universität, Postfach 11 19 32, D-60054 Frankfurt am Main, Germany.

E-mail addresses: krause@th.physik.uni-frankfurt.de (W. Krause), Jan.C.Scholz@physik.uni-giessen.de (J. Scholz), martin.greiner@siemens.com (M. Greiner).

0378-4371/\$ - see front matter © 2005 Elsevier B.V. All rights reserved.

doi:10.1016/j.physa.2005.06.085

1. Introduction

Nowadays, the complexity of many engineered networks has increased to such a high level that conceptually new approaches for their operational control have to be looked for. Key aspects like self-organization and artificial intelligence become increasingly important. It is here where engineering and computer science is beginning to exchange ideas and concepts with the natural sciences like physics and biology. In particular, the new cross-disciplinary branch known as the Statistical Physics of complex networks [1–3] appears to catalyze such efforts.

We pick up on this latest momentum to continue the discussion of a challenging complex communication network in abstracted form [4–6]. In wireless multihop ad hoc networks [7–9] nodes are connected by wireless links. A central control infrastructure is missing. Each node does not only act as a communication source and sink, but also forwards communication for others. All of this requires a lot of self-organized and decentralized coordination amongst the nodes. The outstanding complexity of this communication network is revealed by mentioning the key mechanisms and the associated problems in some more detail.

With regulation of its transmission power, each node is able to modify its transmission range and its neighborhood, to which it builds up wireless communication links. Here the node faces frustration for the first time. On the one hand it wants to save energy and keep its transmission power as low as possible, but on the other it might have to choose a larger neighborhood in order to help the network to gain strong connectivity, so that each node will be able to communicate to any other via multihop routes. This brings us to another protocol layer, from link control to routing control. End-to-end routes have to be explored and maintained. During their execution the communication hops from one node to the next. This is where yet another protocol layer, called medium access control, sets in. It blocks all neighbors attached to an ongoing one-hop transmission in order to avoid interference within the same communication channel. This is the origin of another frustration, now across layers. Whereas routing efficiency prefers short end-to-end routes with the consequence of large one-hop neighborhoods, medium access control prefers to block small neighborhoods with the consequence of long end-to-end routes. A delicate balance between these two layers is necessary for the overall network to gain a large end-to-end throughput capacity, which measures the amount of communication traffic the network is able to handle without overloading.

In a previous paper [4] we have already addressed the connectivity issue, with special emphasis on the development of a simple self-organizing topology control. More self-organization has been proposed in Ref. [6], where a reactive routing and congestion control has been discussed, which adapts to the current congestion state of the wireless multihop ad hoc network. Another investigation [5] has demonstrated that the end-to-end throughput capacity does sensitively depend on the underlying network structure. It is exactly here where we continue and begin to ask for throughput optimization: What is the optimized network structure? What are its properties? Is it possible to construct the optimized network structure with a self-organizing topology control? Are there also other means to enhance the end-to-end

throughput and how do these compare to the approach with optimized network structures?

These are a lot of questions. We group them into the following organizational form of the paper. Section 2 addresses the network structure optimization of wireless multihop ad hoc communication networks. It explains the level of abstraction needed to construct an objective function for the global maximization of end-to-end throughput. A modified version of betweenness centrality is introduced, the cumulative betweenness centrality, which suites well the particular throughput needs of wireless multihop communication. The optimality of the resulting networks is checked with generic packet traffic simulations. Scaling laws for the end-to-end throughput with respect to network size are given. The structure of the globally optimized networks is analyzed and found to be difficult to construct with a decentralized, self-organizing topology control. As a consequence, a new approach is advocated in Section 3 to increase the end-to-end throughput. It uses the cumulative betweenness centrality as key input into a routing metric. This allows to determine throughput-optimizing end-to-end routes iteratively in a self-organizing manner. The increase in throughput turns out to become even slightly larger than for the optimized network structure of the previous section. Conclusion and outlook are given in Section 4.

2. Optimization of network structure

2.1. Abstraction: geometric minimum-node-degree networks

Some level of abstraction is required to make wireless multihop ad hoc communication amenable to the Statistical Physics of complex networks. The first simplification is to neglect mobility and to distribute N nodes onto a unit square in a random homogeneous way. The transmission power P_i then decides which other nodes j are able to be reached by node i via directed links $i \rightarrow j$. These are the nodes which, according to a simple propagation–receiver model, fulfill the inequality $P_i/R_{ij}^\alpha \geq \text{SNR}$. R_{ij} denotes the relative Euclidean distance. The path-loss exponent α is assumed to be constant and SNR represents the signal-to-noise ratio. With these simplifications, wireless multihop ad hoc communication networks can be modeled as geometric graphs. The N nodes are networked together via the set $\{i \rightarrow j\}$ of all directed links.

Not all of the directed links will be used for wireless multihop ad hoc communication. Since operation requires instant one-hop feedback, only bidirected links $i \leftrightarrow j$ qualify for the routing of communication traffic. It is the bidirected links attached to node i which define its communication neighborhood \mathcal{N}_i and its node degree k_i .

One further step is needed to fully specify wireless multihop ad hoc network graphs: assignment of the transmission power P_i for all nodes. The simplest procedure is to assign the same value P to all nodes [10–13]. We prefer to employ a different procedure [4], which contrary to the first one is distributive, self-organizing

and adaptive. In a nutshell, each node i forces its k_{\min} closest nodes j to adjust their transmission powers to at least $P_j = R_{ij}^\alpha$, while adopting the value $P_i = \sup_j P_j$ for itself. Its own value can be increased further whenever another, still close-by node, which seeks for its minimum communication neighborhood, forces i in return to have an even larger transmission power. In this respect each node has at least k_{\min} bidirected neighbors. As a consequence transmission power values differ from node to node. This heterogeneity leads to the occasional emergence of directed links.

We will call wireless multihop ad hoc network graphs generated with this heterogeneous power assignment as geometric minimum-node-degree networks. Already the choice $k_{\min} = 8$ is sufficient to guarantee strong network connectivity almost surely for network sizes up to several thousand nodes [4]. A realization of a minimum-node-degree network with $k_{\min} = 8$ is shown in the upper left part of Fig. 3.

2.2. Objective function for end-to-end throughput

Maybe the most important performance measure of wireless multihop ad hoc networks is given by the end-to-end throughput capacity T_{e2e} . It represents the amount of end-to-end communication traffic the network is able to handle without overloading. Ref. [5] has shown that T_{e2e} does depend on the underlying network structure. We are now interested to find network structures with increased throughput capacity.

Based on a simple random traffic model, a suitable objective function for the end-to-end throughput has been proposed in analytical form [5]:

$$T_{e2e} = \min_i \left(\frac{N(N-1)}{B_i^{\text{cum}}} \right). \quad (1)$$

It introduces the cumulative betweenness centrality

$$B_i^{\text{cum}} = B_i + \sum_{j \in \mathcal{N}_i^{\text{in}}} B_j \quad (2)$$

as the sum of the betweenness centralities of the picked node i and its ingoing neighbors $j \in \mathcal{N}_i^{\text{in}}$. Out of all $N(N-1)$ end-to-end combinations the betweenness centrality

$$B_i = \sum_{\substack{m \neq n=1 \\ (n \neq i)}}^N \frac{b_{mn}(i)}{b_{mn}} \quad (3)$$

counts the number of end-to-end routes, for which i has to forward a packet. b_{mn} represents the number of used routes from m to n , of which $b_{mn}(i)$ pass through i . Throughout this section we will base the betweenness centrality on shortest multihop routes.

The expression (1) is consistent with $T_{e2e} = 1$ for fully connected networks, where each node comes with the maximum degree $k_i = N - 1$, as well as $B_i = N - 1$ and

$B_i^{\text{cum}} = N(N - 1)$. Initial sender and final recipient of each end-to-end communication are only one hop away from each other. Then, due to medium access control, each single one-hop end-to-end communication blocks the overall network, leading to a maximum throughput of one completed end-to-end communication per time step.

Moreover, expression (1) also agrees with the end-to-end throughput of a central-hub network. All end-to-end communications first go from the initial sender to the central hub, and from there to the final recipient. In each of the two involved one-hop transmissions the overall network is blocked by medium access control. First the receiving central hub blocks all its neighbors, and then all its neighbors are again blocked during the subsequent forwarding to the final recipient. This limits the maximum throughput to $T_{e2e} = 0.5$, i.e., one completed end-to-end communication per two time steps. In the central-hub network, it is the central hub which yields the largest B_i^{cum} . Its betweenness centrality amounts to $B_{\text{c.h.}} = N(N - 1)$. Each of its N neighbors counts $B_{\text{ngb(c.h.)}} = N - 1$. All this totals to $B_{\text{c.h.}}^{\text{cum}} = B_{\text{c.h.}} + NB_{\text{ngb(c.h.)}} = 2N(N - 1)$, so that Eq. (1) produces $T_{e2e} = 0.5$.

Beyond these two limiting network examples, the quality of (1) is decided with the minimum-node-degree network structures. Generic packet traffic simulations with shortest-path routing, as described in Ref. [5], have been used to determine their end-to-end throughput. The same network realizations, as used for the simulations, have then been taken to determine (1). The betweenness centrality based on shortest multihop paths has been calculated with an algorithm similar to that described in Ref. [14]. The overall agreement between the estimate (1) and the throughput curves obtained from the generic packet traffic simulations turns out to be remarkable for various k_{min} values; see Fig. 2 for $k_{\text{min}} = 8$, Table 1 and Ref. [5]. This proves the high

Table 1
Scaling exponent γ and parameter N_0 of the end-to-end throughput $T_{e2e} \sim (N - N_0)^\gamma$

$T_{e2e} \sim (N - N_0)^\gamma$	Estimate (1)		Simulation	
	N_0	γ	N_0	γ
$k_{\text{min}} = 8$	24	0.23	65	0.22
$k_{\text{min}} = 12$	69	0.25	127	0.22
$k_{\text{min}} = 20$	179	0.24	219	0.24
$k_{\text{min}} = 40$	(400)	(0.22)	(389)	(0.29)
opt($k_{\text{min}} = 8$)	36	0.41	37	0.43
opt($k_{\text{min}} = 12$)	84	0.40	(52)	(0.49)
opt($k_{\text{min}} = 20$)	(94)	(0.47)	(65)	(0.54)
$k_{\text{min}} = 8, B_i^{\text{cum}}$ -metric	0	0.42	23	0.41
$k_{\text{min}} = 12, B_i^{\text{cum}}$ -metric	22	0.43	63	0.41
$k_{\text{min}} = 20, B_i^{\text{cum}}$ -metric	93	0.40	127	0.41

Rows 1–4 are for minimum-node-degree networks and rows 5–7 are for the respective structure-optimized networks, all with shortest-multihop-path routing. Rows 8–10 are again for minimum-node-degree networks, but now with use of the B_i^{cum} -routing metric. Column blocks 2 and 3 represent the estimate (1) and the generic packet traffic simulations, respectively. In some cases, extracted parameters depend to some extent on the interval size used for the fit; brackets indicate these less reliable values.

quality of expression (1), which will now serve as objective function for the network-structure optimization of the end-to-end throughput.

Note, that for large network sizes the results for the end-to-end throughput suggest a scaling law of the form $T_{e2e} \sim (N - N_0)^\gamma$. Fitted values for N_0 and γ are given in Table 1. Except for $k_{\min} > 20$, the scaling exponent $\gamma = \gamma(k_{\min})$ is found to depend only weakly on the minimum-node degree. For all cases it falls well inside the range $0 < \gamma < 0.5$. The upper estimate $\gamma < 0.5$ has been first given by Ref. [11]. Despite a homogeneous end-to-end traffic pattern this overestimation neglects the heterogeneities in the one-hop traffic as a consequence of the spatial network geometry. In general, nodes in the spatial center of the network have to carry a higher load than nodes in the periphery. Taken alone, $\gamma > 0$ proves that for sufficiently large enough network sizes multihop networks produce a larger throughput than central-hub networks. However, this statement is much too modest, since for all curves of Fig. 2 and for all network sizes, the absolute value of the end-to-end throughput is always larger than $T_{e2e} = 0.5$.

2.3. Algorithmic details of the optimization process

Based on (1), the search for optimized network structures is challenging. First of all, the expression for the end-to-end throughput depends on the network structure in a non-linear and non-local manner. Local addition or removal of links might change the end-to-end routes and thus the traffic distribution on a global scale. Moreover, the search space of all testable network configurations is very large. It is of the order $(N - 1)^N$. Each of the N nodes has its own transmission power ladder with $N - 1$ rungs. Being on rung k means that the picked node is able to reach its k closest neighbors. Of course not all of these configurations are meaningful for wireless multihop ad hoc communication. Hence, it is important on the one hand to confine the search operations only to the meaningful ones and on the other hand to start with good initial network configurations.

As initial configurations the geometric minimum-node-degree networks are chosen. For the moment we stick to $k_{\min} = 8$. This sets a minimum node degree $k_i^{\min} \geq k_{\min}$ for each node i . During subsequent optimization operations, the respective transmission power values of all nodes are not decreased below their initial value, thus ensuring strong connectivity for all times [4]. Search operations are performed in rounds. Per round, each node is randomly picked once. A picked node explores in two directions. In the first move it increases its transmission power by one rung and, if the newly reached node does not already have a large enough transmission power, forces the latter to climb up its ladder until its rung suffices to successfully build a new mutual bidirectional communication link. In the other move the picked node steps down its transmission power ladder by one rung, implying that the lost neighbor might also move down its ladder until it reaches the rung just before another communication link is broken. Both moves modify the local network structure, require a global update of the shortest end-to-end routes and the betweenness centralities for all nodes, and lead to two modified estimates of the end-to-end throughput (1), which are then compared to the old estimate before the two

explorative moves. The network structure yielding the largest estimate is accepted. This gradient update procedure guarantees meaningful wireless multihop ad hoc network structures and keeps the occurrence of interfering one-directed links to a minimum.

A local maximum of (1) is reached, if during a complete search round no improvement of the throughput estimate is found. Fig. 1 shows a typical evolution of the end-to-end throughput in dependence of the number of search rounds until the first local maximum is reached. It only takes a modest number of rounds. The increase of the throughput performance is remarkable. Once a local maximum is reached, the respective network realization is perturbed by forcing a small, randomly chosen fraction of the nodes to step up or down by one rung on their transmission power ladder, including respective new or lost neighbor operations as explained before. We denote the period until the next local maximum is found as meta-round. Fig. 1 also illustrates the evolution of the end-to-end throughput in terms of meta-rounds. The striking feature is that if more than one node is perturbed out of its local-maximum state, the throughput performance decreases with the number

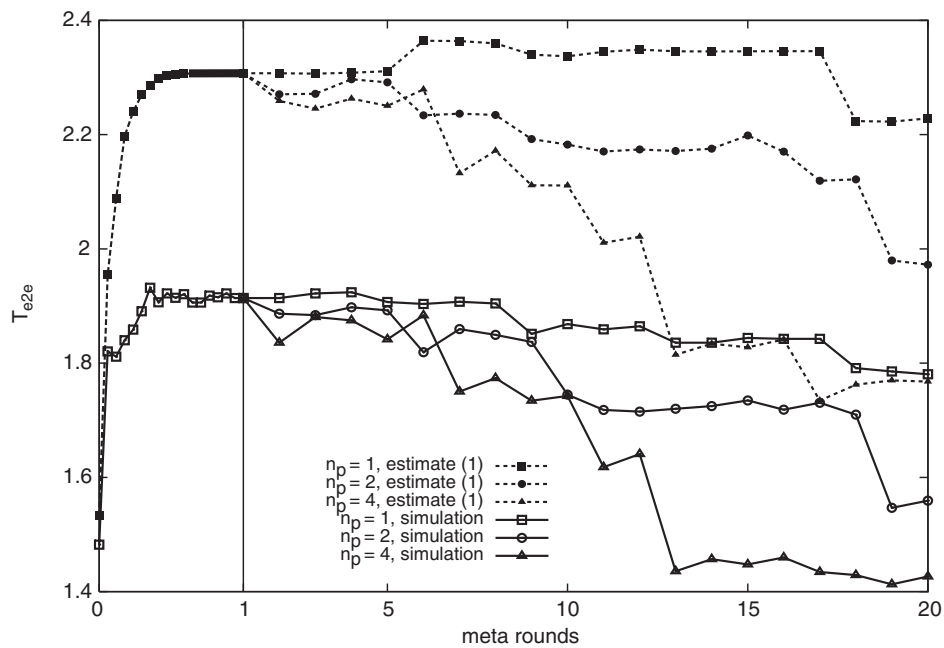


Fig. 1. Evolution of end-to-end throughput with progressing meta rounds. Each meta-round is kicked off with a random perturbation of $n_p = 1$ (squares), 2 (circles), 4 (triangles) randomly selected nodes from a local-maximum network configuration. Within the first meta round, the evolution in terms of optimization rounds is shown until the first local maximum of expression (1) is reached. A minimum-node degree network based on $k_{min} = 8$ and $N = 300$ has been chosen as initial network realization. The upper family of curves (with filled symbols) is for (1), whereas the lower family of curves (with open symbols) represents its counterpart from packet traffic simulations.

of meta-rounds. If only one node is perturbed, the throughput performance remains more or less the same as found for the first local-maximum network realization.

If we use other minimum-node-degree networks as initial network configurations instead of $k_{\min} = 8$, like $k_{\min} = 12$ and 20 , we arrive at the same qualitative findings. Independent of the network size, the first local throughput maximum is reached after only a few update rounds. Subsequent meta rounds do not lead to a significant performance increase; on the contrary, those initiated by larger perturbations again result in a decrease of end-to-end throughput.

It is important to check all of these results with packet traffic simulations. As also demonstrated in Fig. 1, a strong correlation between the simulation results and the throughput estimate (1) is found. This is a non-trivial and important statement. It has been clear from the beginning that the empirical expression (1) is not fully exact. A small discrepancy to the unknown true expression remains. A subsequent optimization with respect to (1) further broadens the gap. The important statement is that the end-to-end throughput of the packet traffic simulation also increases significantly and in correlation to (1).

Taken together, the results obtained from (1) and from packet traffic simulations show that the first found local maximum yields the largest throughput. All further maxima show a lower performance. This allows to terminate the optimization after the first meta-round. We are well aware that such an early termination most likely will not provide the global maximum, maybe even not a close-by network realization. However, in view of an engineer's pragmatism, our maximization policy produces a well defined and fast search into a strong local maximum for this hard and very costly optimization problem.

2.4. Scalability of optimized end-to-end throughput

For various network sizes ranging from $N = 100$ to 2000 and in dependence of the initial minimum-node degree k_{\min} , ensembles consisting of 5 to 25 throughput-optimized network realizations have been generated. Besides the optimized estimate (1) the end-to-end throughput has also been calculated from packet traffic simulations. It is the numerical cost of the network structure optimization, which forbids larger ensemble sizes. Results are shown in Fig. 2.

The optimized network topologies have an end-to-end throughput significantly larger than their initial counterparts. The end-to-end throughput of the optimized topologies again reveals the scaling behavior $T_{e2e} \sim (N - N_0)^\gamma$ in the limit of large network sizes. Fitted parameter values N_0 , γ are given in Table 1. The values found for the scaling exponent are very close to the upper bound $\gamma = 0.5$ given in Ref. [11]. The increase of γ to almost 0.5 demonstrates that within the optimized network topologies the heterogeneities of the one-hop traffic have been considerably reduced. With other words, the network structure has been modified in such a way that the new shortest-path end-to-end routes distribute the overall network traffic more evenly and reduce the peak traffic loads of the bottleneck nodes.

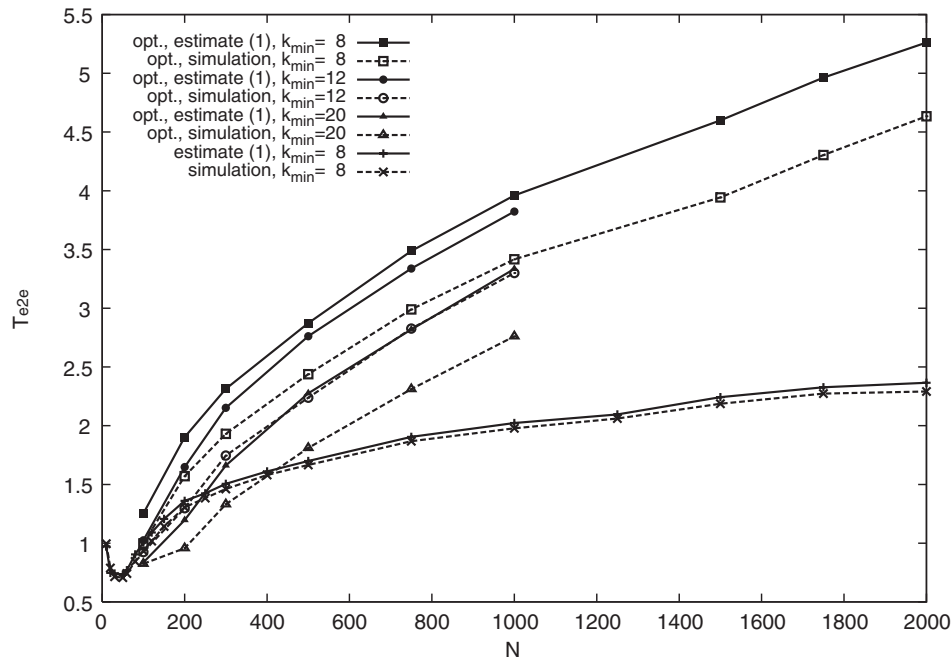


Fig. 2. End-to-end throughput of optimized networks as a function of network size, obtained from the objective function (1) (full symbols) and from generic packet traffic simulations (open symbols). Initial minimum-node-degree networks have been chosen with $k_{\min} = 8$ (squares), 12 (circles), 20 (triangles). An average over 25 (squares, $N \leq 1000$), 9 (squares, $N > 1000$), 5 (circles, triangles) independent network realizations has been performed for each symbolized N . For comparison the results obtained with the initial $k_{\min} = 8$ minimum-node-degree networks are also shown (crosses).

2.5. Structural properties of optimized networks

The optimized network structures resulting from the initial $k_{\min} = 8$ minimum-node-degree networks produce the largest end-to-end throughput; consult again Fig. 2. Optimized counterparts resulting from initial $k_{\min} = 12$ have almost the same end-to-end throughput. However, for the larger initial $k_{\min} = 20$ the respective optimized networks already come with a noticeably smaller end-to-end throughput. These findings are in accordance with the intuitive philosophy expressed in Ref. [11]: the largest throughput is obtained once the network is just barely strongly connected and blockings due to medium access control are smallest. The minimum-node degree $k_{\min} = 8$ just barely guarantees strong network connectivity and due to the small neighborhoods the blockings from medium access control are also small.

Fig. 3 (top right) shows a typical realization of an optimized network. It still looks similar to the initial $k_{\min} = 8$ network, which is illustrated in Fig. 3 (top left). For this example, only 391 new communication links have been added within the $N = 300$ nodes during the optimization procedure. Fig. 3 (bottom right) shows the bidirected

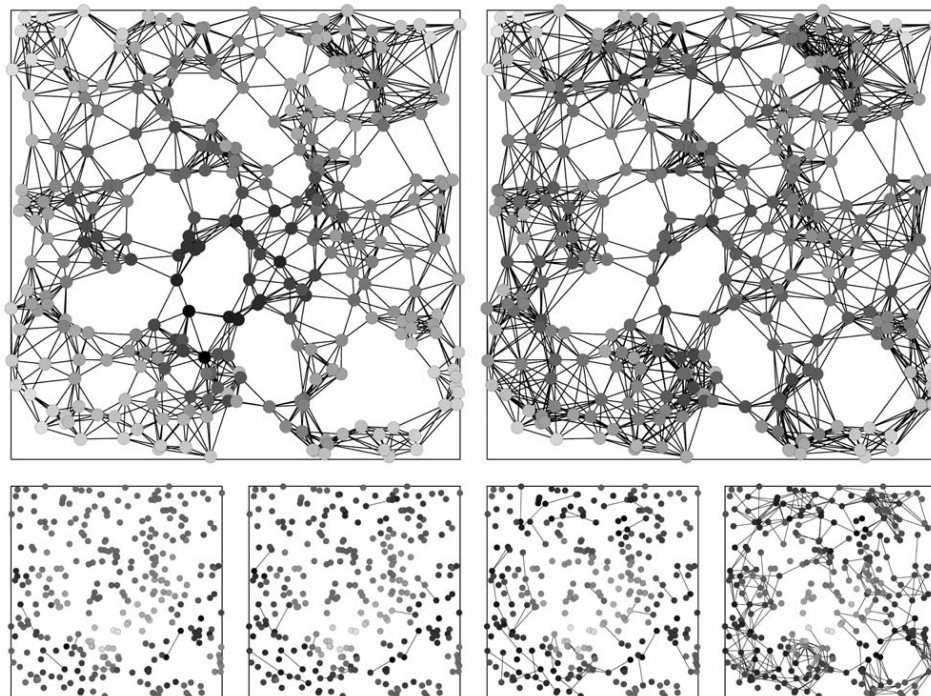


Fig. 3. Analysis of network structure optimization: (upper left) typical initial $k_{\min} = 8$ network configuration and (upper right) respective optimized network configuration. Only bidirectional communication links are shown; for reasons of readability, one-directed links have been suppressed. The gray scale of the nodes encodes B_i^{cum} , with zero (white) to maximum (black). From left to right, the subfigures in the lower row illustrate the most important 5, 15, 50 and 391 (all) new links. Here, light colored nodes come with strongly reduced B_i^{cum} values, whereas dark nodes have experienced a strong increase.

links added during the optimization. Almost none of them attaches to the spatially centered nodes, which are the bottleneck nodes with the largest overall cumulative betweenness centralities. Instead, nearly all of the new links are located in the greater surrounding of the most loaded nodes, including the outer parts of the network. The introduction of these new communication links modifies the shortest-path end-to-end routes in such a careful way that on the one hand the largest B_i^{cum} values of the most-loaded nodes are decreased and on the other the end-to-end throughput performance is increased significantly.

Not all of the 391 new links are important. A ranking of the new links reveals that the five most important new links are in charge of already 49% of the throughput increase, found with the generic packet traffic simulations. The ranking has been performed in the following way: at first, each of the 391 new links has been added singly to the minimum-node-degree network and the respective throughput (1) has been determined. The single link addition which yields the largest throughput defines

the most important link. This link is then included into the network. Next, this procedure is repeated for the remaining 390 new links, leading to the second most important new link, and so on. For the 15 and 50 most important links 73% and 104% of the final throughput increase are reached, respectively. For the remaining 341 new links the throughput increase fluctuates closely around 100%. This demonstrates that a fraction of only about 50 out of the 391 new links is necessary to reach the optimal performance.

From left to right, the lower row of Fig. 3 shows the 5, 15, 50 and 391 most important out of the 391 new links for this typical optimized network structure. The change of the nodes' B_i^{cum} values is shown with a gray scale, where black/light gray means increase/decrease. A close investigation of the five most important links reveals that two of them are formed between one- and two-hop neighbors of the bottleneck nodes. The other three are further away. All five form shortcuts in the periphery of the network. By reducing the hop distance between certain nodes they create new shortest path routes. This leads to a redistribution of traffic away from the highly loaded core of the network to the low-loaded periphery. For the 15, respectively, 50 most important links this behavior even becomes more visible. All of them are also only added in the periphery and not in the center of the network.

Similar findings hold for all other examined network realizations and for all network sizes. From initial $k_{\min} = 8$ minimum-node-degree network to optimized network the average node degree has increased from more-or-less N -independent $\langle k \rangle = 9.9$ to 12.8 for $N = 100$ nodes and 13.8 for $N = 2000$.

So far, the throughput optimization of network structure has been from a global perspective. To become technologically more relevant, a distributive optimization analog has to be found. This is a highly non-trivial and tough problem. The additional, throughput-enhancing new links are not directly attached to the most-loaded nodes, but further away within the periphery of the network. Due to this strong non-local dependence between network structure and end-to-end throughput several simple-minded greedy attempts based on cumulative betweenness centrality have not resulted in a significant increase in throughput performance. This is the time to think about conceptually other ways!

3. Performance increase with a routing metric based on cumulative betweenness centrality

A different approach will now be taken to increase the end-to-end throughput. In the previous section, the optimized modification of network structure has been relying on a simple, fixed routing policy. The end-to-end communications have always been routed along the shortest multihop paths. What about the other way around? Keeping the network structure fixed and modifying the end-to-end routes in such a way that the most-loaded nodes get a substantial relief, thus increasing end-to-end throughput. For this endeavor we will introduce a new routing metric. Given the experience of the last section, the latter will be based on cumulative betweenness

centrality. This alternative approach will also allow for a distributed implementation with only moderate costs for coordination overhead and computation.

3.1. Routing metric based on cumulative betweenness centrality

In general, a routing metric is needed to determine the length of an end-to-end route. The simplest example is the hop-count metric. In this case the length of an end-to-end route is equal to the number of hops or links traversed along this route. For any pair of initial sender and final recipient, shortest-path routing only picks those routes which have the smallest multihop length. This has the disadvantage that a small number of nodes, especially those in the spatial center of the network, have to carry a large fraction of the overall network traffic, thus reducing the overall end-to-end throughput performance.

The cumulative betweenness centrality represents a measure of a node's load. We will now employ it as routing metric. The length of an end-to-end route between endpoints i, f then becomes

$$d_{i \rightarrow f} = \sum_{k \neq f} \sigma_{i \rightarrow f}(k) B_k^{\text{cum}}. \quad (4)$$

All nodes k belonging to the end-to-end route have $\sigma_{i \rightarrow f}(k) = 1$, otherwise $\sigma_{i \rightarrow f}(k) = 0$. The distance (4) sums up the cumulative betweenness centralities of all one-hop transmitting nodes along the end-to-end route, including the initial sender i , but excluding the final recipient f . The shortest end-to-end route between i and f is the one with minimum $d_{i \rightarrow f}$.

Note, that the shortest end-to-end routes are based on the actual routing metric, which itself is determined by the end-to-end routes; consult again Eqs. (3) and (2). Consequently, shortest end-to-end routes and routing metric have to be calculated in alternating order, until some form of convergence is reached.

The self-consistent, iterative determination of all end-to-end routes subject to the B_k^{cum} metric consists of two parts: initialization and iteration. Initially, we set $B_k^{\text{cum}} = 1$ for all nodes. In one round of iterations, all nodes are picked one after the other. A picked node, say i , explores and updates all shortest end-to-end routes originating from itself. In doing so, it uses a Dijkstra-like procedure [15] with the presently assigned routing metric. Directly after i 's end-to-end routing updates, the routing metric is also updated. All nodes in the network determine their new cumulative betweenness centrality. Formally, due to the decomposition $B_k = \sum_{i,f} B_{i \rightarrow f}(k)$ of the betweenness centrality, only the contribution $B_{i \rightarrow f}(k)$ resulting from all routes with initial sender i needs to be updated. Then the next node in this round is picked. It already uses the freshly updated B_k^{cum} values to proceed further. This procedure can also be performed in a distributive manner. Only information about the link state of all nodes has to be exchanged between the nodes.

In order to fix the number of iteration rounds, generic packet traffic simulations have been performed, as described in Ref. [5]. Minimum-node-degree networks with $k_{\min} = 8$ and $N = 30\text{--}300$ have been chosen to investigate the influence of the number of iteration rounds. The simulation results reveal that already two iteration

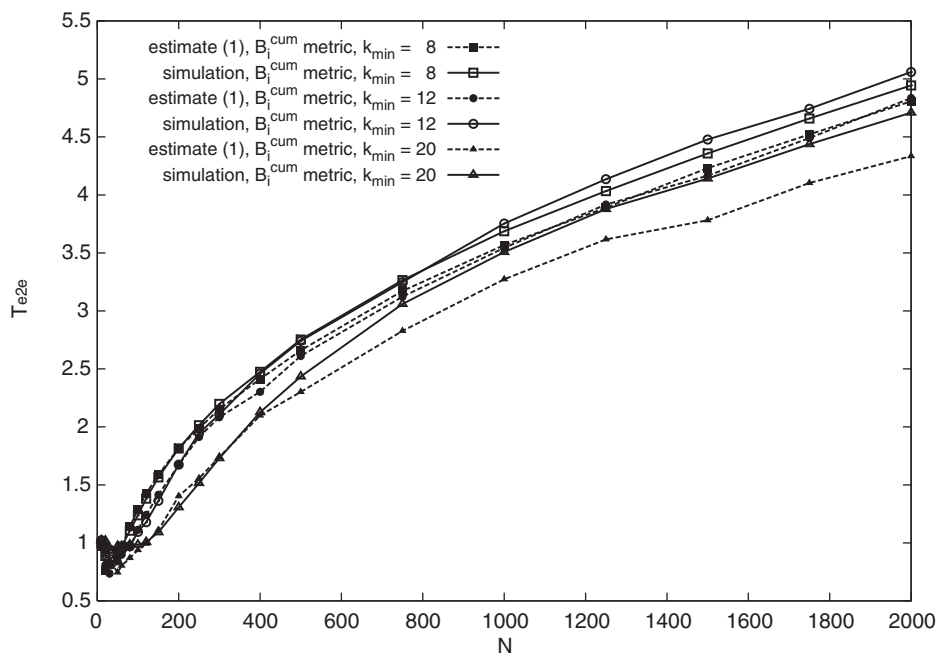
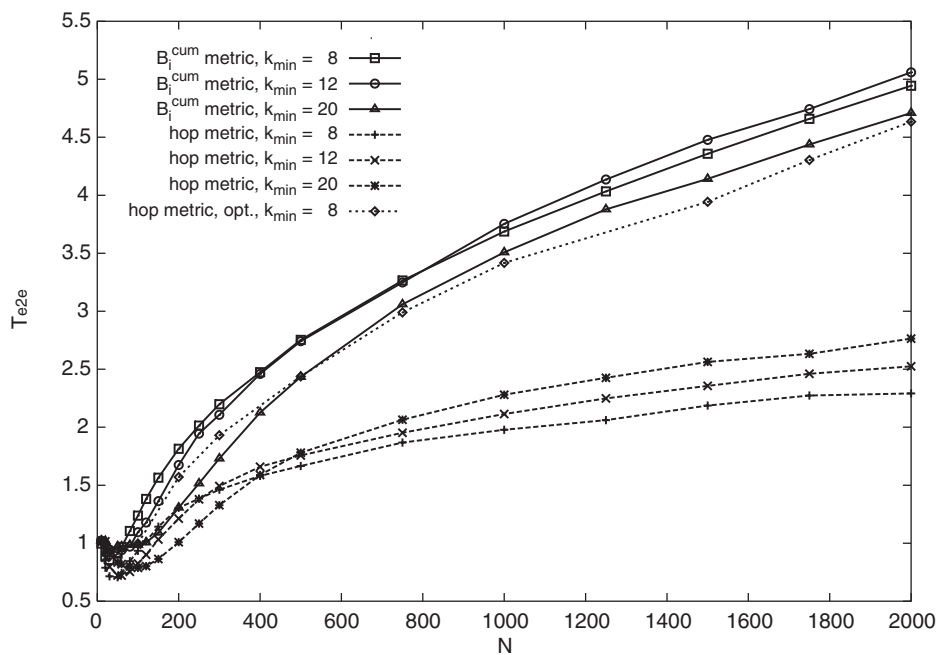
rounds are sufficient. Beyond two rounds the end-to-end throughput does not increase further, although end-to-end routes are still subject to modifications. This defines a weak convergence. It is contrary to strong convergence, for which also the end-to-end routes would become stable. For the following we will only concentrate on the algorithm using two iteration rounds.

3.2. Results on end-to-end throughput

For various minimum-node-degree networks with sizes up to $N = 2000$ we have calculated the end-to-end throughput from a generic packet traffic simulation, which uses the end-to-end routes obtained from the routing metric based on cumulative betweenness centrality. Averages over 100 independent network realizations have been taken for $k_{\min} = 8$; for $k_{\min} = 12, 20$ it have only been 20. Fig. 4 (top) illustrates T_{e2e} as a function of N . Again the scaling expression $T_{e2e} \sim (N - N_0)^\gamma$ produces a good description for $N > 200$. The resulting parameter values are listed in Table 1. The scaling exponent $\gamma = 0.41$ is found to be independent of k_{\min} . It is much larger than the respective $\gamma = 0.22\text{--}0.24$ resulting from the hop-count metric. Moreover, this scaling exponent is of the same order as those obtained from the optimized network structures based on shortest-multihop-path routing. In fact, on absolute scales the end-to-end throughput has become even slightly larger.

In principle, the expression (1) is not restricted to shortest-multihop-path routing. So far, in Section 2 it has only been tested for this case and found to produce a good estimate for the end-to-end throughput. A similar quality statement can now also be given for the routing based on the metric with the cumulative betweenness centrality. Fig. 4 (bottom) and the bottom of Table 1 compare the respective end-to-end throughput obtained from (1) with its counterpart obtained from packet traffic simulations. For the various minimum-node-degree networks with $k_{\min} = 8, 12, 20$ the agreement is remarkable, although not perfect, and of the same order as in the previous discussions illustrated in Fig. 2. This proves again the high relevance of the cumulative betweenness centrality for the generic modeling of the end-to-end communication traffic in wireless multihop ad hoc networks.

A consequence of the large end-to-end throughputs obtained with the routing metric based on cumulative betweenness centrality must be that the end-to-end communication traffic is then more evenly distributed over the network. Fig. 5 illustrates the point. It shows the routes of three selected end-to-end communication partners. In case of the hop-count metric, two of the routes are very similar. They have the same initial node and neighboring final nodes. Both routes have a long common part, using the same highly congested nodes in the spatial center of the network. In case of the B_k^{cum} metric, these two routes are pushed apart. In this way they decrease the load of the highly congested centered nodes. Another property of the new routing metric is illustrated with the third end-to-end route. Whereas the hop-count metric chooses a geometrically rather direct path, the metric based on cumulative betweenness centrality pushes the same end-to-end communication to the periphery of the network. This increases the load of those nodes situated at the



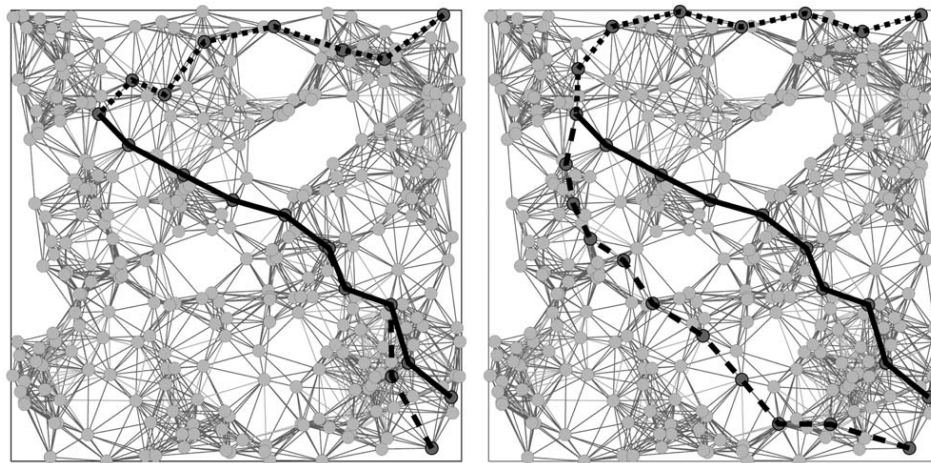


Fig. 5. Selected end-to-end routes based on the hop-count metric (left) and on the metric with cumulative betweenness centrality (right). The underlying network is of minimum-node-degree type with $k_{\min} = 8$ and $N = 300$.

periphery to some extent. However, such nodes are not critical to the network, and in return, the other close-by nodes experience a certain amount of traffic relief.

We recapitulate: cumulative betweenness centrality describes well the average traffic load of nodes networked together via wireless multihop ad hoc communication. A routing metric based on this quantity has the strong tendency to distribute the end-to-end communication traffic evenly over the network. It pushes end-to-end routes towards the periphery. This is achieved without any geographical information and suffices to increase the end-to-end throughput to realms, which even slightly exceed those obtained with the optimization of network structure based on the hop count metric.

4. Conclusion and outlook

We have discussed wireless multihop ad hoc communication networks from the perspective of the Statistical Physics of complex networks. A modification of betweenness centrality, which we have denoted as cumulative betweenness centrality,

Fig. 4. (Top) N -dependent end-to-end throughput obtained with the routing metric based on cumulative betweenness centrality for $k_{\min} = 8$ (open squares), 12 (open circles), 20 (open triangles) minimum-node-degree networks. All curves have been determined from a generic packet traffic simulation. An average over 100 (for $k_{\min} = 8$) and 10 (for $k_{\min} = 12, 20$) independent network realizations has been performed for each symbolized N . For comparison, respective curves (crosses, rotated crosses, stars) based on the hop-count routing metric are also shown, as well as the analog (open diamonds; see also Fig. 2) resulting from the $k_{\min} = 8$ network structure optimization. (Bottom) Comparison of the first three curves (open symbols) from (top) with their counterparts (closed symbols) determined from Eq. (1).

has been shown to be very relevant for the intricate modeling of the end-to-end throughput performance. The maximization of a respective objective function has led to optimized geometric network structures. Roughly, those are such that the networks are just barely strongly connected and that the size of the blockings resulting from the nodes' competition to gain wireless medium access are kept to a minimum. However, the significant increase in end-to-end throughput depends on only a few important links. These are not attached to the highly loaded nodes in the spatial center of the geometric network, but are found in the network's periphery. This pronounced non-local relationship makes it almost impossible to construct the optimized network structures in a technologically relevant distributive manner.

A second approach has been presented to increase the end-to-end throughput. It also relies on the cumulative betweenness centrality. The latter is used as routing metric and leads to an iterative determination of end-to-end routes, which decrease the traffic load of the most utilized nodes. With this routing metric the end-to-end throughput performance of non-optimized network structures becomes even larger than for the structure-optimized networks with the hop-count routing metric.

This alternative approach with the new routing metric also allows for a technologically relevant distributed implementation. Only moderate costs for link-state coordination overhead between the nodes and subsequent computation within the nodes are needed. More details will be given in Ref. [16]. A performance comparison with other distributive implementations for routing and congestion control, like the promising ant algorithms [17], still needs to be done.

Potential further applications of the routing metric based on cumulative betweenness centrality are not restricted to static multihop ad hoc and sensor networks. There is spinoff potential for more cyber physics related to the Internet, Ethernet and computer traffic engineering.

The last remark is again on network structure optimization. A very intriguing distributive approach could be network game theory. In Ref. [18] a coupling of playing games with neighboring nodes and network structure evolution has been introduced. Consequently, the optimization strategy would be: give a game to the nodes, let them play, and by doing so they will automatically end up in a game-dependent network structure, serving the optimization objective. Of course, for the moment this is only an idea and a lot of tough conceptual work is still necessary to prove it right or wrong.

Acknowledgement

W.K. gratefully acknowledges support by the Frankfurt Center for Scientific Computing.

References

- [1] R. Albert, A.-L. Barabási, Statistical mechanics of complex networks, *Rev. Mod. Phys.* 74 (2002) 47–97.

- [2] S.N. Dorogovtsev, J.F.F. Mendes, *Evolution of Networks—From Biological Nets to the Internet and www*, Oxford University Press, Oxford, UK, 2003.
- [3] M.E.J. Newman, The structure and function of complex networks, *SIAM Rev.* 45 (1) (2003) 167–256.
- [4] I. Glauche, W. Krause, R. Sollacher, M. Greiner, Continuum percolation of wireless ad hoc communication networks, *Physica A* 325 (2003) 577–600.
- [5] W. Krause, I. Glauche, R. Sollacher, M. Greiner, Impact of network structure on the performance of wireless multihop ad hoc communication, *Physica A* 338 (2004) 633–658.
- [6] I. Glauche, W. Krause, R. Sollacher, M. Greiner, Distributive routing & congestion control in wireless multihop ad hoc communication networks, *Physica A* 341 (2004) 677–701.
- [7] Proceedings of the 3rd ACM International Symposium on Mobile Ad Hoc Networking and Computing (MobiHoc 2002), ACM, Lausanne, Switzerland, 2002.
- [8] Proceedings of the 4th ACM International Symposium on Mobile Ad Hoc Networking and Computing (MobiHoc 2003), ACM, Annapolis, MD, USA, 2003.
- [9] Proceedings of the 5th ACM International Symposium on Mobile Ad Hoc Networking and Computing (MobiHoc 2004), ACM, Roppongi, Japan, 2004.
- [10] P. Gupta, P.R. Kumar, Critical power for asymptotic connectivity in wireless networks, in: *Stochastic Analysis, Control, Optimization and Applications*, Birkhauser, Boston, 1998, pp. 547–566.
- [11] P. Gupta, P.R. Kumar, The capacity of wireless networks, *IEEE Trans. Inf. Theory* IT-46 (2) (2000) 388–404.
- [12] C. Bettstetter, On the minimum node degree and connectivity of a wireless multihop network, in: *MobiHoc*, vol. 7, 2002, pp. 80–91.
- [13] O. Dousse, P. Thiran, M. Hasler, Connectivity in ad-hoc and hybrid networks, in: *Proceedings of IEEE Infocom*, New York, NY, USA, 2002, pp. 1079–1088.
- [14] M.E.J. Newman, Scientific collaboration networks ii: shortest paths, weighted networks, and centrality, *Phys. Rev. E* 64 (2001) 016132.
- [15] E. Dijkstra, A note on two problems in connection with graphs, *Numerische Mathematik* 1 (1959) 269–271.
- [16] W. Krause, Structure and dynamics of wireless multihop ad hoc communication networks, Ph.D. Thesis, Johann-Wolfgang-Goethe Universität Frankfurt/Main, Germany, 2005.
- [17] G.D. Caro, F. Ducatelle, L.M. Gambardella, Anthocnet: an ant-based hybrid routing algorithm for mobile ad hoc networks, in: *8th International Conference on Parallel Problem Solving from Nature, PPSN VIII*, Birmingham, UK, September 2004.
- [18] H. Ebel, S. Bornholdt, Evolutionary games and the emergence of complex networks, *arXiv:cond-mat/0211666*, 2002.

Bibliography

- R. Albert and A.-L. Barabási. Statistical mechanics of complex networks. *Rev. Mod. Phys.*, 74:47–97, 2002.
- R. Albert, H. Jeong, and A.-L. Barabási. Internet: Diameter of the world-wide web. *Nature*, 401(6749):130–131, Sept. 1999. ISSN 0028-0836. doi: [10.1038/43601](https://doi.org/10.1038/43601).
- E. Anshelevich, A. Dasgupta, E. Tardos, and T. Wexler. Near-optimal network design with selfish agents. In *STOC '03: Proceedings of the thirty-fifth annual ACM symposium on Theory of computing*, pages 511–520, New York, NY, USA, 2003. ACM Press. ISBN 1-58113-674-9. doi: [10.1145/780542.780617](https://doi.org/10.1145/780542.780617).
- R. Axelrod and W. D. Hamilton. The Evolution of Cooperation. *Science*, 211(4489):1390–1396, 1981. doi: [10.1126/science.7466396](https://doi.org/10.1126/science.7466396).
- V. Bala and S. Goyal. A noncooperative model of network formation. *Econometrica*, 68(5):1181–1229, 2000.
- A.-L. Barabási and R. Albert. Emergence of scaling in random networks. *Science*, 286(5439):509–512, 1999.
- M. Barthélemy. Comment on “Universal Behavior of Load Distribution in Scale-Free Networks”. *Phys. Rev. Lett.*, 91(18):189803, Oct. 2003. doi: [10.1103/PhysRevLett.91.189803](https://doi.org/10.1103/PhysRevLett.91.189803).
- M. Barthélemy. Betweenness centrality in large complex networks. *European Physical Journal B*, 38(2):163–168, 2004.
- B. Bollobás. *Random Graphs*. Cambridge studies in advanced mathematics. Academic Press, London, 1985.
- B. Bollobás. *Modern Graph Theory*. Graduate Texts in Mathematics. Springer, 1998.
- U. Brandes. A faster algorithm for betweenness centrality. *Journal of Mathematical Sociology*, 25(2):163–177, 2001. doi: [10.1080/0022250X.2001.9990249](https://doi.org/10.1080/0022250X.2001.9990249).
- CAIDA Macroscopic Topology Project Team. The CAIDA AS relationships dataset. <http://www.caida.org/data/active/as-relationships/>, 2000–2006.
- H. Chang, S. Jamin, and W. Willinger. Internet connectivity at the AS-level: an optimization-driven modeling approach. In *MoMeTools '03: Proceedings of the*

Bibliography

- ACM SIGCOMM workshop on Models, methods and tools for reproducible network research, pages 33–46, New York, NY, USA, 2003. ACM Press. ISBN 1-58113-748-8. doi: 10.1145/944773.944780.
- H. Chang, R. Govindan, S. Jamin, S. J. Shenker, and W. Willinger. Towards capturing representative AS-level internet topologies. *Computer Networks — The International Journal Of Computer And Telecommunications Networking*, 44(6):737–755, 2004.
- F. R. K. Chung. *Spectral Graph Theory*. Regional Conference Series in Mathematics. CBMS, 1997.
- Cisco Systems, Inc. Cisco IOS IP configuration guide. http://www.cisco.com/en/US/docs/ios/12_2/ip/configuration/guide/1cfbook.pdf, 2006.
- Cisco Systems, Inc. Introduction to EIGRP. <http://www.cisco.com/warp/public/103/1.html>, Aug. 2005.
- J. Dall and M. Christensen. Random geometric graphs. *Phys. Rev. E*, 66(1):016121, July 2002. doi: 10.1103/PhysRevE.66.016121.
- B. Danila, Y. Yu, S. Earl, J. A. Marsh, Z. Toroczkai, and K. E. Bassler. Congestion-gradient driven transport on complex networks. *Physical Review E*, 74(4):046114, 2006a.
- B. Danila, Y. Yu, J. A. Marsh, and K. E. Bassler. Optimal transport on complex networks. *Physical Review E*, 74(4):046106, 2006b.
- R. Diestel. *Graph Theory*, volume 173 of *Graduate Texts in Mathematics*. Springer, 2005.
- S. N. Dorogovtsev and J. F. F. Mendes. Evolution of networks – from biological nets to the internet and WWW. *Oxford University Press*, 2003.
- J. Doyle. *Routing TCP/IP*, volume I of *CCIE Professional Development*, chapter Dynamic Routing Protocols. Cisco Press, 1998.
- H. Ebel and S. Bornholdt. Coevolutionary games on networks. *Physical Review E*, 66(5):056118, Nov. 2002a. doi: 10.1103/PhysRevE.66.056118.
- H. Ebel and S. Bornholdt. Evolutionary games and the emergence of complex networks. *arXiv:cond-mat/0211666*, 2002b. <http://arxiv.org/abs/cond-mat/0211666>.
- H. Ebel, L.-I. Mielsch, and S. Bornholdt. Scale-free topology of e-mail networks. *Phys Rev E Stat Nonlin Soft Matter Phys*, 66(3 Pt 2A):035103, Sept. 2002.

- S. Eidenbenz, V. S. A. Kumar, and S. Zust. Equilibria in topology control games for ad hoc networks. In *DIALM-POMC '03: Proceedings of the 2003 joint workshop on Foundations of mobile computing*, pages 2–11, New York, NY, USA, 2003. ACM Press. ISBN 1-58113-765-6. doi: [10.1145/941079.941081](https://doi.org/10.1145/941079.941081).
- P. Erdős and A. Rényi. On the evolution of random graphs. *Publ. Math. Inst. Hung. Acad. Sci.*, 5:17–61, 1960.
- L. Euler. Solutio problematis ad geometriam situs pertinentis. *Commentarii Academiae Scientiarum Imperialis Petropolitanae*, 8:128–140, 1736.
- A. Fabrikant, A. Luthra, E. Maneva, C. H. Papadimitriou, and S. Shenker. On a network creation game. In *PODC '03: Proceedings of the twenty-second annual symposium on Principles of distributed computing*, pages 347–351, New York, NY, USA, 2003. ACM Press. ISBN 1-58113-708-7. doi: [10.1145/872035.872088](https://doi.org/10.1145/872035.872088).
- M. Faloutsos, P. Faloutsos, and C. Faloutsos. On power-law relationships of the internet topology. In *SIGCOMM '99: Proceedings of the conference on Applications, technologies, architectures, and protocols for computer communication*, pages 251–262, New York, NY, USA, Aug. 1999. ACM Press. ISBN 1-58113-135-6. doi: [10.1145/316188.316229](https://doi.org/10.1145/316188.316229).
- R. Ferrer and R. V. Solé. Optimization in complex networks. In R. Pastor-Satorras, M. Rubi, and A. Diaz-Guilera, editors, *Statistical Mechanics of Complex Networks*, volume 625 of *Lecture Notes in Physics*, pages 114–126. Springer Berlin / Heidelberg, 2003. doi: [10.1007/978-3-540-44943-0_7](https://doi.org/10.1007/978-3-540-44943-0_7).
- B. Fortz and M. Thorup. Internet traffic engineering by optimizing OSPF weights. In *INFOCOM 2000. Nineteenth Annual Joint Conference of the IEEE Computer and Communications Societies. Proceedings*, volume 2, pages 519–528. IEEE, 2000.
- L. C. Freeman. A set of measures of centrality based on betweenness. *Sociometry*, 40(1):35–41, Mar. 1977.
- H. Fukś and A. T. Lawniczak. Performance of data networks with random links. *Mathematics and Computers in Simulation*, 51(1-2):101–117, 1999. ISSN 0378-4754. doi: [10.1016/S0378-4754\(99\)00125-1](https://doi.org/10.1016/S0378-4754(99)00125-1).
- M. Gardner. Mathematical games: The fantastic combinations of John Conway's new solitaire game "life". *Scientific American*, 223:120–123, Oct. 1970.
- I. Glauche, W. Krause, R. Sollacher, and M. Greiner. Continuum percolation of wireless ad hoc communication networks. *Physica A: Statistical Mechanics and its Applications*, 325(3-4):577–600, 2003. ISSN 0378-4371. doi: [10.1016/S0378-4371\(03\)00249-8](https://doi.org/10.1016/S0378-4371(03)00249-8).
- K. I. Goh, B. Kahng, and D. Kim. Universal behavior of load distribution in scale-free networks. *Physical Review Letters*, 87(27):278701, 2001.

Bibliography

- R. Guimera, A. Arenas, A. Diaz-Guilera, and F. Giralt. Dynamical properties of model communication networks. *Physical Review E*, 66(2):026704, 2002.
- R. Guimerà, A. Díaz-Guilera, F. Vega-Redondo, A. Cabrales, and A. Arenas. Optimal network topologies for local search with congestion. *Phys. Rev. Lett.*, 89(24):248701, Nov. 2002. doi: [10.1103/PhysRevLett.89.248701](https://doi.org/10.1103/PhysRevLett.89.248701).
- H. Haller and S. Sarangi. Nash networks with heterogeneous links. *Math. Social Sciences*, 50:181–201, 2005.
- C. Hauert and M. Doebeli. Spatial structure often inhibits the evolution of cooperation in the snowdrift game. *Nature*, 428(6983):643–646, Apr. 2004. ISSN 1476-1122. doi: [10.1038/nature02360](https://doi.org/10.1038/nature02360).
- P. Holme and G. Ghoshal. Dynamics of networking agents competing for high centrality and low degree. *Physical Review Letters*, 96(9):098701, Mar. 2006. doi: [10.1103/PhysRevLett.96.098701](https://doi.org/10.1103/PhysRevLett.96.098701).
- T. C. Hu. *Integer programming and network flows*. Addison-Wesley, 1969.
- H. Jeong, B. Tombor, R. Albert, Z. N. Oltvai, and A.-L. Barabasi. The large-scale organization of metabolic networks. *Nature*, 407(6804):651–654, Oct. 2000. ISSN 0028-0836. doi: [10.1038/35036627](https://doi.org/10.1038/35036627).
- H. Jeong, S. P. Mason, A.-L. Barabási, and Z. N. Oltvai. Lethality and centrality in protein networks. *Nature*, 411(6833):41–42, May 2001. ISSN 0028-0836. doi: [10.1038/35075138](https://doi.org/10.1038/35075138).
- C. Jin, Q. Chen, and S. Jamin. Inet: Internet topology generator. Technical Report CSE-TR443-00, Department of EECS, University of Michigan, 2000.
- D. G. Kendall. Stochastic processes occurring in the theory of queues and their analysis by the method of the imbedded markov chain. *The Annals of Mathematical Statistics*, 24(3):pp. 338–354, 1953. ISSN 00034851. <http://www.jstor.org/stable/2236285>.
- B. Kerr, M. A. Riley, M. W. Feldman, and B. J. M. Bohannan. Local dispersal promotes biodiversity in a real-life game of rock-paper-scissors. *Nature*, 418(6894):171–174, July 2002. ISSN 0028-0836. doi: [10.1038/nature00823](https://doi.org/10.1038/nature00823).
- G. Kirchhoff. Über die Auflösung der Gleichungen, auf welche man bei der Untersuchung der linearen Verteilung galvanischer Ströme geführt wird. *Annalen der Physikalischen Chemie*, 72:497–508, 1847.
- A. S. Klovdahl. Social networks and the spread of infectious diseases: The AIDS example. *Social Science & Medicine*, 21(11):1203–1216, 1985. ISSN 0277-9536. doi: [10.1016/0277-9536\(85\)90269-2](https://doi.org/10.1016/0277-9536(85)90269-2).

- D. Koschützki, K. A. Lehmann, L. Peeters, S. Richter, D. Tenfelde-Podehl, and O. Zlotowski. *Network Analysis*, volume 3418 of *Lecture Notes in Computer Science*, chapter Centrality Indices, pages 16–61. Springer, 2005.
- W. Krause, I. Glauche, R. Sollacher, and M. Greiner. Impact of network structure on the capacity of wireless multihop ad hoc communication. *Physica A: Statistical Mechanics and its Applications*, 338(3-4):633–658, 2004. ISSN 0378-4371. doi: [10.1016/j.physa.2004.03.013](https://doi.org/10.1016/j.physa.2004.03.013).
- W. Krause, J. Scholz, and M. Greiner. Optimized network structure and routing metric in wireless multihop ad hoc communication. *Physica A — Statistical Mechanics and its Applications*, 361(2):707–723, 2006. doi: [10.1016/j.physa.2005.06.085](https://doi.org/10.1016/j.physa.2005.06.085).
- D. Krioukov, F. Chung, kc claffy, M. Fomenkov, A. Vespignani, and W. Willinger. The workshop on internet topology (WIT) report. *ACM SIGCOMM Computer Communication Review*, 37(1):69–73, 2007. ISSN 0146-4833. doi: [10.1145/1198255.1198267](https://doi.org/10.1145/1198255.1198267).
- A. T. Lawniczak, K. P. Maxie, and A. Gerisch. From individual to collective behaviour in CA like models of data communication networks. In P. M. A. Sloot, B. Chopard, and A. G. Hoekstra, editors, *Cellular Automata*, volume 3305 of *Lecture Notes in Computer Science*, pages 325–334. Springer Berlin / Heidelberg, 2004. doi: [10.1007/978-3-540-30479-1_34](https://doi.org/10.1007/978-3-540-30479-1_34).
- L. Li, D. Alderson, W. Willinger, and J. Doyle. A first-principles approach to understanding the internet’s router-level topology. *Computer Communication Review*, 34(4):3–14, 2004.
- G. Malkin. RIP version 2. <http://www.ietf.org/rfc/rfc2453.txt>, Nov. 1998.
- A. Medina, I. Matta, and J. Byers. BRITE: A flexible generator of internet topologies. Technical Report 2000-005, Boston University, Boston, MA, USA, 2000.
- S. Milgram. The small-world problem. *Psychology Today*, 1(1):61–67, May 1967.
- A. E. Motter and Y.-C. Lai. Cascade-based attacks on complex networks. *Phys. Rev. E*, 66(6):065102, Dec. 2002. doi: [10.1103/PhysRevE.66.065102](https://doi.org/10.1103/PhysRevE.66.065102).
- J. F. Nash. Equilibrium points in n-person games. *Proceedings of the National Academy of Sciences of the United States of America*, 36(1):48–49, 1950. ISSN 00278424. <http://www.jstor.org/stable/88031>.
- J. F. Nash. Non-cooperative games. *The Annals of Mathematics*, 54(2):286–295, 1951. ISSN 0003486X. <http://www.jstor.org/stable/1969529>.
- M. E. J. Newman. The structure of scientific collaboration networks. *Proc Natl Acad Sci U S A*, 98(2):404–409, Jan. 2001a. doi: [10.1073/pnas.021544898](https://doi.org/10.1073/pnas.021544898).

Bibliography

- M. E. J. Newman. Scientific collaboration networks. I. network construction and fundamental results. *Phys Rev E Stat Nonlin Soft Matter Phys*, 64(1 Pt 2):016131, July 2001b. doi: [10.1103/PhysRevE.64.016131](https://doi.org/10.1103/PhysRevE.64.016131).
- M. E. J. Newman. The structure and function of complex networks. *SIAM Review*, 45(1):167–256, 2003.
- M. A. Nowak and R. M. May. Evolutionary games and spatial chaos. *Nature*, 359(6398):826–829, Oct. 1992. doi: [10.1038/359826a0](https://doi.org/10.1038/359826a0).
- M. A. Nowak and R. M. May. The spatial dilemmas of evolution. *International Journal of Bifurcation and Chaos*, 3:35–78, Feb. 1993. doi: [10.1142/S0218127493000040](https://doi.org/10.1142/S0218127493000040).
- H. Ohtsuki, C. Hauert, E. Lieberman, and M. A. Nowak. A simple rule for the evolution of cooperation on graphs and social networks. *Nature*, 441(7092):502–505, May 2006. ISSN 0028-0836. doi: [10.1038/nature04605](https://doi.org/10.1038/nature04605).
- J. M. Pacheco, A. Traulsen, and M. A. Nowak. Coevolution of strategy and structure in complex networks with dynamical linking. *Physical Review Letters*, 97(25):258103, 2006a. doi: [10.1103/PhysRevLett.97.258103](https://doi.org/10.1103/PhysRevLett.97.258103).
- J. M. Pacheco, A. Traulsen, and M. A. Nowak. Active linking in evolutionary games. *Journal of Theoretical Biology*, 243(3):437–443, 2006b. ISSN 0022-5193. doi: [10.1016/j.jtbi.2006.06.027](https://doi.org/10.1016/j.jtbi.2006.06.027).
- G. Palla, A.-L. Barabási, and T. Vicsek. Quantifying social group evolution. *Nature*, 446(7136):664–667, Apr. 2007. ISSN 0028-0836. doi: [10.1038/nature05670](https://doi.org/10.1038/nature05670).
- Y. Rekhter and T. Li. A border gateway protocol 4 (BGP-4). <http://www.ietf.org/rfc/rfc1771.txt>, Mar. 1995.
- F. C. Santos and J. M. Pacheco. Scale-free networks provide a unifying framework for the emergence of cooperation. *Physical Review Letters*, 95(9):098104, Aug. 2005. doi: [10.1103/PhysRevLett.95.098104](https://doi.org/10.1103/PhysRevLett.95.098104).
- M. Schäfer, J. Scholz, and M. Greiner. Proactive robustness control of heterogeneously loaded networks. *Physical Review Letters*, 96(10):108701, Mar. 2006. doi: [10.1103/PhysRevLett.96.108701](https://doi.org/10.1103/PhysRevLett.96.108701).
- J. J. Schneider and S. Kirkpatrick. Selfish versus unselfish optimization of network creation. *Journal of Statistical Mechanics: Theory and Experiment*, 2005(08):P08007, 2005. doi: [10.1088/1742-5468/2005/08/P08007](https://doi.org/10.1088/1742-5468/2005/08/P08007).
- J. Scholz, M. Dejori, M. Stetter, and M. Greiner. Noisy scale-free networks. *Physica A — Statistical Mechanics and its Applications*, 350(2-4):622–642, 2005. ISSN 0378-4371. doi: [10.1016/j.physa.2004.11.012](https://doi.org/10.1016/j.physa.2004.11.012).

- J. Scholz, W. Krause, and M. Greiner. Decorrelation of networked communication flow via load-dependent routing weights. *Physica A — Statistical Mechanics and its Applications*, 387:2987–3000, Jan. 2008. doi: [10.1016/j.physa.2008.01.011](https://doi.org/10.1016/j.physa.2008.01.011).
- J. C. Scholz and M. O. W. Greiner. Topology control with IPD network creation games. *New Journal of Physics*, 9(6):185, 2007. doi: [10.1088/1367-2630/9/6/185](https://doi.org/10.1088/1367-2630/9/6/185).
- Y. Shavitt and E. Shir. DIMES: Let the internet measure itself. *arXiv.org*, cs/0506099, 2005. <http://arXiv.org/abs/cs/0506099v1>.
- R. V. Solé and S. Valverde. Information transfer and phase transitions in a model of internet traffic. *Physica A*, 289(3-4):595–605, 2001.
- G. Szabó and G. Fáth. Evolutionary games on graphs. *Physics Reports*, 446(4-6): 97–216, 2007. ISSN 0370-1573. doi: [10.1016/j.physrep.2007.04.004](https://doi.org/10.1016/j.physrep.2007.04.004).
- B. Tadić, G. J. Rodgers, and S. Thurner. Transport on complex networks: Flow, jamming and optimization. *International Journal of Bifurcation and Chaos*, 17(7): 2363–2385, July 2007. <http://arxiv.org/abs/physics/0606166>.
- University of Oregon. RouteViews project, 2001. <http://www.routeviews.org/>.
- A. Vázquez, R. Pastor-Satorras, and A. Vespignani. Large-scale topological and dynamical properties of the internet. *Phys. Rev. E*, 65(6):066130, June 2002. doi: [10.1103/PhysRevE.65.066130](https://doi.org/10.1103/PhysRevE.65.066130).
- F. Vega-Redondo. *Evolution, Games, and Economic Behaviour*. Oxford university Press, 1996.
- J. von Neuman and O. Morgenstern. *Theory of Games and Economic Behavior*. Princeton University Press, 1944.
- A. Wagner and D. A. Fell. The small world inside large metabolic networks. *Proceedings of the Royal Society of London. Series B: Biological Sciences*, 268(1478): 1803–1810, 2001. doi: [10.1098/rspb.2001.1711](https://doi.org/10.1098/rspb.2001.1711).
- D. J. Watts and S. H. Strogatz. Collective dynamics of 'small-world' networks. *Nature*, 393(6684):440–442, June 1998. doi: [10.1038/30918](https://doi.org/10.1038/30918).
- G. Wild and P. D. Taylor. Fitness and evolutionary stability in game theoretic models of finite populations. *Proceedings of the Royal Society of London. Series B: Biological Sciences*, 271(1555):2345–2349, 2004. doi: [10.1098/rspb.2004.2862](https://doi.org/10.1098/rspb.2004.2862).
- S. Wolfram. Statistical mechanics of cellular automata. *Reviews Of Modern Physics*, 55(3):601–644, July 1983. doi: [10.1103/RevModPhys.55.601](https://doi.org/10.1103/RevModPhys.55.601).
- S. Wolfram. Cellular automata as models of complexity. *Nature*, 311(5985):419–424, 1984. ISSN 0028-0836.

Bibliography

- G. Yan, T. Zhou, B. Hu, Z.-Q. Fu, and B.-H. Wang. Efficient routing on complex networks. *Physical Review E*, 73(4):046108, Apr. 2006. doi: [10.1103/PhysRevE.73.046108](https://doi.org/10.1103/PhysRevE.73.046108).
- S.-H. Yook, Z. N. Oltvai, and A.-L. Barabási. Functional and topological characterization of protein interaction networks. *Proteomics*, 4(4):928–942, Apr. 2004. doi: [10.1002/pmic.200300636](https://doi.org/10.1002/pmic.200300636).
- W. W. Zachary. An information flow model for conflict and fission in small groups. *Journal of Anthropological Research*, 33(4):452–473, 1977. ISSN 00917710. <http://www.jstor.org/stable/3629752>.
- S. Zhou and R. J. Mondragon. Accurately modeling the internet topology. *Physical Review E*, 70(6):066108, 2004.
- M. G. Zimmermann, V. M. Eguíluz, and M. S. Miguel. Cooperation, adaptation and the emergence of leadership. In A. Kirman and J.-B. Zimmermann, editors, *Economics with Heterogeneous Interacting Agents*, volume 503 of *Lecture Notes in Economics and Mathematical Systems*, pages 73–86. Springer, 2001. <http://arxiv.org/abs/nlin/0105004>.
- M. G. Zimmermann, V. M. Eguíluz, and M. S. Miguel. Coevolution of dynamical states and interactions in dynamic networks. *Physical Review E (Statistical, Nonlinear, and Soft Matter Physics)*, 69(6):065102, June 2004. doi: [10.1103/PhysRevE.69.065102](https://doi.org/10.1103/PhysRevE.69.065102).

Acknowledgments

While the present work may be the product of an individual, it wouldn't have come into being without the support of other people.

Firstly, I have to express my appreciation to my adviser Prof. Dr. Martin Greiner for guidance, support and feedback.

I'd also like to thank my colleagues Mirko Schäfer and Dominik Heide for the fruitful discussions, collaborations, and for proofreading of the manuscript.

For financial support, thanks go to Prof. Dr. Bernd Schürmann and Dr. Thomas Runkler (Siemens AG, Munich) and Prof. Dr. Carsten Greiner (Institute for Theoretical Physics, University of Frankfurt), and to the Frankfurt Institute for Advanced Studies (FIAS) for providing the working and computing infrastructure. Also the Center for Scientific Computing (CSC), located in Frankfurt has to be acknowledged, as their super computing infrastructure enabled the thorough numerical studies conducted during preparation of the thesis.

I'd also like to thank the other colleagues at FIAS, first of all my best buddies at FIAS, Andreea Lazar and Urs Bergmann, but all other people at FIAS as well, for discussions regarding scientific topics, which provided me with interesting insights in fields of science ranging from theoretical physics, over quantum chemistry, to neuro science, and theoretical biology, and apart from that, for generally making the time at FIAS enjoyable.

Furthermore I've got to thank my family and friends for support and encouragement through all these years. Most important of all I am indebted to Maike Hild, who would have surely liked if I hadn't spend so many hours working late.

Jan Carsten Scholz

Wilhelm-Leuschner-Straße 9
35440 Linden, Germany
✉ scholz@fias.uni-frankfurt.de

Personal Information

Date of birth April 5, 1978
Place of birth Lahn/Gießen, Germany
Nationality German

Education

2005 – today **obtaining Ph.D. in Theoretical Physics**, *Frankfurt Institute for Advanced Studies (FIAS)*, Goethe University Frankfurt, Germany.
Ph.D. thesis on *Self-organizing structure and metrics of complex networks*
Supervisor: Prof. Dr. Martin Greiner

1998 – 2005 **Diploma in Physics**, *Institute for Theoretical Physics*, Justus-Liebig-Universität Gießen, Germany, *Grade: "sehr gut" (excellent)*.
Diploma thesis title: *Network Game Theory*
Supervisors: Prof. Dr. Werner Scheid, Prof. Dr. Martin Greiner

1990 – 1997 **Abitur (High School equivalent)**, *Liebigschule*, Gießen.
specialized courses: *Mathematics, Physics*

Internships and Teaching

2. – 3. 2004 **Student Internship**, *Siemens Corporate Technology, Information and Communication*, Munich, Germany.
Research on *Noisy scale-free networks*

2001 – 2003 **Experimental Physics tutor for undergraduate students**, *Institute for Atomic and Molecular Physics*, Universität Gießen.

Computer Literacy

Programming C/C++, Python, Php, sed, awk, bash, Perl, SQL, (e)lisp
Scientific Computing boost graph library, SciPy, octave/matlab, gnuplot, maxima, mathematica
Office L^AT_EX, emacs, OpenOffice
System Administration GNU/Linux, MacOS X, other UNIX systems, Windows

Publications

- in preparation Jan Scholz and Martin Greiner. Transport capacity of Internet-like scale-free networks with tunable clustering coefficient. in preparation.
- 2008 Jan Scholz, Wolfram Krause, and Martin Greiner. Decorrelation of networked communication flow via load-dependent routing weights. *Physica A — Statistical Mechanics and its Applications*, 387:2987–3000, 2008.
- 2007 Jan C Scholz and Martin O W Greiner. Topology control with IPD network creation games. *New Journal of Physics*, 9(6):185, 2007.
- 2006 Mirko Schäfer, Jan Scholz, and Martin Greiner. Proactive robustness control of heterogeneously loaded networks. *Physical Review Letters*, 96(10):108701, 2006.
- 2006 Wolfram Krause, Jan Scholz, and Martin Greiner. Optimized network structure and routing metric in wireless multihop ad hoc communication. *Physica A — Statistical Mechanics and its Applications*, 361(2):707–723, 2006.
- 2005 Jan Scholz, Mathäeus Dejori, Martin Stetter, and Martin Greiner. Noisy scale-free networks. *Physica A — Statistical Mechanics and its Applications*, 350(2-4):622–642, 2005.

Conferences and Workshops

3. 2009 **DPG Frühjahrstagung**, *Deutsche Physikalische Gesellschaft*, Dresden, Germany, Spring meeting of the german physical society.
Talk: *The impact of clustering on the transport capacity of scale-free communication networks*
3. 2008 **DPG Frühjahrstagung**, *Deutsche Physikalische Gesellschaft*, Berlin, Germany.
Talk: *Decorrelation of networked communication flow via load-dependent routing weights*
10. 2007 **European Conference on Complex Systems 2007**, *European Complex Systems Society (ECSS)*, Dresden, Germany, Complex Networks: Dynamics and Topology Interplay.
Talk: *The impact of clustering on the transport capacity of scale-free communication networks*
Poster: *Topology control with IPD network creation games*
5. 2007 **COST Working Group 3 Meeting**, *European Cooperation in the field of Scientific and Technical Research*, Belgrade, Serbia.
Invited talk: *Efficient routing weights in communication networks*
2. 2007 **Workshop Econophysics, FoKo 2007**, Bad Hersfeld, Germany, Annual Colloquium of the *Institut für Wirtschaftsinformatik, Frankfurt*.
Talk: *Topology control with IPD network creation games*
5. 2006 **NetSci 2006**, *Indiana University*, Bloomington IN, USA, International Workshop and Conference on Network Science.
Talk: *IPD network creation games*
3. 2006 **DPG Frühjahrstagung**, *Deutsche Physikalische Gesellschaft*, Dresden, Germany.
Poster: *IPD network creation games*
5. 2005 **School and Workshop on Structure and Function of Complex Networks**, *International Centre for Theoretical Physics (ICTP)*, Trieste, Italy.